THESIS

DEVELOPMENT OF A SCALABLE, HIGH THROUGHPUT, LOW ENERGY CONSUMING, RAPID VACCINE PRODUCTION DEVICE

Submitted by

Andrew J. Andraski

Department of Mechanical Engineering

In partial fulfillment of the requirements

For the Degree of Master of Science

Colorado State University

Fort Collins, Colorado

Fall 2022

Master's Committee:

Advisor: Jason Quinn
Co-Advisor: John Mizia

Raymond Goodrich

ABSTRACT

DEVELOPMENT OF A SCALABLE, HIGH THROUGHPUT, LOW ENERGY CONSUMING, RAPID VACCINE PRODUCTION DEVICE

Producing vaccines rapidly and efficiently is an incredibly important task. To accomplish this, we are required to develop novel vaccine manufacturing methods and technologies. With the onset of the COVID-19 pandemic and the prolonged struggle to mitigate its spread and devastating impacts, an entirely new approach to making an inactivated, whole virus vaccine was pioneered by a team of researchers at Colorado State University's (CSU) Infectious Disease Research Center (IDRC). The novel method employs ultraviolet light and riboflavin (Vitamin B2) to inactivate the virus so that it is suitable for use as a vaccine candidate. The novel method has been coined the "SolaVAX" process, and the efficacy of a COVID-19 vaccine produced using the SolaVAX process was proven in an animal challenge study during pre-clinical testing.

An existing pathogen reduction technology (PRT) called Mirasol PRT was capable of manufacturing small batches of vaccine material in the laboratory. The Mirasol PRT was developed for inactivating pathogen in blood products. The technology's batch processing design is not suitable for efficiently producing large quantities of vaccine material and meeting the needs for current and future pandemic preparedness. To safely and efficiently inactivate large volumes of pathogen for vaccine production, flow-through processing rather than batch processing is necessary.

In a collaborative effort, a team of engineering researchers at CSU's Energy Institute developed a device called the VacciRAPTOR that is estimated to be capable of processing 71 liters of pathogen solution per hour. This processing rate equates to producing over 100,000

human COVID-19 vaccine doses per hour. The VacciRAPTOR uses 18 broadband UV lamps to illuminate and inactivate a flowing solution of whole virus. It has reliably and repeatably inactivated Zika virus during preliminary testing. In addition to using broadband UV lamps for pathogen inactivation, high intensity narrowband UV LEDs were also explored. Both broadband UV emission from lamps and narrowband UV emission from LEDs proved to effectively inactivate whole Zika virion.

Since both broadband and narrowband UV light emission from lamps and LEDS effectively inactivated Zika virus during lab testing, a combined Life Cycle Assessment (LCA) and Technoeconomic Analysis (TEA) was performed to compare the differences in global warming potential (GWP) and economic impact as a result of utilizing UV lamps versus UV LEDs for illumination. The LCA results indicate that using UV lamps is 24x less impactful (5.7 g-CO2-eq per liter of treated virion solution produced) than using UV LEDs (136 g-CO2-eq per liter of treated virion solution produced) when considering use-phase GWP. The TEA results indicate that using UV lamps is 14x less expensive ($6,300) than using UV LEDs ($87,600) when considering overnight capital and lifetime use-phase energy consumption costs.

Since the SolaVAX method and VacciRAPTOR technology utilize ultraviolet light and Vitamin B2 rather than hazardous chemicals such as Formalin, this technology can be integrated into production centers without requiring that the center to be capable of handling the toxic and environmentally hazardous materials that are often associated with vaccine production. The device is scalable, compact, and low energy consuming. Scalability, compact design, and chemical-free processing opens the potential to distribute vaccine production capabilities when and where it is needed throughout much of the world.

ACKNOWLEDGEMENTS

My deepest thanks go out to those who have supported my trajectory both on and off the beaten paths through college, outdoor education, wilderness therapy, South America, Spain, and the mountain west. The people, forces, and places that have supported me and challenged me are abundant, and to each of you I am profoundly grateful.

I am particularly grateful for John Mizia who has served as a personal and professional mentor for nearly a decade. Without his guidance and openness, I can definitively say that I would not be where I am today. My friends and colleagues at Colorado State University's Energy Institute, Industrial Assessment Center, and Infectious Disease Research Center have fostered an enjoyable, growth-oriented atmosphere throughout my experience as a master's student.

The following collection of names are people who have inspired me and guided me through my experience as a master's student. The collection is in no particular order, nor is it complete: Allison Andraski, Brian and Janet Andraski, Matt Willman and the RPL staff, Raymond Goodrich, Lindsay Hartson, Izzy Ragan, Alina Vise, Katherine Compton, Kelly Banta, Carl Jung and associates, Maynard James Keenan, Todd Sheaffer, Carlos Castaneda, don Juan Matus, Corvus Corax, S.N. Goenka, my loving family, and my incredible friends.

TABLE OF CONTENTS

LIST OF TABLES

LIST OF FIGURES

CHAPTER 1 BACKGROUND – VACCINE HISTORY AND TRADITIONAL VACCINES

1.1 A Brief History of Vaccine Discovery and Development

Humankind and the viruses that infect it perpetually combat one another as humans and viruses evolve and adapt. Vaccination is defined as the "intentional inoculation of a person or animal with a harmless form of a pathogen" [1]. The earliest known vaccination efforts began in China with variolation in attempt to reduce the spread and mortality rate of smallpox. In these early vaccination efforts, well before the existence of viruses had been discovered, dried smallpox scabs were pulverized and inhaled or injected into uninfected humans. This practice reduced the mortality rate from around 30% to 2-3% and led to a milder form of the disease [1]. These rudimentary methods of variolation spread throughout China, India, and Africa before it was introduced in Europe and the Americas in the 1700s [1].

In the late 1700s, smallpox continued to infect and spread rampantly. At this time, country doctors began noticing that milkmaids who had contracted cowpox from the cows they were milking were immune to contracting smallpox. In 1776, country doctor Edward Jenner collected puss from a cowpox sore that was on the hand of milkmaid and injected it into a young man named James Phipps, who, when later exposed to smallpox, did not contract the disease. Edward Jenner's methods had their share of criticism, but he continued to promote his practice [1]. The crude vaccination procedures became widespread throughout the next century. Jenner coined the term "vaccine" which is derived from the Latin word *vacca* which means "cow". Jenner is given credit for creating the first vaccine [1].

1.2 Modern Traditional Viral Vaccine Types

There are five primary types of vaccines in use today as shown in ***Table 1.1 below***. The first three types are approved for use in humans and the fourth and fifth are experimental. Although the fourth vaccine type listed in the table is, in general, considered experimental, the first nucleic acid vaccine approved for human use is the mRNA vaccine that was developed to combat SARS-CoV-2, the virus that causes COVID-19. The three types of vaccines that are approved for use in humans are live attenuated, recombinant subunit, and inactivated. These three vaccine types are discussed briefly in the following paragraphs. Detail of the experimental vaccine types (types 4 and 5 in ***Table 1.1 below***) are beyond the scope of this report.

Table 1.1: Modern types of viral vaccines for use in humans [1, 2].

	Vaccine Type	Examples
1	Live attenuated	Measles, mumps, rubella (MMR); influenza, yellow fever,
2	Recombinant subunit	Hepatitus B, human papillomavirus (HPV)
3a	Inactivated	Poliovirus, hepatitus A, rabies, seasonal influenza
4a	Nucleic acid	SARS-CoV-2 (Pfizer, Moderna)
4b	Nucleic acid (experimental)	Influenza, HIV, West Nile, herpes viruses
5a	Recombinant vector	SARS-CoV-2 (Johnson and Johnson)
5b	Recombinant vector (experimental)	Rabies, HIV, West Nile, measles, Ebola, avian influenzas

Live attenuated (meaning weakened so that the virus no longer replicates effectively) is the most common type of vaccine. One method for attenuating a virus is by repeatedly growing the virus in non-human cells where the non-human cell environment is not well suited for effective virus replication. As the virus replicates in the non-human cells, mutations occur as the virion adapts so that it can replicate more effectively in the non-human cells. After multiple passages of this process, the virus mutates so that it effectively replicates in non-human cells

while losing its ability to replicate effectively in human cells. Another way to achieve attenuation is by genetically modifying the virus to remove genes that make it virulent. It still grows, but it cannot cause infection. When injected into humans, the human host generates an immune response that protects the host from infection from live attenuated virus. The immune response developed in the process helps protect the vaccinated human from infection if it is exposed to the live "non-attenuated" virus.

Recombinant subunit vaccines can be developed for virus strains that do not replicate well in a laboratory setting. The inability to replicate well in a laboratory prevents the possibility of producing a live virus for vaccine [1]. A recombinant subunit vaccine is composed of only certain viral proteins rather than the whole virus. In a simplified description, recombinant subunit vaccines are produced by placing nucleic acids from one organism into another organism. For vaccine production, a viral nucleic acid protein is inserted into a small piece of non-human DNA called a plasmid. When the plasmid containing the virus-protein is inserted into a cell culture (typically a bacteria), the bacteria transcribe and translate the protein as if it were its own. Introducing these proteins (viral subunits) into a human elicits an immune response that causes the human to generate protective antibodies that strengthen the immune system against infection from the virus [3, 1].

Inactivated virus vaccines are traditionally produced by subjecting whole virions to high heat or an inactivating chemical such as formalin which is an aqueous solution of formaldehyde [1]. These traditional inactivation pathways can cause significant unwanted damage to a virus's structure which reduces its potency as an antigen. An antigen is the substance that elicits an immune response within the body. A weak antigen yields minor immune protection while a potent antigen will yield a more protective immune response. As such, the efficacy of producing

inactivated virus vaccines using traditional methods (high heat or chemical) can be relatively low. As is discussed in greater detail in the ***Chapter 2***, a novel inactivated virus vaccine production method has been developed by a team of researchers at Colorado State University's (CSU) Infectious Disease Research Center (IDRC). The novel method is theorized to yield higher portions of vaccine-ready inactivated virions than traditional inactivation methods.

CHAPTER 2 INTRODUCTION – THE SOLAVAX PATHOGEN INACTIVATION PROCESS AND ITS DEVELOPMENT

2.1 SolaVAX – A Novel, Whole Virion Inactivation Method

Worldwide, it is estimated that as of August 2022, 579 million people have been infected by the COVID-19 virus and, of those 579 million cases, 6.4 million deaths have resulted from the disease [4]. This equates to a global mortality rate of 1.1%. In 2020, in response to the urgent need to mitigate the spread of COVID-19, a novel method coined the "SolaVAX method" was developed for inactivating whole virion by a team of researchers at Colorado State University's (CSU) Infectious Disease Research Center (IDRC). Instead of subjecting whole virion to high heat or Formalin, a formaldehyde derivative, the SolaVAX method uniquely inactivates the virion by dosing a liquid solution of whole virion and riboflavin (vitamin B2) with broad-spectrum ultraviolet (UV) light [5]. Efficacy of the SolaVAX method has been demonstrated in an animal challenge model [5].

2.2 SolaVAX – Developing the Process

The SolaVAX inactivation method was inspired by techniques that are currently used for pathogen inactivation/reduction in blood products. There are three principal blood pathogen reduction methods commonly practiced worldwide. In the United States, the only approved blood pathogen reduction technology (PRT) is called the Intercept PRT by Cerus. Other common PRT systems used worldwide are the Mirasol PRT and a plasma only process technology called Theraflex by Macopharma.

The SolaVAX inactivation method was most directly inspired by the Mirasol PRT. The Mirasol PRT treats blood products in small batches (typically around 500mL per batch

depending upon the type of blood product being treated). ***Figure 2.1 below*** illustrates the process by which blood products are treated using the Mirasol PRT system. The blood product is mixed with a liquid solution of riboflavin (vitamin B2) in a UV transparent bag where it is then placed in the Mirasol illuminator. In the illuminator, the solution is mechanically agitated and dosed with broad-spectrum UV light. The photochemical reaction between riboflavin and UV light damage the pathogen's nucleic acid to cause inactivation. Riboflavin is a non-toxic, non-mutagenic compound that is classified by the Food and Drug Administration as a Generally Recognized as Safe (GRAS) product (21 CFR 184, 1695, 2001) [6]. Riboflavin acts as a photosensitizer which increases the inhibition effect of UV light on the pathogen. The photochemical reaction between riboflavin and UV light pathogen inactivation is discussed in greater detail in ***Chapter 3.2***.

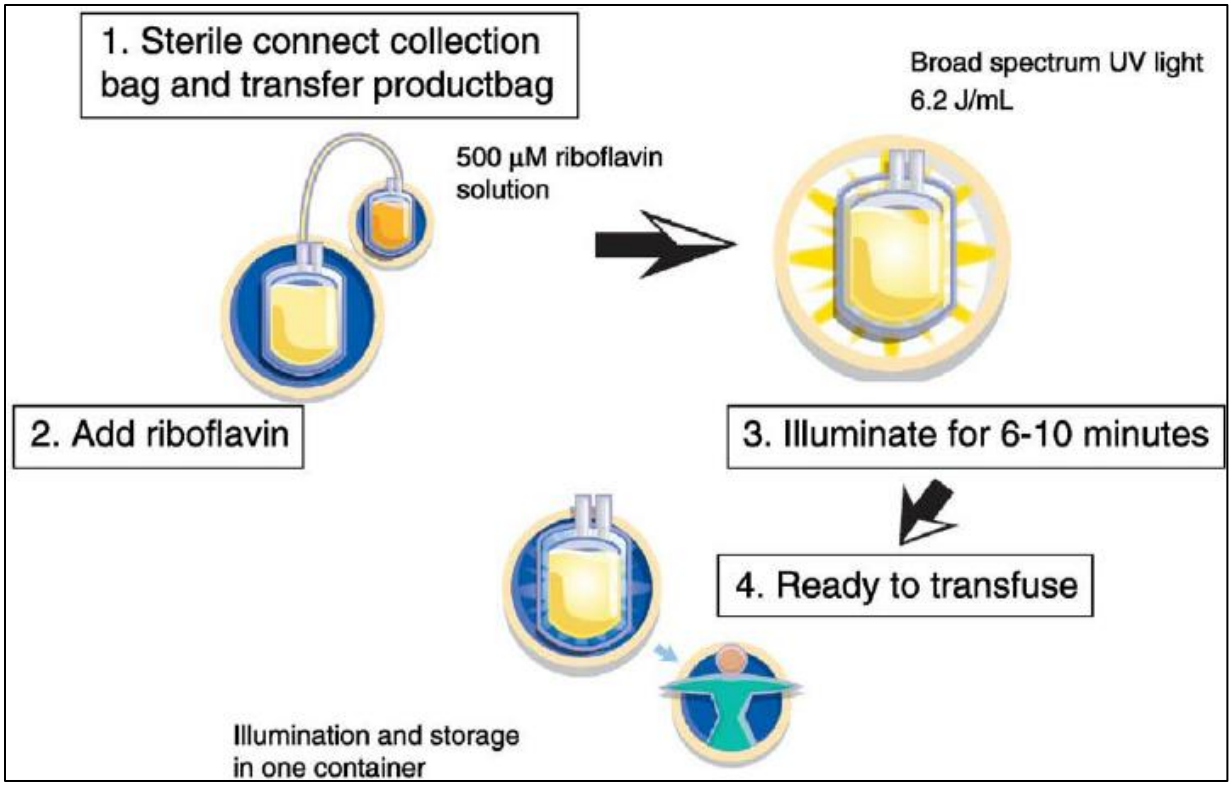

Figure 2.1: The Mirasol PRT system utilizes broad-spectrum UV light and a solution of blood product with riboflavin (vitamin B2) to reduce pathogens in blood products so that they are transfusion ready. This method inspired the development of the SolaVAX whole virion inactivation process [7].

When pathfinding the SolaVAX process, it was hypothesized that the photochemical reaction between riboflavin and UV light may not only be capable of pathogen reduction in blood products, but it may also be capable of whole virion inactivation for vaccine production. Producing a solution of inactivated yet structurally undamaged virion is the basis for producing inactivated virus vaccines. Lab tests performed at the CSU IDRC confirmed that the process of exposing a solution of riboflavin and live whole virion to broad-spectrum UV light inactivates whole virion and yields a potent antigen. As such, the basis for a novel inactivation method for whole virion vaccine production was conceived and coined “SolaVAX”.

Through further exploration of the novel SolaVAX process, a whole virion vaccine candidate for SARS-CoV-2 was produced and efficacy in an animal challenge model was demonstrated. The data suggests that preparation of a whole virion vaccine using the SolaVAX-

specific photochemical method for SARS-CoV-2 may have utility in the preparation of a broad array of whole virion vaccine candidates [5].

2.3 Future Pandemic Preparedness

To prepare for future pandemics and to help mitigate the present COVID-19 crisis, the creation of rapid, scalable, and distributed vaccine production technology is imperative. Using the Mirasol PRT System, a system specifically designed for batch processing of blood products (as opposed to a continuous manufacturing type of device), multiple operators can process up to about 7.2L of virion solution per hour. The "batch" treatment process of the Mirasol PRT System requires multiple operators, several steps, presents challenges with maintaining a sterile environment, and requires many single-use disposable plastic devices. As a batch processing device, the Mirasol PRT System is neither readily scalable nor suitable for high volume processing.

To rapidly produce large quantities of inactivated whole-virion vaccine material on a highly scalable and readily distributed platform, a novel technology that employs the SolaVAX method is under development. CSU's Energy Institute and Infectious Disease Research Center are collaborating to develop and test an energy efficient, high-throughput, flow through device that employs the SolaVAX process. ***Chapter 4*** details the development of the novel technology and ***Chapter 5*** details preliminary pathogen inactivation testing and results.

CHAPTER 3 ELECTROMAGNETIC RADIATION, RIBOFLAVIN PHOTOCHEMISTRY, AND PATHOGEN INACTIVATION

3.1 Electromagnetic Radiation

Electromagnetic radiation (EMR) is an electric and magnetic disturbance that travels through space at the speed of light and contains neither mass nor charge. EMR travels in packets of radiant energy known as photons or quanta and exhibits both particle and wave nature [8]. Examples of EMR are x-rays, ultraviolet light, visible light, and infrared. The following section narrows the EMR focus to the visible and ultraviolet light spectra.

3.1.1 Visible and Ultraviolet Light

The visible spectrum of light is the "visible" spectrum because these wavelengths of electromagnetic radiation are detectable/visible to the naked human eye as light and color. Spectrometry studies have quantified the wavelengths of electromagnetic radiation over a large spectrum of wavelengths. The ultraviolet (UV) region and the visible region of the electromagnetic radiation spectrum reside between 100nm and 780nm. The ultraviolet (UV) region exists between 100nm to 400nm and the visible region exists between 400nm to 780nm. The shorter the electromagnetic radiation wavelength, the greater the energy it possesses. This relationship is described in the equation below. ***Figure 3.1 below*** illustrates these regions and their associated wavelengths.

$$\boldsymbol{Energy\ of\ a\ Photon} = \boldsymbol{E} = \frac{Planck's\ Constant\ \times speed\ of\ light}{wavelength} = \frac{h\ \times c}{\lambda}$$

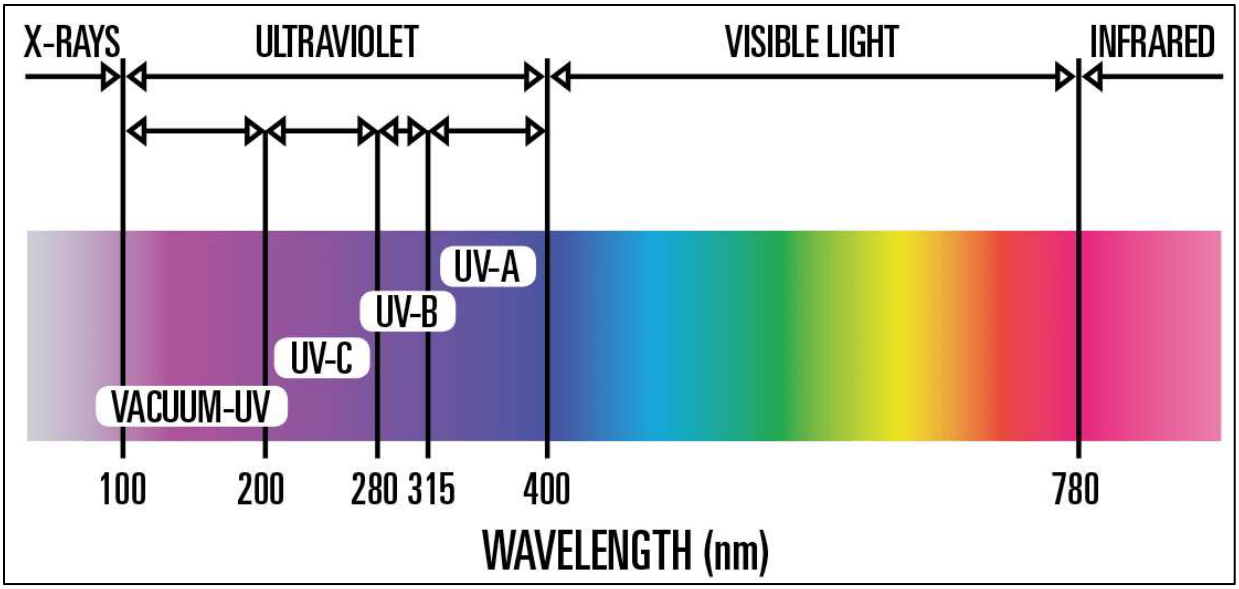

Figure 3.1: Ultraviolet and visible regions of the electromagnetic spectrum. Shorter wavelength radiation is more energetic than longer wavelength radiation [9].

In the visible region of light, white light can be separated and categorized into its seven principal colors: red, orange, yellow, green, blue, indigo, and violet (ROYGBIV). The separation of white light into its seven principal colors is best illustrated in nature by a rainbow. When sunlight is refracted by water molecules in the atmosphere, from a certain viewing angle and distance, an arc comprised of these seven principal colors will appear.

In the ultraviolet (UV) region, UV light is characterized by four regions UVA, UVB, UVC, and Vacuum-UV. UVA is the least energetic UV region and Vacuum-UV is the most energetic UV region [10]. Here, UVA, UVB, and UVC rays will be examined. While UVA, B or C rays are not visible to the human eye, they can be experienced in nature and/or utilized for a multitude of applications. Human exposure to UVA (~315nm to 400nm) can elicit a tanning effect on our skin while exposure to UVB (~280nm to 315nm) is responsible for Vitamin D synthesis and sun burns. UVC rays (~200nm to 280nm) are highly energetic and very damaging to skin and other cells. Fortunately, UVC sun rays are filtered out by atmospheric ozone. The most damaging component of sunlight for humans is UVB [9].

Scientific devices have been created to emit UVC radiation as a means of disinfecting surfaces, air, and liquid. UVC radiation is 99.99% effective at inactivating bacteria and viruses [9]. The highly energetic, short wavelengths of UVC penetrate the DNA and cellular structure of pathogens rendering them “inactive” or incapable of replication [9].

3.2 Ultraviolet Light, Riboflavin Photochemistry, and Pathogen Inactivation

Understanding the nature of UV light and its effects on pathogen cell and nucleic acid structure is paramount to successfully designing and characterizing the VacciRAPTOR’s illumination field. The UV radiation delivered to the flowing pathogen solution must be sufficiently energetic to render the pathogen inactive (i.e. incapable of replication) without damaging its overall structure. If the goal were simply to inactivate a virus so that it could not replicate, then selecting a UVC light source would be the most efficient UV source to select. UVC radiation is highly energetic and can easily render viruses inactive through irreversible DNA and structure damage. UVC however, causes indiscriminate/excess damage to pathogen’s protein structure during inactivation. The indiscriminate damage reduces the inactivated pathogen’s potency as an antigen.

To successfully carry out the SolaVAX process, the VacciRAPTOR must render viruses inactive by only damaging the portion of viral nucleic acid that allows it to replicate. UVC is too energetic to inactivate whole virion without also causing unwanted structural damage. As a result, other targeted modes of inactivation are necessary to yield a solution of inactivated whole-virion that is viable for use in vaccine production. In the following section, riboflavin photochemistry and its modes of action are discussed over several EMR regions: UVC, UVB,

UVA, and visible UV. The following section illuminates why broadband UVB lamps were selected for use in the VacciRAPTOR's design.

3.2.1 Ultraviolet Light and Riboflavin – Sharpening Inactivation Precision and Sensitivity

Riboflavin (RB), also known as vitamin B2, is a naturally occurring substance that is found in many foods and is sold as a dietary supplement. In humans, RB plays a role in the growth, development, and function of cells in the body and helps convert consumed food into energy that's available to the body [11]. In pathogen inactivation, RB has proven to have a sensitizing effect on the interaction between pathogen nucleic acids UV light. In simple terms, RB acts as a photosensitizer that enhances UVB and UVA radiation's ability to precisely target and damage a specific portion of nucleic acid that, in turn, decreases reactivation (i.e. increases log kill) of the virus [12].

The absorption spectrum of RB in water is shown in ***Figure 3.2 below***. RB is characterized by its absorption peaks at 222nm, 226nm, 373nm and in the visible region at 445nm (blue color) [13]. The action spectra (yellow line) in ***Figure 3.3 below*** illustrates the effect of RB on log virus kill within the UVC to UVA spectrum (200nm to 400nm) as well as a portion of the visible spectrum (400nm to 780nm). RB enhances pathogen kill levels when solutions of RB and pathogen are exposed to EMR wavelengths between approximately 300nm and 500nm. Note that the action spectra (yellow line) in ***Figure 3.3*** is greater than zero between 300 and 500nm.

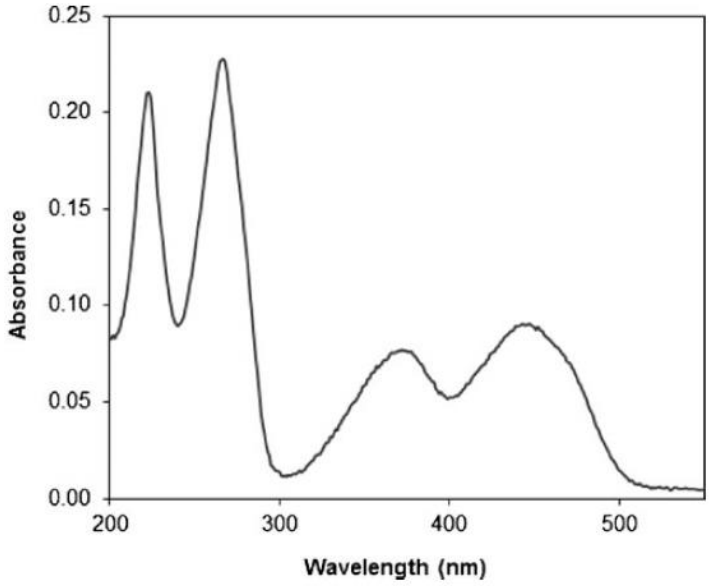

Figure 3.2: Absorption spectrum of riboflavin in water (0.08mg/mL). RB is characterized by absorption peaks in the UV spectrum of 222nm, 226nm, 373nm and in the visible region near 445nm [13].

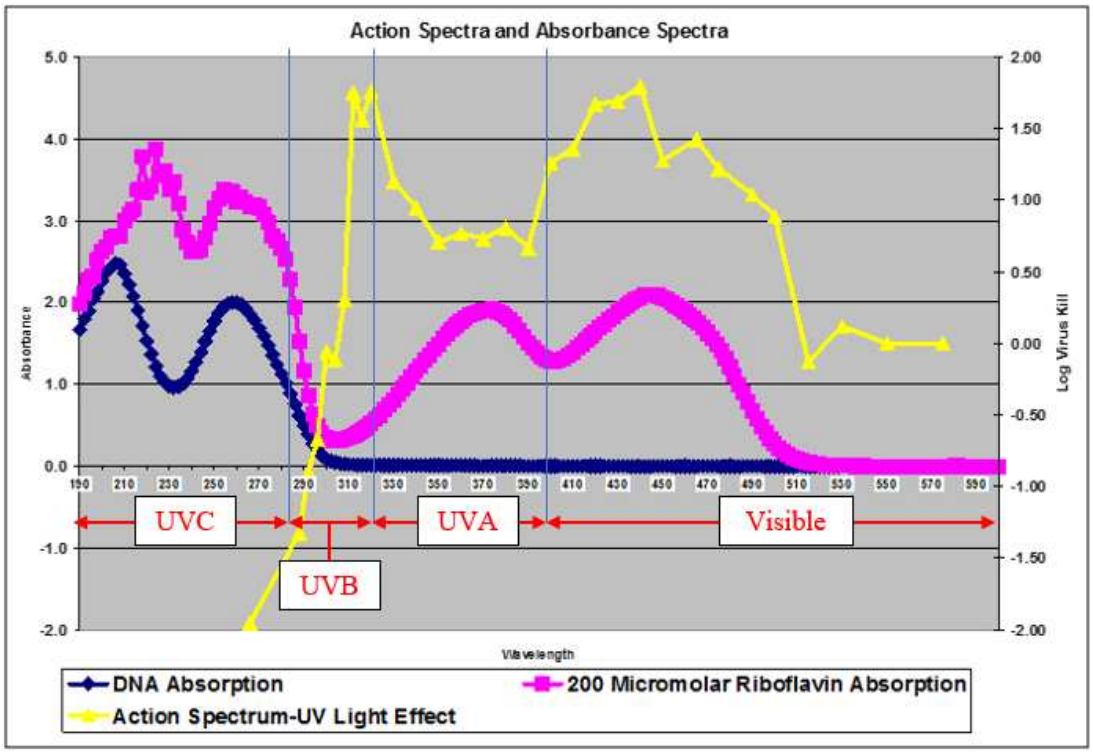

Figure 3.3: The action spectrum (yellow line) indicates the difference in pathogen kill levels with and without RB. The action spectrum is positive between 300nm and 500nm. This indicates that inactivation is enhanced due to RB-UV photochemical reactions between 300nm and 500nm [14].

The action spectrum (yellow line) indicates the difference in pathogen kill levels with and without the presence of RB. Note that the action spectrum at wavelengths between 300 and 500nm is positive and log kill is up to ~1.75 log greater with RB than without RB. At wavelengths below 300nm, the action spectra are negative, indicating that the presence of RB inhibits log virus kill at wavelengths below ~300nm. UVC alone is effective at damaging DNA and thus inactivating viruses because DNA readily absorbs electromagnetic radiation in the UVC region. This is illustrated by the two absorption peaks of DNA (blue line) in the UVC region. When inactivating viruses for use in vaccine production, the highly energetic UVC radiation causes excess damage to the virus's structure yielding it unusable for vaccine applications [14, 15, 16].

In the UVB spectrum, DNA does not readily absorb electromagnetic radiation. This is shown by the blue curve in ***Figure 3.3 above***. In this region, RB presence is highly effective at improving log virus kill and is most prominent between ~310 and 330nm. UVB radiation is less energetic than UVC radiation, so it is less likely to cause unwanted damage to viral protein structure. The damage is understood to be limited to the DNA location that is responsible for promoting viral replication. UVB and UVA electromagnetic radiation have proven to be highly effective at viral inactivation without causing excess damage [16].

In the UVA region, RB-UV photochemical inactivation is less effective than in the UVB region. In the UVA region, RB continues to act as a photosensitizer, but log virus kill is not as prominent. It is theorized that the RB + UVA radiation is less effective than RB + UVB because UVA radiation is less energetic, and it is not absorbed by DNA [14, 15, 16].

In the visible region, the RB photochemistry is distinct from the photochemistry that occurs in the UVA and UVB region. In the visible region, RB does not need to be bound to DNA

to undergo a photochemical reaction. The photochemical reaction generates reactive oxygen species that cause irreversible nucleic acid damage through various oxidative reactions. These oxidative reactions will inactivate the virus but will also cause additional non-discriminate damage to the virus structure. Similar to UVC, RB + visible UV will inactivate a virus, but the inactivation mechanism causes excessive damage to the viral structure that lowers its potency as an antigen. Thus, the excessively damaged, yet inactivated virus, is less suitable for whole virion vaccines [14, 15, 16].

In summary, riboflavin and UV electromagnetic radiation will inactivate pathogens through different modes of action depending on the wavelength of the incident electromagnetic radiation. Each region of wavelength discussed (UVA, UVB, UVC, and visible) will elicit a riboflavin-photochemical reaction to occur that effectively inactivates pathogen. Of these four regions, with the presence of riboflavin, UVB and short-wavelength UVA yield the most desirable results for whole virion vaccine production because the damage targets a specific portion of viral DNA that inhibits replication without causing excess damage to the rest of the virus's structure. The favorable results of UVB/short wavelength UVA + RB for whole virion vaccine production directly influenced the decision to utilize broadband UVB illumination in the VacciRAPTOR. The broadband UVB lamps used in the device have a peak emission spectrum centered over the UVB/short wavelength UVA region. ***Figure 4.5 on page 24*** shows the emission spectra of the lamps used in the VacciRAPTOR.

CHAPTER 4 VACCIRAPTOR SYSTEM DESIGN AND CHARACTERIZATION

4.1 The need for the technology

The onset of the COVID-19 pandemic has illuminated, with remarkable clarity, that the battle between human health and pathogen infection is ever-evolving and ever-present. Humans and technology must continue to adapt and improve along with viruses as they continue to change and emerge. Presently, humanity is struggling to thwart the spread of COVID-19. Humankind was not able to protect itself from this virus through means of traditional vaccine production nor natural immunity protection before it became a worldwide pandemic. The need to create an improved process and a high-volume processing technology that can be readily distributed and deployed worldwide is clear. A major stride was taken towards meeting this need when the SolaVAX method was developed, and its efficacy was demonstrated in an animal challenge model [5].

The SolaVAX method was pioneered using the Mirasol PRT system, a small batch processing technology. The Mirasol PRT is not suitable for high-volume processing and, as such, a new technology called the VacciRAPTOR device was pioneered to carry out the SolaVAX method. The VacciRAPTOR technology is another nascent effort towards future pandemic preparedness that provides a scalable, high volume throughput processing platform for SolaVAX inactivation. The name “RAPTOR” is an acronym derived from the team of collaborators involved in the SolaVAX and VacciRAPTOR development. “RAPTOR” is an abbreviation for Rapid Response Technical / Operations / Research Team. ***Figure 4.1*** and ***Figure 4.2 below*** show the Mirasol PRT batch processing system and the VacciRAPTOR high-volume, flow through processing device.

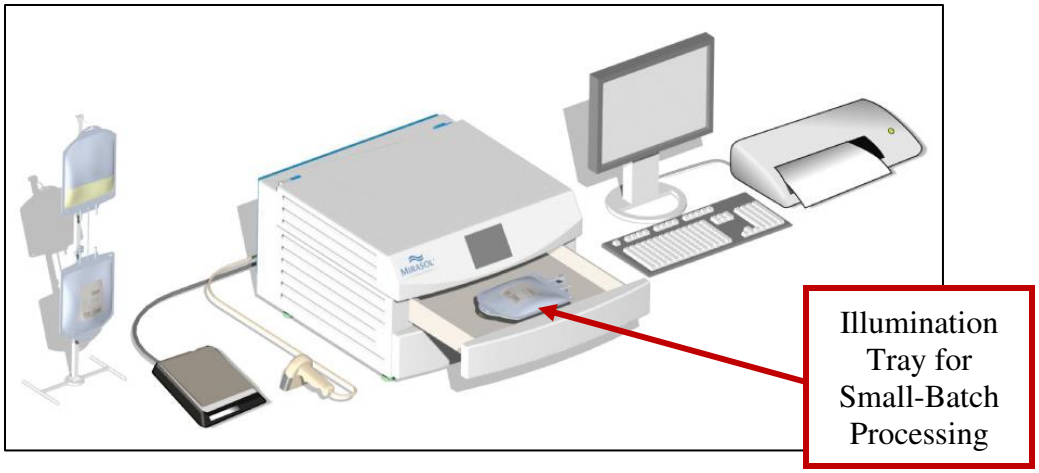

Figure 4.1: The small batch processing capabilities of the Mirasol PRT system shown here are suitable for pathogen reduction in blood productions, but the platform is not suitable for high-volume vaccine production processing. This technology can only process about 7L of viral solution per hour [7].

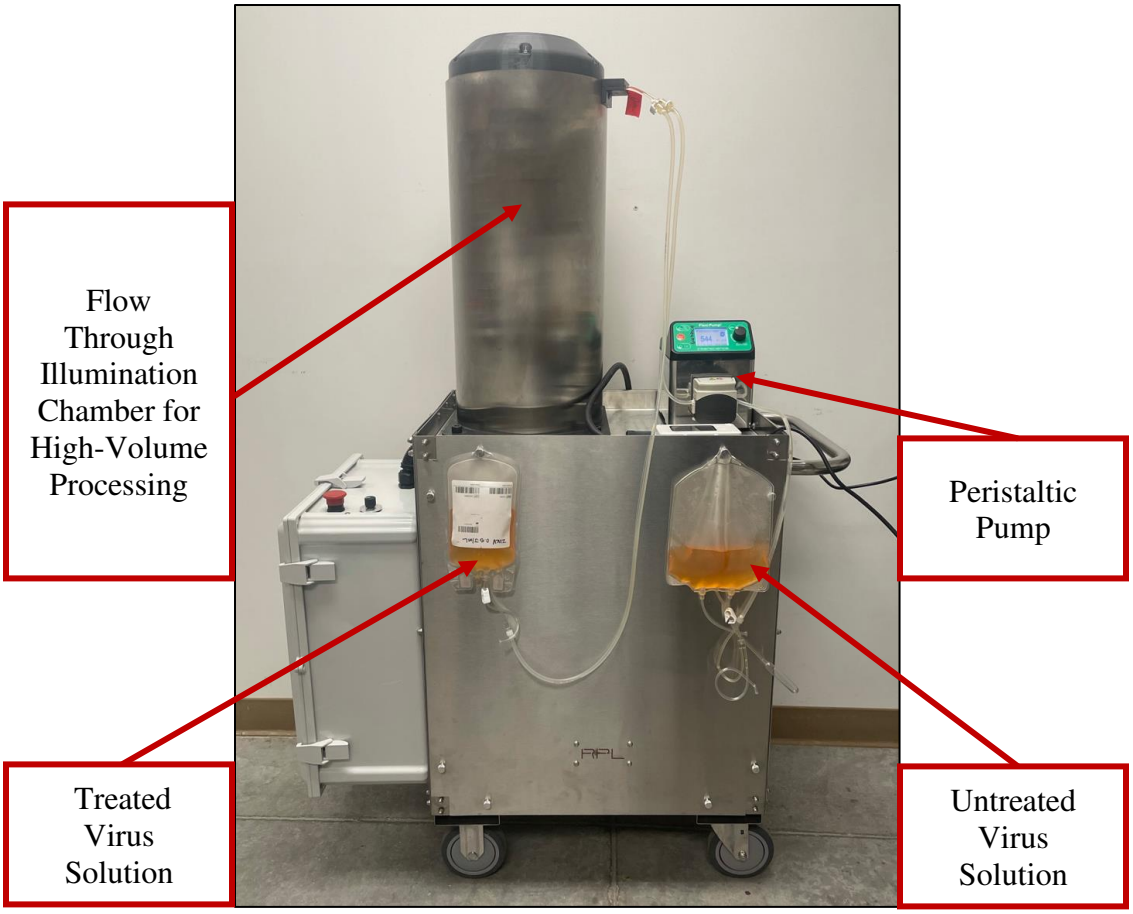

Figure 4.2: The VacciRAPTOR is capable processing approximately 87 liters of viral solution per hour. Active virus flows in solution from the "untreated" reservoir, through the peristaltic pump, into the UV illumination chamber and then out of the chamber and into the "treated" reservoir after receiving a UV dosage of 1.5J/mL.

4.2 General Concept Development

In 2019, the Infectious Disease Research Center (IDRC) and CSU's Energy Institute began working together to develop the high-throughput riboflavin/UV photochemical device for vaccine manufacturing that has the capability of distributed deployment. The device must be able to deliver 1.5 J of UV energy per milliliter of viral solution and have the capacity to treat between 1 L/hr and 150 L/hr. In order to meet the need for distributed deployment, the device's footprint was constrained to be no larger than a shopping cart and able to fit inside of a fume hood.

Figure 4.3 below provides a more detailed illustration of the VacciRAPTOR's treatment process compared to ***Figure 4.2 above***. A peristaltic pump moves the untreated bulk virus and riboflavin solution from a reservoir into a UV-transparent reactor coil. In the reactor coil region, the solution is dosed with the UV energy from broadband phototherapy lamps. Inactivation of the whole virion occurs due to the resulting UV-riboflavin photochemical reaction. From the reactor coil, the solution flows into a "treated" solution reservoir. The treated solution of inactivated, whole virion is now ready for final processing to create the vaccine itself.

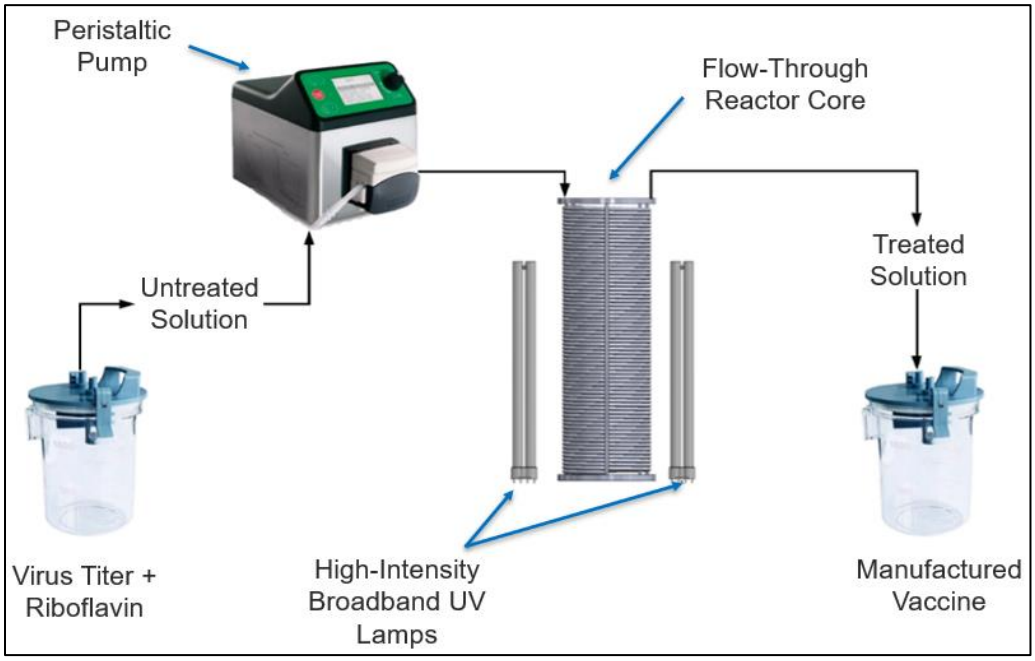

Figure 4.3: Process and Instrumentation Diagram – An untreated solution of virus titer and riboflavin (RB) is pumped from an untreated solution reservoir into the flow-through reactor core. In the reactor core, the virus solution is dosed with high-intensity UV light energy where a photochemical reaction occurs between the UV light, the RB, and the virus. The reaction inactivates the virus (i.e. renders the virus unable to replicate). Ultimately, the inactivated virus solution flows from the reactor core into the treated solution reservoir.

In summary, the initial design concept was simple and broad design criteria were defined. The SolaVAX process, has proven to be effective at producing a COVID-19 vaccine in an animal challenge model, however, the science of the process has not been sufficiently defined to impose strict design criteria for the VacciRAPTOR. The nuances of the SolaVAX process are

being studied in parallel with the design of the VacciRAPTOR flow-through technology. The first iteration of the prototype was designed to meet the following basic design criteria:

1. Illumination source's emission spectra is comparable to that of the Mirasol PRT system
2. High volume, flow-through processing device that can treat up to 150 L/hr while delivering 1.5J/mL of UV radiant energy to a flowing, liquid virion solution
3. Removable, disposable, medical grade UV-transparent tubing and tubing housing (reactor core)
4. Compact footprint (no larger than a large shopping cart) to support ease of distributed vaccine manufacturing
5. Ensure virion solution temperature does not exceed 40°C during the inactivation process.

4.3 Characterization of the Illumination Field and Treatment Capacity

4.3.1 Terms and Definitions

When discussing electromagnetic radiation emission, several terms are interchangeable/synonymous. For example, the terms "irradiance" and "intensity" are synonymous. Both terms refer to the power per unit area of EMR incident on a surface. Further, "radiant flux" and "radiant power" are synonyms which describe the radiant energy per unit time that is emitted, transmitted, reflected, or received by an object. Throughout this paper, the terms "irradiance" and "radiant power" will be used rather than their respective synonyms. For reference, a list of terms and definitions is provided in ***Table 4.1 below***.

Table 4.1: Terms and definitions related to electromagnetic radiation and its measurements.

Term	Symbol	Unit	Definition/Description
Irradiance	E_e	mW/cm^2	Power per unit area of radiation incident on a surface, the power is constant but spread over an area
Intensity	E_e	mW/cm^2	Synonymous with irradiance (less commonly used relative to "irradiance")
Spectral Irradiance	$E_{e,\lambda}$	mW/cm^2/nm	Power per unit area of radiation at a given wavelength
Radiant Flux	Φ_e	mW	Radiant energy per unit time which is emitted, transmitted, reflected or received by an object
Radiant Power	Φ_e	mW	Synonymous with radiant flux (less common than "radiant flux")
Optical Power	Φ_e	mW	Same as radiant power or radiant flux, but is a term specifically for light emission
Radiant Energy	Q_e	J	Electromagnetic radiation energy emitted by a source into the surrounding environment

4.3.2 Key Design Criteria – Treatment Capacity Up to 150 L/hr

Understanding the illumination field is essential for ensuring a successful design that meets the criteria outlined in ***Chapter 4.2***. Initial research on broadband UVB phototherapy lamps revealed that, on average, about 13% of a broadband UVB lamp's rated power consumption is converted to UVB light output at wavelengths between ~280nm and ~320nm [17]. Based on this information, it was assumed that most broadband UVB lamps are 13% efficient at converting electrical power to UVB light emission.

Daavlin 36W phototherapy lamps were chosen during prototype development due to their compact, high output design. Assuming 13% efficiency in converting electrical power consumption to UVB output, a 36W lamp would output approximately 4.7W of UVB radiant power. The following equation was used to approximate the theoretical treatment capacity (i.e. volumetric flow rate) of a single lamp, assuming 100% of the UV radiant power is transferred to

the liquid solution. The approximation indicates that a single lamp can treat 11.3 L/hr with a radiant energy dosage of 1.5 J/mL.

$$Single\ Lamp\ Theoretical\ Treatment\ Capacity = \frac{UVB\ Radiant\ Power\ Emission}{Required\ UVB\ Treatment\ Dosage}$$

$$= \frac{4.7W}{1.5J/mL} = \frac{4.7\ J/s}{1.5\ J/mL} = 3.1\frac{mL}{s} = 11.3\frac{L}{hr}$$

Given the design specification to treat between 1 L/hr and 150 L/hr, the first prototype was constructed using eighteen (18) 36W Daavlin lamps. Assuming 100% of the available UV radiant power transfers into the solution, it was estimated that utilizing 18 lamps would result in a theoretical treatment capacity of up to 203 L/hr while delivering 1.5 J/mL of UV radiant energy.

$$Total\ Theoretical\ Treatment\ Capacity$$

$$= Single\ Lamp\ Treatment\ Capacity * \#\ of\ Lamps$$

$$= 11.3\frac{L}{hr}\ per\ lamp * 18\ lamps = 203\frac{L}{hr}$$

These assumptions were the basis the 18-lamp prototype and estimate a theoretical treatment capacity of about 200 L/hr. Once the prototype's illumination field was built and operational, spectral irradiance measurements of the device's actual illumination field were taken. See ***Chapter 4.3.4*** for a description of the methods used to measure the actual spectral irradiance of the VacciRAPTOR;s illumination field and the calculations that determined the treatment capacity.

4.3.3 Comparing emission spectra between the Mirasol PRT and the VacciRAPTOR

The SolaVAX whole virion inactivation process was developed and validated in batches using the Mirasol PRT system. Since kill kinetics and inactivation pathways will vary depending on the emission spectra of the incident UV radiation, it was important to employ UV lamps in the VacciRAPTOR that have a comparable emission spectrum to that of the lamps in the Mirasol PRT. The emission spectra measurements of the Mirasol PRT and the VacciRAPTOR lamps were taken using the spectrometer shown in ***Figure 4.4***. The spectrometer probe tip was inserted into the illumination chamber of each device while the lamps were illuminated, and measurements were taken.

The emission spectra measurements for each device are compared in ***Figure 4.5 below***. Since the emission profiles are very similar, it can be assumed that the kill kinetics and inactivation pathways are the same in the Mirasol PRT as well as in the VacciRAPTOR. Herein, the VacciRAPTOR inactivation studies can build directly off of the inactivation studies that were performed with the Mirasol PRT throughout the initial development of the SolaVAX method.

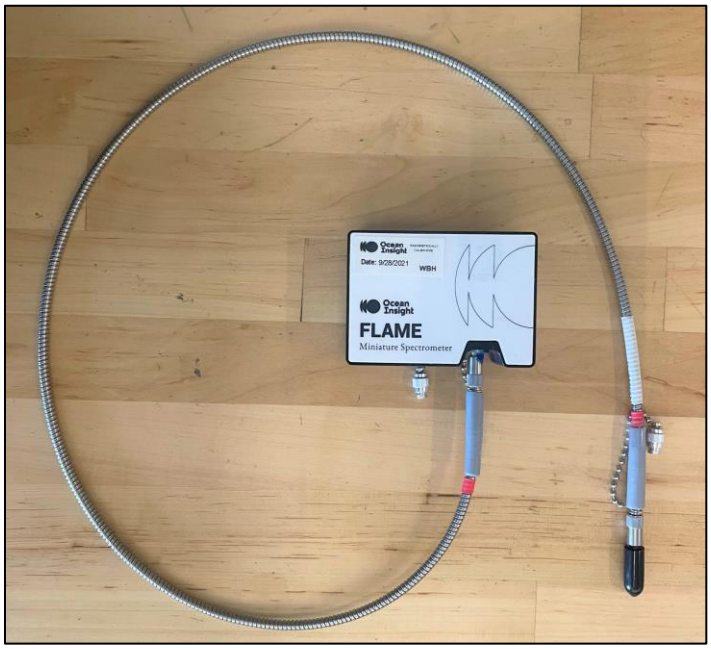

Figure 4.4: Spectrometer used to measure emission spectra.

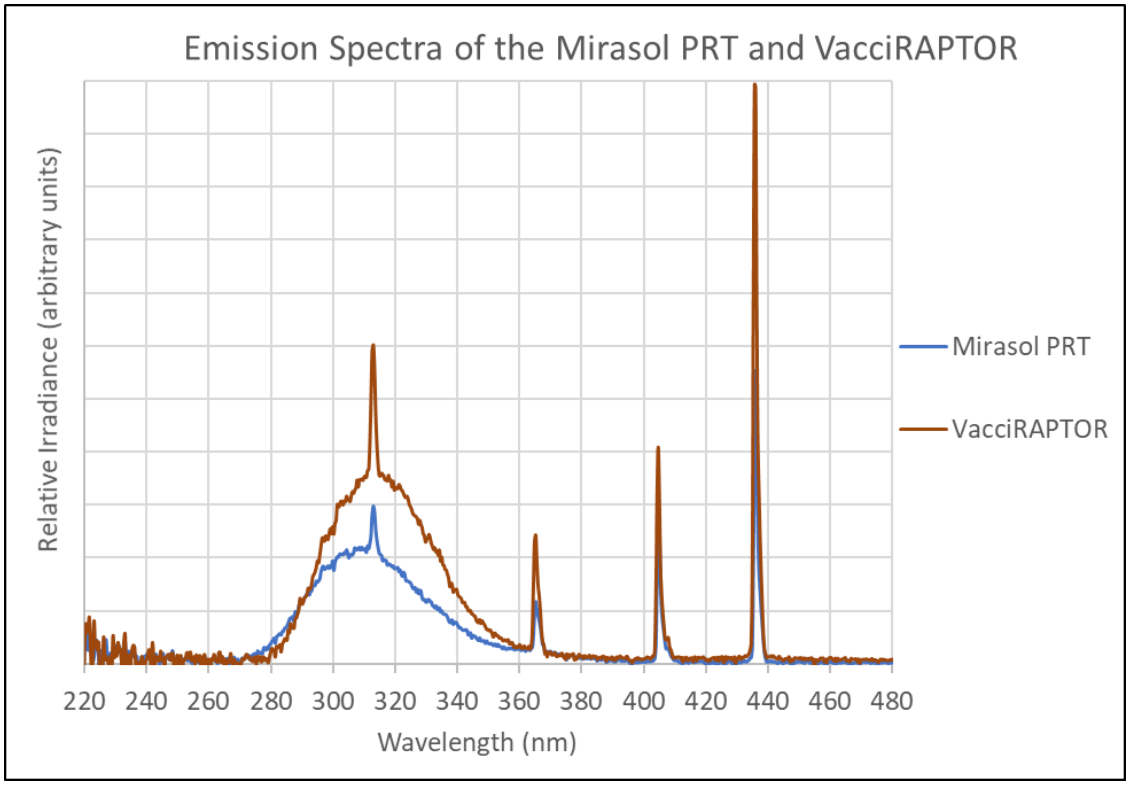

Figure 4.5: Spectral intensity profile comparison between the Mirasol PRT and VacciRAPTOR

4.3.4 Calculating the VacciRAPTOR's Treatment Capacity Given Spectral Irradiance Measurements

To calculate the VacciRAPTOR's true treatment capacity, as opposed to the theoretical treatment capacity calculated in ***Chapter 4.3.2***, the spectral irradiance within the illumination chamber must be measured at the location where the UV radiation intersects the flowing virus solution. ***Figure 4.6 below (left)*** shows the reactor coil is being inserted into the illumination chamber. The red ring in ***Figure 4.6 (right)*** shows where the illumination coil slides in between the inner and outer rings of UV lamps. The reactor coil sits equidistant between the inner ring (4 lamps) and the outer ring (14 lamps). The spectral irradiance of the VacciRAPTOR was measured by removing the reactor coil, inserting the tip of the spectrometer probe into the chamber at the same location as the reactor coil, and recording irradiance with the spectrometer

The measurement was recorded after turning on the lamps and allowing the lamps to reach steady state operating temperatures before recording the measurement.

A single measurement was taken at the midpoint along the length of the illumination chamber. This midpoint measurement may not represent the average spectral irradiance value throughout the chamber. Irradiance gradients are likely present. The irradiance may be greatest at the middle of the lamp and taper as you move away from the center along the length of the lamp. ***Figure 4.7 below*** illustrates a potential irradiance gradient field. The lamps alternate orientation as shown in ***Figure 4.6 (right)***, but it is not known what the actual irradiance gradient looks like. The alternating lamp orientation creates a more compact array and is intended to help resolve non-uniform irradiance emissions along the length of the lamps that are due to lamp orientation. Further work is needed to characterize how irradiance values may vary along the length of the lamps.

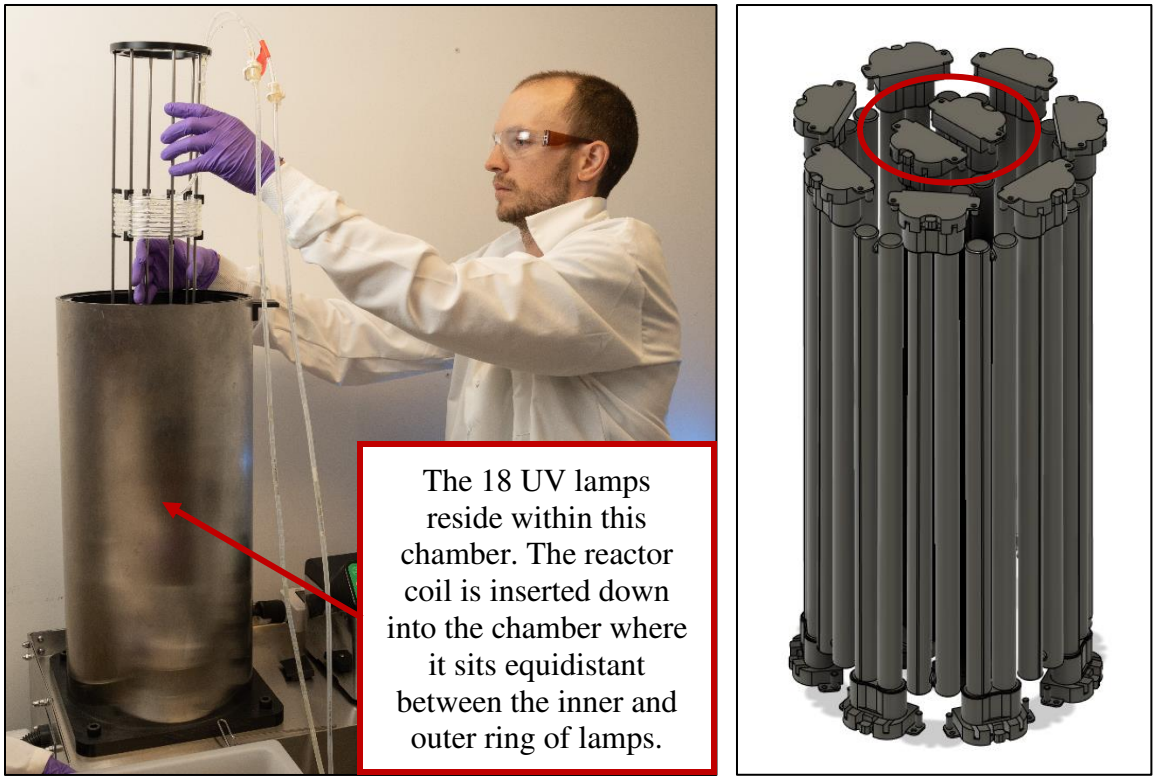

Figure 4.6: High-density lamp package with alternating lamp orientation delivers a compact and uniform high-intensity illumination field.

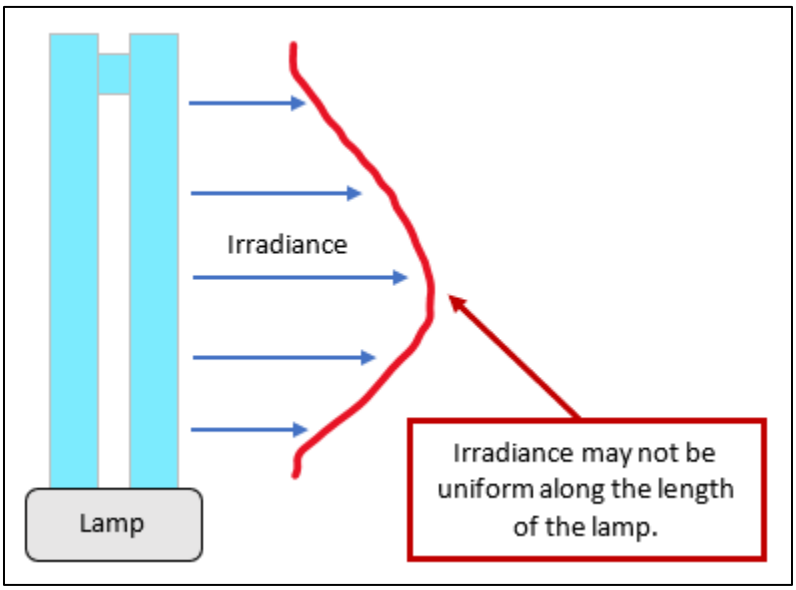

Figure 4.7: Irradiance gradients are likely to exist along the length of the lamp due to edge effects and thermal gradients. Further work needs to be performed to characterize how irradiance may vary along the length of the lamps.

Spectral irradiance is often measured in units of μW/cm^2/nm. The area under this curve is equivalent to the device's irradiance (measured in mW/cm^2). ***Figure 4.8 below*** shows the spectral irradiance profile of the VacciRAPTOR's illumination field. To calculate irradiance (area under the curve), a midpoint Riemann sum was calculated from 220nm to 480nm. The spectrometer utilized (shown in ***Figure 4.4 on page 23***) measures irradiance at even wavelength intervals every 0.385nm. The 0.385nm measurement determined the width of each midpoint Riemann area. The measured irradiance at each wavelength determined the height of each midpoint Riemann area. The total irradiance between 220nm and 480nm for the VacciRAPTOR it is 20.6 mW/cm^2.

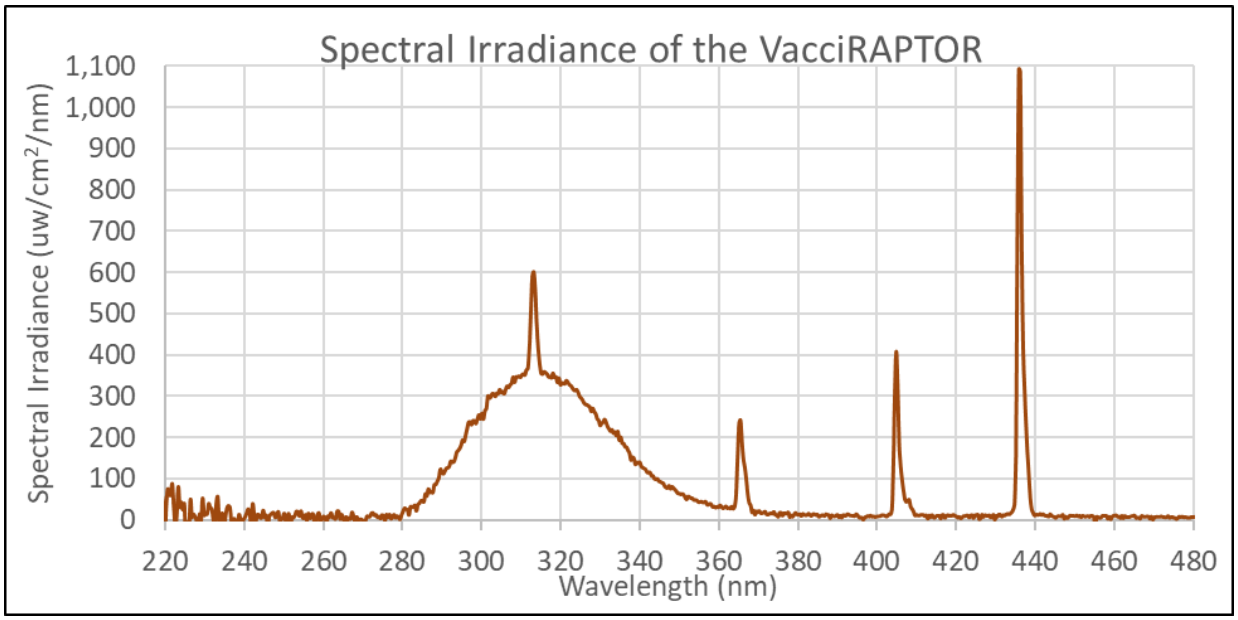

Figure 4.8: Spectral irradiance of the VacciRAPTOR's illumination chamber.

It is important to note that due to the limitations of the spectrometer and the narrow geometry of the VacciRAPTOR, the spectral irradiance measurement was taken parallel to the orientation of the UV lamps. Measuring spectral irradiance parallel to lamp orientation, as opposed to perpendicular, yields a conservatively low irradiance amplitude at each wavelength.

To understand how conservative parallel irradiance measurements are relative to perpendicular measurements, the irradiance of a single Daavlin 36W broad-spectrum UVB lamp was measured parallel to the lamp and perpendicular to the lamp. The perpendicular irradiance measurement was 2.8 times greater than the parallel measurement. It is theorized that the true irradiance of the VacciRAPTOR is bound between 20.6mW/cm^2 (parallel) and 2.8 times that at 57.7mW/cm^2 (perpendicular).

Once irradiance is calculated, the radiant power (mW) of an illumination field can be determined by multiplying irradiance by the surface area of the object receiving the irradiance. In this case, the surface receiving the incident irradiance is the surface area of the tubing coil. As shown by ***Figure 4.9 below***, the tubing coil forms a cylinder whose diameter is 13.0cm (center-to-center) and height is 43.0cm. The tubing coils incident surface area was approximated by treating the tubing coil as an infinitely thin cylinder with a height of 43cm and a diameter of 13cm. Given these dimensions, the surface area is approximately 1,756cm^2. Multiplying the coil surface area by the VacciRAPTOR's irradiance and rounding to three significant figures results in a calculated radiant power of 36,200mW (parallel) and 101,000mW (perpendicular).

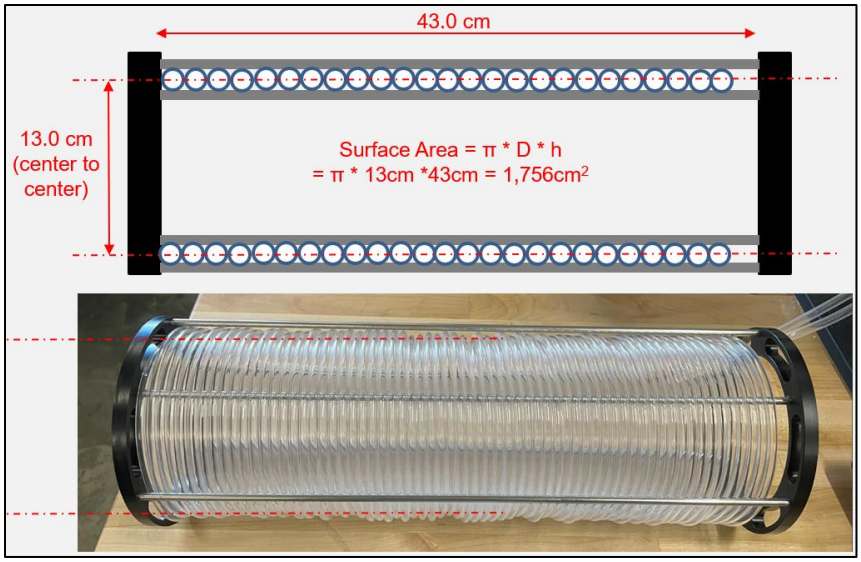

Figure 4.9: Approximating the tubing coil surface area as a smooth cylinder that is 43cm high and has a diameter of 13cm.

Treatment capacity (i.e. volumetric flow rate) can be determined based on the required radiant energy dosage per unit volume of solution that flows through the device. Recalling the design criteria outlined in ***Chapter 4.2***, inactivating whole virion in solution with riboflavin under a broad-spectrum UVB illumination field, requires roughly 1,500 Joules of radiant energy to be delivered to each liter of virus solution. By converting irradiance units from mW to J/hr and dividing by the radiant energy dosage rate of 1,500J/L, the treatment capacity is estimated to be between 87L/hr (parallel) and 242L/hr (perpendicular), assuming 100% of the radiant power is delivered to the solution. Treatment capacity equations and calculations are provided below.

$$\boldsymbol{Irradiance} = area\ under\ the\ spectral\ irradiance\ curve$$

$$(approximated\ using\ midpoint\ Riemann\ sum)$$

$$= \left(20.6\frac{mW}{cm^2}\right)_{parallel\ measurment} to \left(57.7\frac{mW}{cm^2}\right)_{perpendicular\ measurment}$$

$$\boldsymbol{Incident\ Surface\ Are} = total\ surface\ area\ that\ receives\ incident\ irradiation$$

$$= \pi \times diameter \times height = \pi \times 13.0cm \times 43cm = 1{,}756cm^2$$

$$\boldsymbol{Radiant\ Power} = radiant\ energy\ per\ unit\ time\ that\ is\ emitted\ by\ an\ object$$

$$= Irradiance \times Incident\ Surface\ Area$$

$$= \left[\left(20.6\frac{mW}{cm^2}\right)_{parallel}\ to\ \left(57.7\frac{mW}{cm^2}\right)_{perpendicular}\right] \times 1{,}756cm^2$$

$$= 36{,}200\ mW_{parallel}\ to\ 101{,}000mW_{perpendicular}$$

$$\boldsymbol{Treatment\ Capacity_{lower\ bound}} = \boldsymbol{Treatment\ Capacity_{parallel}}$$

$$= Irradiance \times Incident\ Surface\ Area \times \frac{1}{Radiant\ Energy\ Dosage}$$

$$= 36{,}200mW \times \frac{1}{1.5\ {}^{J}/_{mL}} \times \frac{1\,J}{1{,}000mJ} \times \frac{60sec}{1min} \times \frac{1mL/min}{16.67L/hr} = 87\frac{L}{hr}$$

$$\boldsymbol{Treatment\ Capacity_{upper\ bound}} = \boldsymbol{Treatment\ Capacity_{perpendicular}}$$

$$= 101{,}000mW \times \frac{1}{1.5\ {}^{J}/_{mL}} \times \frac{1\,J}{1{,}000mJ} \times \frac{60sec}{1min} \times \frac{1mL/min}{16.67L/hr} = 242\frac{L}{hr}$$

In summary, the upper and lower bounds of the VacciRAPTOR's treatment capacity, as calculated above, indicate that design criteria requiring a treatment capacity of up to 150L/hr is within the bounds of the estimated upper and lower treatment capacity. The terms "treatment capacity" and "volumetric flow rate" are synonymous in this context. In other words, a treatment

capacity of 87L/hr means that to deliver 1.5J of UV energy to each mL of viral solution that flows through the device, the viral solution must flow at a volumetric flow rate of 87L/hr. The upper and lower bound treatment capacities calculated above do not account for UV transmittance losses through the tubing that houses the flowing solution.

4.4 Design and Characterization of The Reactor Coil

4.4.1 What is the Reactor Coil

As mentioned in ***Chapter 4.2***, the reactor coil is a helically coiled tube and housing assembly that gets inserted into the illumination field of the VacciRAPTOR. The reactor coil is designed to be removable and disposable after use. As shown in ***Figure 4.3 on page 19***, viral solution is pumped from a reservoir and into the reactor coil where the solution is receives high intensity UV electromagnetic radiation energy. The solution then exits the illumination field and enters a reservoir of treated solution. The reactor coil tubing is made of highly UV-transparent tubing known as THV (tetrafluoroethylene hexafluoropropylene vinylidene fluoride).

4.4.2 Key Design Criteria – Material Selection for UV-Transparency, Medical Grade, Chemical Resistance, and Appropriate Working Temperature Tolerance

THV most readily meets the needs of the key design criteria that were defined for the reactor coil. The key criteria are high UV-transparency, medical grade, good chemical resistance, and a working temperature that is sufficiently high to withstand maximum operating temperatures. The working temperature of THV is 150°C which is well above the maximum air temperature experienced within the VacciRAPTOR's illumination field (~30°C). The tubing is available in a variety of medical grade options and is reported to have good chemical resistance.

In order to test the UV transmittance through the tubing, the fixture in ***Figure 4.10 below*** was designed. The fixture clips onto the same type of lamp as those used in the VacciRAPTOR. The spectrometer insertion ports are sized to snugly fit the diameter of the spectrometer probe tip and block ambient light. The fixture ensures that the probe measures spectral irradiance at a constant angle and constant distance from the light source during testing. The spectrometer measurements are very sensitive to distance and angle. Two tubing insertion ports are on top of the fixture. The tubing can be inserted either in a double or single wall configuration. For the single-wall insertion port, a portion of the tubing is removed circumferentially, and the remainder is inserted into the port. The port maintains the original curvature of the tubing. ***Figure 4.11 below*** shows two tubing samples. The top tube sample is trimmed to test single-wall transmittance. The bottom tube sample is untrimmed to test double-wall transmittance.

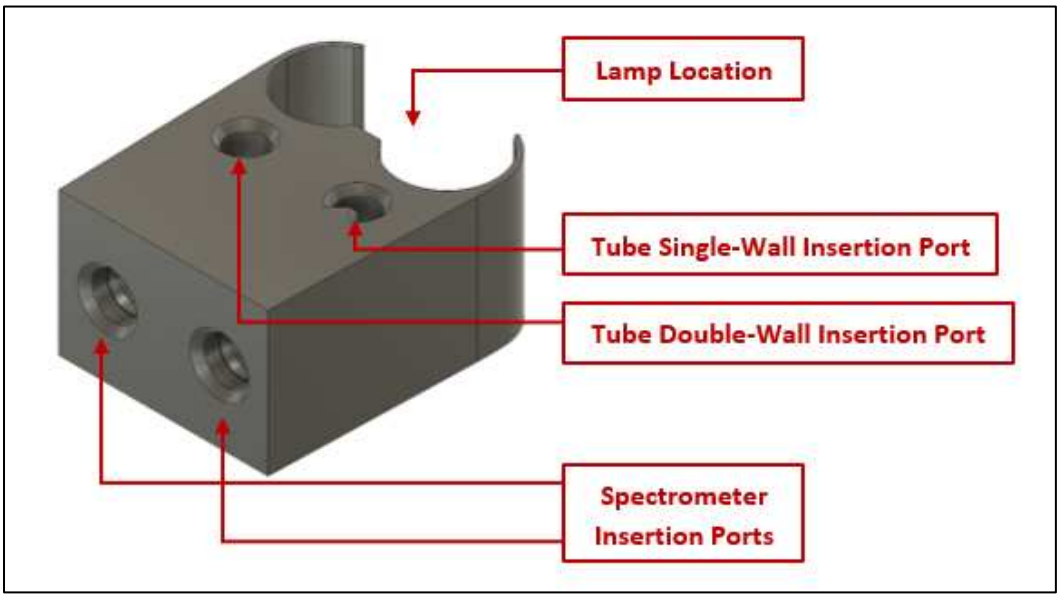

Figure 4.10: The specially designed lamp clip ensured constant measurment angle, distance, and blocking of ambient light during UV-transmission testing.

Figure 4.11: The top tube sample is trimmed for insertion into the single-wall insertion port. The bottom tube sample is untrimmed for double-wall transmittance testing.

The transmittance spectra curves are shown in ***Figure 4.12 below***. The control measurement (blue line) represents 100% UV transmittance. The measurement was taken without any tubing in the fixture. The next most prominent line (red line) shows the UV transmittance through THV. THV demonstrates the highest UV transmittance at 82%. UV transmittance, THV tubing was the best performer. The second-best performing tubing was PFA (perfluoroalkoxy) at 49% (grey line). The illumination bag UV transmittance was comparable to the PFA at 50% (yellow line). ***Table 4.2 below*** summarizes the results for all of the materials tested. At 82% transmittance, the THV exhibited much greater transmittance than any of the other materials. The second-best performer was PFA (perfluoroalkoxy) at 49%.

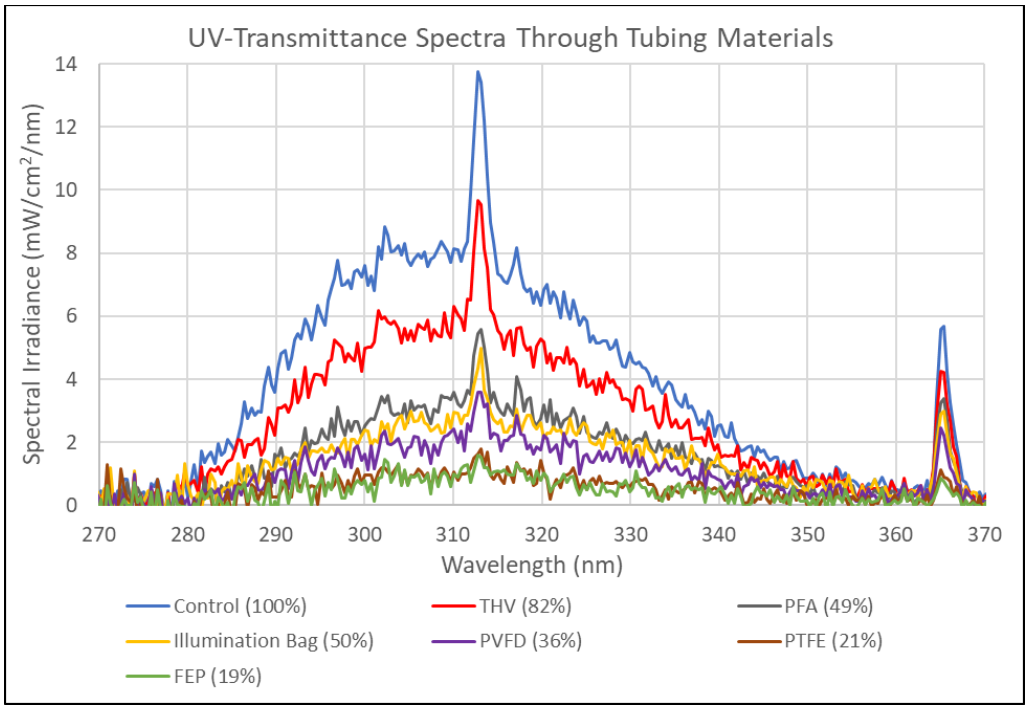

Figure 4.12: Percent UV-transmittance is based on the calculated area (midpoint Riemann approximation) under each curve between 220nm and 480. For clarity and relative comparison of transmittance, the graph is zoomed in to compare irradiance transmittance between 270nm and 370nm. The transmittance spectra for each tubing material do not exhibit shifting in the spectra curves.

Table 4.2: Percent UV transmittance through a single wall of various medical grade tubings.

Material	Polymer Name	Wall Thickness (mm)	Transmission %
Control	No material	n/a	100%
THV	Tetrafluoroethylene Hexafluoropropylene Vinylidene Fluoride	1.2	82%
PFA	Perfluoroalkoxy	1	49%
Illumination Bag	Material type not determined	0.4	50%
PVFD	Polyvinylidene Fluoride	1	36%
PTFE	polytetrafluoroethylene	1	21%
FEP	Fluorinated Ethylene Propylene	1	19%

It was also important to see if there was a shift in the spectra as a result of transmitting the lamp's UV light through the material. In all cases, as seen in ***Figure 4.12 above***, there was only a reduction in the overall irradiance, no significant spectral shifting was exhibited. In other

words, the area under the curve (irradiance) decreased, but the shape of the spectral intensity curve was unaffected.

4.4.3 Reactor Coil Scalability and its Influence on Treatment Capacity

The reactor coil is designed to be highly scalable so that the treatment capacity of the unit itself can be scaled simply by adjusting the size of the reactor coil. The chamber can accommodate a helically coiled tube that is up to 43cm in height. The largest helical tubing coil is illustrated on the left of ***Figure 4.13 below***. Treatment capacity is directly proportional to the tubing coil size. A large coil provides a long path of tubing for the liquid solution to traverse within the illumination field while a smaller coil provides a sorter path. Since the radiant power output is constant, the volumetric flow rate must be adjusted proportionally to the length of the tubing within the chamber in order to not over- or under-dose a solution with radiant energy. A longer path increases the treatment capacity (i.e. volumetric flowrate) while a shorter path decreases the treatment capacity.

Figure 4.13: Images of the scalable reactor coil design (left = full size, middle = quarter size, right = eighth size). Treatment capacity of the VacciRAPTOR scales directly with the size of the tubing coil. Larger coils allow for greater treatment capacities than smaller coils.

In ***Chapter 4.3.3***, the upper and lower bound treatment capacities of the device were calculated for a full-size coil (43cm height) and assumed that 100% of the UV radiant energy emitted by the lamps reached the liquid. Adjusting for 82% UV-transmittance through the THV tubing, the upper and lower bound treatment capacities reduce from 242 L/hr and 87 L/hr to 199 L/hr and 71 L/hr, respectively for a full-size coil. Images of full, quarter, and eighth-size coils are shown in ***Figure 4.13 above***. A "full size" coil covers the entire coil housing height while a "quarter coil" covers only one quarter of the housing height and an "eighth coil" covers 1/8th of the height. Each helix is wrapped so that it is centered between the top and bottom of the black coil housing endcaps.

Going forward, this report will only use the "parallel" radiant power and corresponding "lower bound" treatment capacity calculated in ***Chapter 4.3.3***. The "perpendicular" radiant power and corresponding "upper bound" treatment capacity calculated in ***Chapter 4.3.3*** is theoretical and was not directly measured with the spectrometer. As a result, the theoretical "perpendicular" radiant power value will not be carried into the remainder of this report. The "parallel" radiant power and corresponding "lower bound" treatment capacity is anchored to a direct spectrometer measurement. To maintain a conservative radiant power and treatment capacity estimate and to anchor associated metrics to actual measurements, only the "parallel" radiant power (36,200mW) and corresponding "lower bound" treatment capacity (87L/hr) will be considered throughout the remainder of this report.

Treatment capacity is a function of reactor coil size. ***Table 4.3 below*** tabulates the relationship between coil size and treatment capacity. Note in ***Table 4.3*** that the reported treatment capacities are adjusted to account for 82% UV transmittance through the THV tubing coil. Recall that the Mirasol PRT System has a treatment capacity of approximately 7L/hr. When compared to a full-size reactor coil, the VacciRAPTOR's treatment capacity is approximately 10x greater than the Mirasol PRT System.

4.4.4 Fluid Dynamics Within the Helical Reactor Coil (Critical Reynolds Number, Reynolds number, and Pressure Drop)

In terms of fluid dynamics, volumetric flow rate and flow path geometry directly influence the critical Reynolds number, Reynolds number, and pressure drop within the helical reactor coil. ***Table 4.3 below*** summarizes the relationship between coil size, treatment capacity,

pressure drop, Reynolds number, and vaccine dose production rate. The vaccine dose production rate is discussed in ***Chapter 4.4.5.***

Table 4.3: Coil size directly influences treatment capacity, pressure drop, Reynolds number, and vaccine does production rate. Note that the pressure drop and Reynolds number calculations apply to the helical tubing section only. They do not apply to the liquid flowing from the untreated solution reservoir to the helix or the liquid flowing from the helix exit to the treated solution reservoir.

Coil Dimensions			*Treatment Capacity (flow rate)		Pressure Drop (in helix only)	Reynolds Number (Re_{cr} = 6,411)	Vaccine Dose Production Rate
Coil Size	Portion of Full Size	No. of Coils					
	%	#	mL/min	L/hr	kPa	unitless	doses/hr
Full size	100%	65	1,187	71	390	4,860	102,000
3/4 size	75%	49	891	53	195	3,650	76,000
1/2 size	50%	33	594	36	73	2,430	51,000
1/4 size	25%	16	297	18	14.0	1,220	25,000
1/8 size	12.5%	8	148	9	2.77	608	13,000

*Treatment capacities are adjusted to account for 82% UV transmittance through the tubing coil

When discussing fluid dynamics, an essential characteristic is the critical Reynolds number (Re_{cr}). The critical Reynolds number defines the approximate value at which fluid flow characteristics transition between laminar and turbulent flow. At $Re < Re_{cr}$, the fluid is assumed to exhibit laminar flow behaviors while at $Re > Re_{cr}$, the fluid is assumed to exhibit turbulent flow behaviors. Near the critical Reynolds number, the fluid may exhibit transitional flow characteristics where the flow is neither entirely laminar nor turbulent. The critical Reynolds number is strongly dependent on surface roughness, disturbances such as tube fittings and connections, and overall geometry.

For straight, smooth tubes, the critical Reynolds number is 2,300 while for helically coiled smooth tubes, the critical Reynolds number increases and depends on the ratio between the helix's diameter (D) and the tube's inner diameter (d) as shown in the equation below [18]. The critical Reynolds number is higher for helically coiled tubes than straight tubes due to the secondary flow behavior and centrifugal forces that occur in the curved tubes [18]. Given the same inside diameter of either a straight tube or a helically coiled tube, the volumetric flow rate

(Q) must be greater in a helically coiled tube to overcome the centrifugal forces within the secondary flow to transition from laminar to turbulent behavior. Schmidt proposes the following correlation for determining the critical Reynolds number in helically coiled, smooth tubes [19]:

$$Re_{cr} = 2{,}300\left[1 + 8.6\left(\frac{d}{D}\right)^{0.45}\right] = 2300\left[1 + 8.6\left(\frac{0.396cm}{13.0cm}\right)^{0.45}\right] = 6{,}410$$

where

Re_{cr} = critical Reynolds number correlation for flow in a helical coil

d = tube inside diameter = 0.396cm

D = helix diameter = 13.0cm

The Reynolds number is a unitless measure of the ratio between inertial forces and viscous shear forces within the flowing fluid. The equation for Reynolds number for fluid flow in a tube of constant cross-sectional area is as follows:

$$Re = \frac{4Q}{\pi d\nu}$$

where

Q = volumetric flow rate

d = tube inside diameter = 0.396cm

ν = dynamic viscosity of the fluid = 1.31x10^{-6} m^2/s (assumes water at 10°)

Table 4.3 above lists the Reynolds number value for several coil sizes from a full-size coil to a 1/8th-size coil. Note that the maximum Reynolds number is estimated to be 4,860 which is about 24% lower than the estimated critical Reynolds number of 6,411. Since the estimated

maximum Reynolds number is about 24% lower than the critical Reynolds number for flow in the helically coiled reactor core, the calculations indicate that the flow is laminar in the helix for all coil sizes. A graphical representation of the treatment capacity as it compares to the Reynolds number for various flow rates is presented in ***Figure 4.14 below***. Note that at its maximum, the Reynolds number (orange line) remains well below the critical Reynolds number for a helical tube (yellow line). If the tubing were linear as opposed to helically coiled, the flow characteristics are likely to transition from laminar to turbulent flow at approximately 550mL/min (intersection of the orange and grey lines).

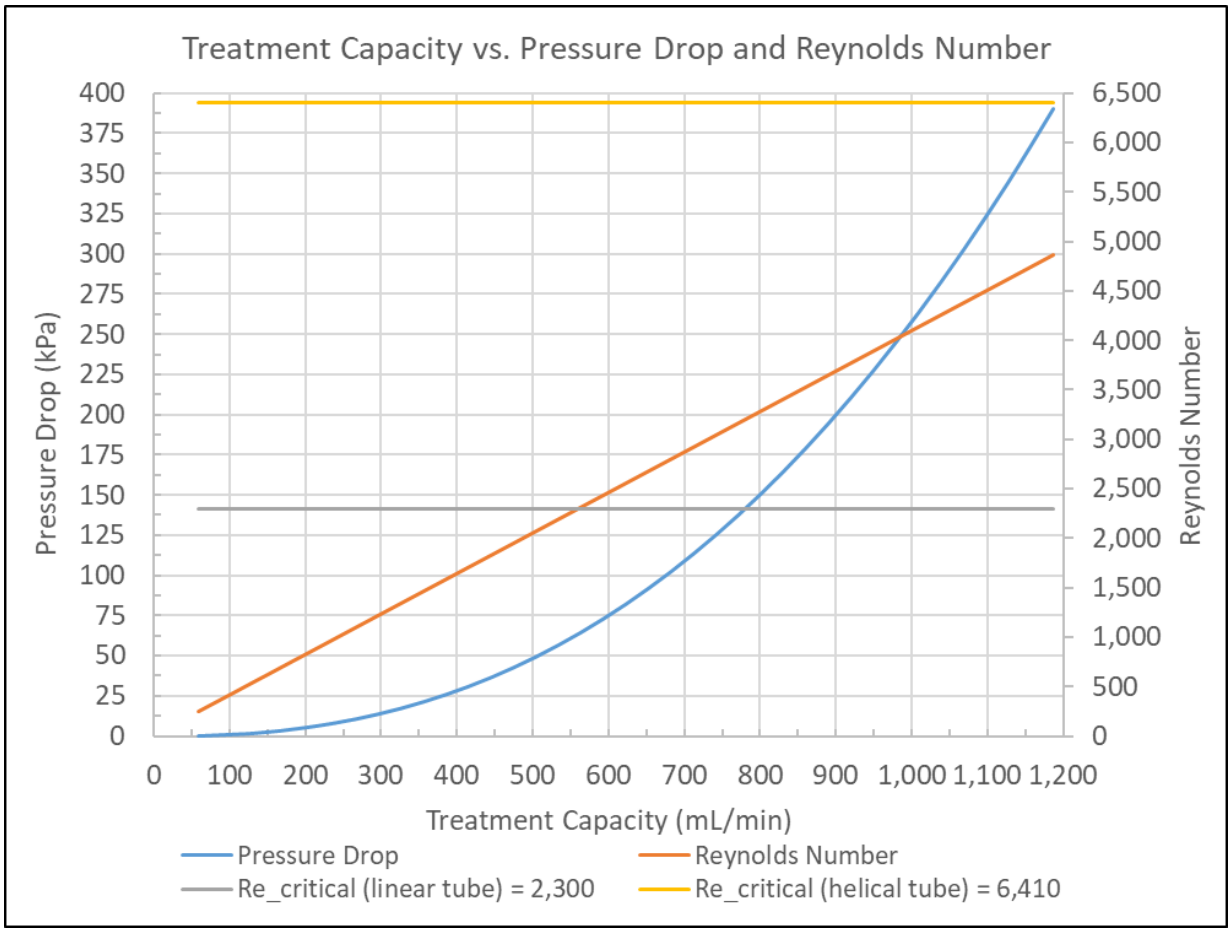

Figure 4.14: Characterizing pressure drop and Reynolds number as a function of treatment capacity for flow within the reactor coil's helically wrapped tubing.

Another important fluid dynamic characteristic to understand is pressure drop through the coil. Several equations can be found in literature that are used to calculate pressure drop in a helically coiled tube. One form of the pressure drop equation is provided below. This form of the equation incorporates a friction factor which, similar to the critical Reynolds equation above, is dependent upon the ratio of diameters (d/D). According to Grundmann and Gneilinski, a helically coiled tube's friction factor (λ) and pressure drop (ΔP) are best calculated by the following equations [18, 20]. Note that the equation for λ used here applies to laminar flow only.

$$\lambda = friction\ factor = \frac{64}{Re}\left[1 + 0.033\left(\log Re\sqrt{\frac{d}{D}}\right)^4\right]$$

$$\Delta P = pressure\ drop = \frac{8\rho}{\pi^2}\frac{\lambda l}{d^5}Q^2$$

where

$d = tube\ inside\ diameter$

$D = helix\ diameter$

$\rho = fluid\ density$

$l = uncoiled\ length\ of\ the\ spiral\ tube$

$Q = volumetric\ flow\ rate = treatment\ capacity$

Referencing ***Table 4.3 on page 38***, numerical values for the pressure drop calculations for various coil sizes are provided. The blue curve in ***Figure 4.14 on page 40*** graphs pressure drop as a function of flow rate. Note that the VacciRAPTOR's treatment capacity (i.e. flow rate) with a full-size coil is 71L/hr and the VacciRAPTOR's treatment capacity with a 1/8th-size coil is

9L/hr. Since pressure drop is directly proportional to tube length and treatment capacity-squared, small increases in coil size and treatment capacity greatly increase the pressure drop through the coil. For an $1/8^{th}$ size coil, the pressure drop is only about 3kPa (~0.4psi) while it is nearly 400kPa (~58psi) for the full-size coil. Further work is required to understand if subjecting viruses to 400kPa and shear forces associated with flow rates of 71L/hr will damage a virus's structure and yield an antigen with reduced potency due to this damage. Additionally, there is greater risk of tubing connection failure or leaks at 400kPa.

4.4.5 Estimating Vaccine Dose Production Rate Given Treatment Capacity

The vaccine dose production rate is defined as the rate at which a single human vaccine dose can be generated by the device. The VacciRAPTOR's estimated vaccine dose production rates are provided in ***Table 4.3 on page 38***. The number of doses per volume of treated whole virion solution depends on the virus type and the required concentration of whole virion particles per dose.

For a human-sized vaccine dose produced using the SolaVAX method for SARS-CoV-2, it is estimated that the dosage concentration should contain roughly $7x10^8$ virions per dose and the concentration of the virion solution treated by the VacciRAPTOR should have a concentration of $1x10^9$ virions per mL. Given the VacciRAPTOR's maximum treatment capacity of ~1,190mL/min, the device is capable of producing approximately 102,000 SARS-CoV-2 vaccine doses per hour. In other words, it is estimated that a single VacciRAPTOR can produce approximately 1,000,000 vaccine doses in 10 hours. The steps for approximating the VacciRAPTOR's vaccine dose production rate are outlined below.

Given

$$Human\ vaccine\ viral\ concentration = HVVC = \ 7x10^{8}\frac{virions}{dose}$$

and

$$Virion\ solution\ concentration = VSC = 1x10^{9}\frac{virions}{mL}$$

and

$$Treatment\ Capacity = TC = 1{,}187\frac{mL}{min} \cong 71{,}400\frac{mL}{hr}$$

then

$$Vaccine\ Dose\ Production\ Rate = \frac{VSC}{HVVC} \times TC = \frac{1x10^{9}\frac{virions}{mL}}{7x10^{8}\frac{virions}{dose}} \times 71{,}400\frac{mL}{hr}$$

$$\cong 102{,}000\frac{doses}{hr}$$

4.5 Thermal Management

4.5.1 Thermal Management System Background and Overview

A significant thermal load is generated during operation due to the (18) 36W UV-lamps. The UV-lamps are arranged in a compact enclosure. The most thermally sensitive components of the VacciRAPTOR are the UV-lamps and the liquid pathogen solution that flows through the reactor coil. If the lamps get too hot, damage and premature failure may result. If the liquid pathogen solution gets too hot, this may cause unwanted damage to the structure of the pathogen as it flows through the device.

Figure 4.15 below illustrates the annular cooling channels that are designed into the top and bottom of the illumination chamber to permit airflow during operation. ***Figure 4.16*** shows the VacciRAPTOR's overall forced air convection cooling configuration. Air enters the device through a large white register, flows through a blower, and is directed up into the annular cooling channels of the illumination chamber. On top of the illumination chamber is the grey "top cap". The top cap is an essential component that prevents harmful UV light from exiting the device and contacting the operator's eyes and skin. The top cap blocks UV light while allowing air to flow through the illumination chamber.

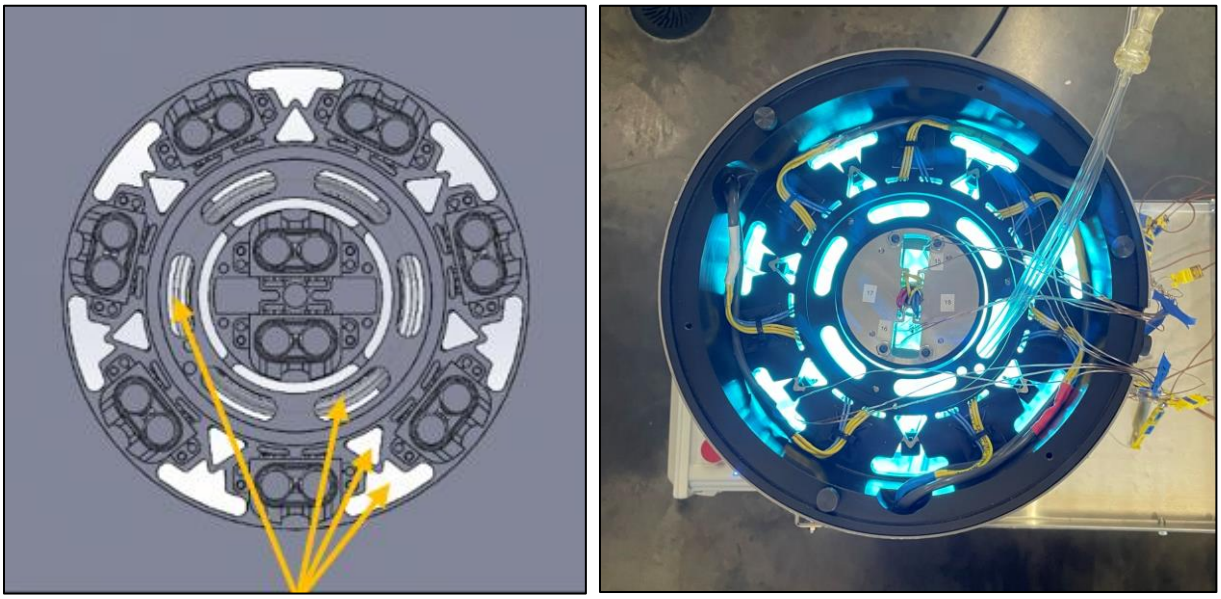

Figure 4.15: Annular cooling channels were added to the design above and below the illumination chamber to permit forced air flow across the lamps. The yellow arrows (left) show the channels in a CAD rendering. The sapphire light (right) showing

through the actual device illuminates the flow path where photons and air exit the illumination chamber. Note that the top cap is not shown in the images.

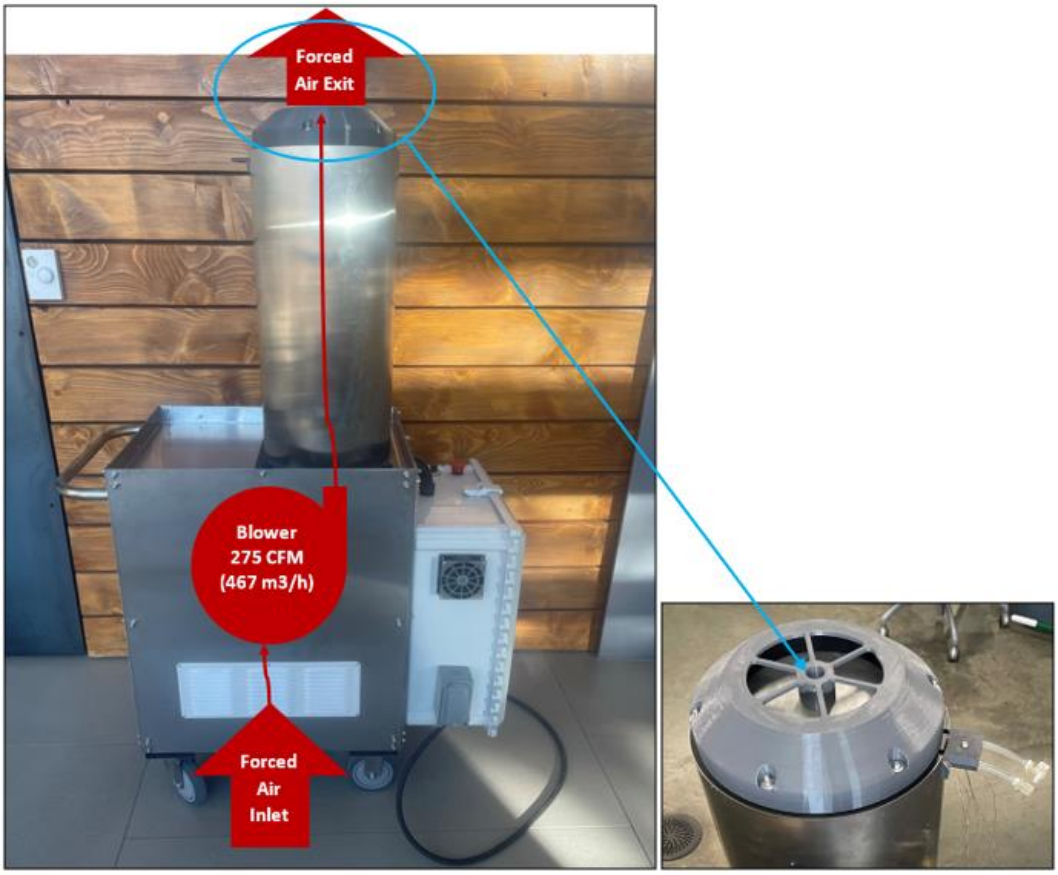

Figure 4.16: Forced air convective cooling configuration of the VacciRAPTOR (left) with a closeup image of the exit configuration. The exit configuration minimizes the amount of harmful UV light that exits the device while permitting sufficient cooling airflow.

An isometric cross-sectional view of the final top cap design is provided in ***Figure 4.17 below***. This is the same top cap as the one shown in the lower right of ***Figure 4.16 above***. Notice that there are channels that permit airflow (roughly illustrated by the blow arrows) and surfaces that minimize light emission from the illumination chamber (green arrows).

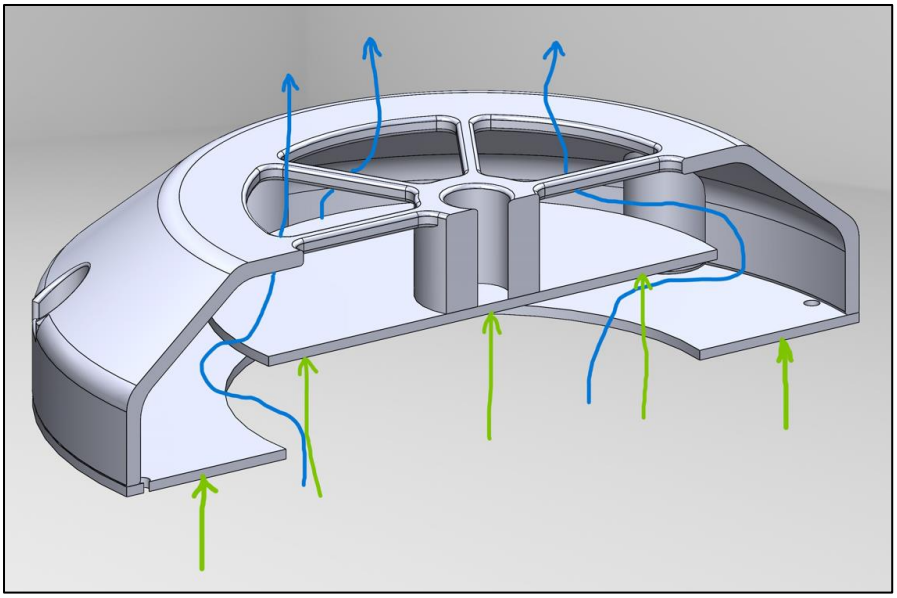

Figure 4.17: Top cap isometric cross-sectional view (blue lines illustrate air flow paths, green lines illustrate where direct UV radiation transmission is blocked by a black plate whose diameter is greater than the diameter of the opening below it).

4.5.2 Forced Air Convective Cooling of the UV Lamps

The VacciRAPTOR's thermal management system, primarily the blower/fan sizing and the top cap geometry, has undergone several design iterations in the process of balancing the need cool the lamps while simultaneously minimizing harmful UV radiation from escaping from the top of the device. It is challenging to prevent photons (UV light) from escaping from the device without restricting the airflow that is needed to provide forced air convective cooling.

To protect the lamps from premature failure due to high operating temperatures, the goal of the thermal management system was to provide enough cooling so that the lamps would maintain an average temperature within the illumination chamber that was equivalent to or less than the average operating temperature of a single lamp operating in open air and in a quiescent room with 20°C ambient air. Thermocouples, as shown in ***Figure 4.18 below***, were attached to the base, middle, and top of lamps that operated in an open, quiescent room (left) and to many of lamps within the illumination chamber (right).

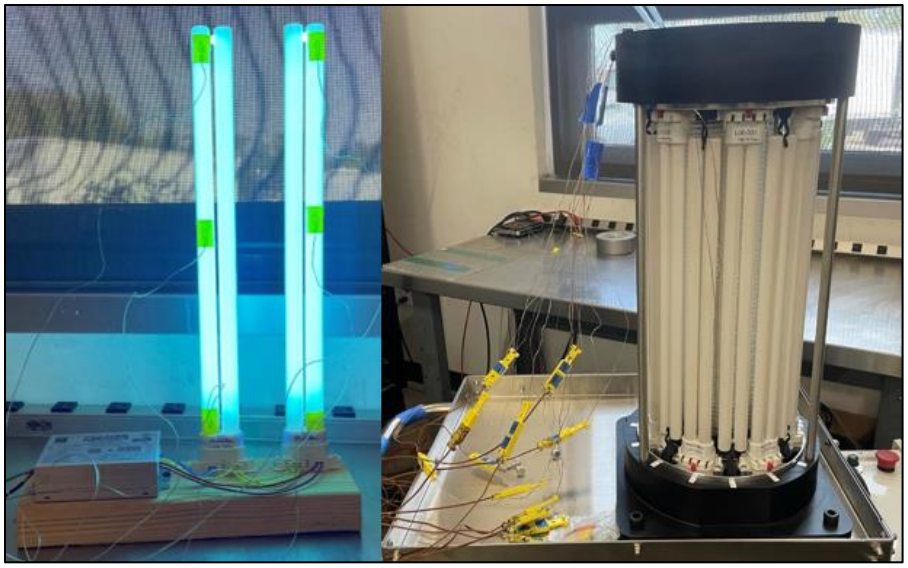

Figure 4.18: Lamp temperature measurements were recorded by attaching several stick-on thermocouples to the surface of several lamps. The left image shows the lamps operating in an open quiescent space. The right image shows the lamps in the illumination chamber being equipped with thermocouples.

After empirically testing several smaller blowers and various top cap geometries, a blower with a volumetric flowrate rating of 275CFM[1] (467 m^3/h) provided sufficiently high volumetric air flow to maintain the lamps at an acceptable operating temperature. A blower was chosen rather than an axial fan with an equivalent volumetric flowrate rating because blowers operate more quietly and produce higher pressures than axial fans of the same flowrate rating.

Figure 4.19 below compares the average operating temperature of the lamps in an open, quiescent room to the average operating temperature of the lamps in the illumination chamber while 20°C ambient air is blown through the chamber with a 275CFM blower. Since the average operating temperature of the lamps in the VacciRAPTOR is approximately equal to the average operating temperature of the lamps in an open room, there is confidence that the lamp temperature thermal management will prevent premature lamp failure due to overheating.

[1] Dayton blower, model 3HMH7

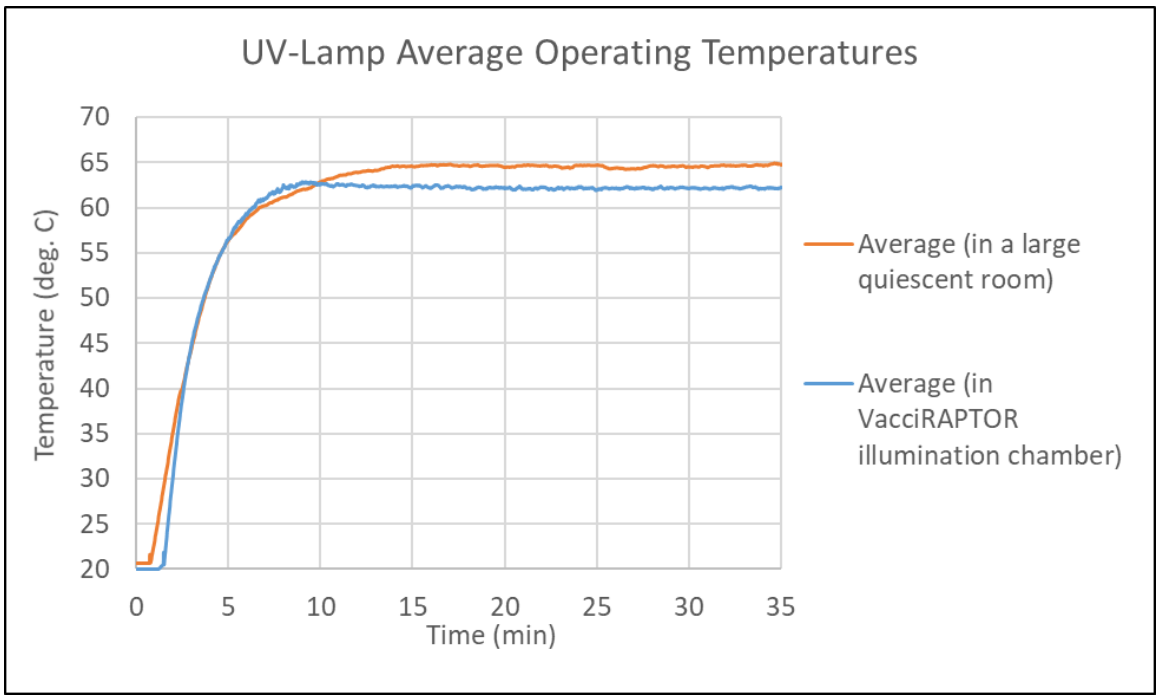

Figure 4.19: Comparing the average lamp operating temperature when the lamps are in an open, quiescent room and when they are in the VacciRAPTOR with the best-performing top cap and 275CFM blower shows that the lamp temperatures are approximately the same. This indicates that the forced air convection system maintains the lamps at a safe operating temperature.

4.5.3 Quantifying the Amount of Heat Rejected by the Forced Air Cooling System

Heat rejection ($\dot{Q}$) through forced air convection, as shown in the equation below, is a function of the mass flow rate of air ($\dot{m}$), specific heat (C_p), and the change in air temperature from the inlet to the exit (ΔT). The mass flow rate of air ($\dot{m}$) is equal to the air density (ρ) times the volumetric flow rate of air (Q). To determine the amount of heat rejected, the air's mass flow rate and change in temperature were measured. The specific heat and the density of the air were assumed to be approximately constant throughout the conditions between the air inlet and air exit. While the VacciRAPTOR was operating at steady conditions, the inlet and exit air temperatures were recorded using thermocouple probes.

$$\dot{Q} = \dot{m} C_p \Delta T \quad where \quad \dot{m} = \rho Q$$

Volumetric airflow measurements were taken using a Testo 405i hot-wire anemometer probe in combination with the methods outlined by the log-linear rule in ASHRAE Standard 111-1988 and over two traverse locations that were 90° apart. To develop the flow stream, a large, long circular duct was placed over the air exit. The inside diameter of the duct was equivalent to the inside diameter of the illumination chamber (26cm) and its length was 10x its inside diameter (260cm). Air flow measurements were taken 208cm (8x the inside diameter) downstream from where the air exited the VacciRAPTOR and entered the large tube. ***Figure 4.20*** shows the test setup and ***Table 4.4 below*** provides the location of the flow measurements along the traverse lines relative to the inside of the tube wall. It was assumed that the flow was fully developed after traveling 8x the inside diameter of the yellow tube.

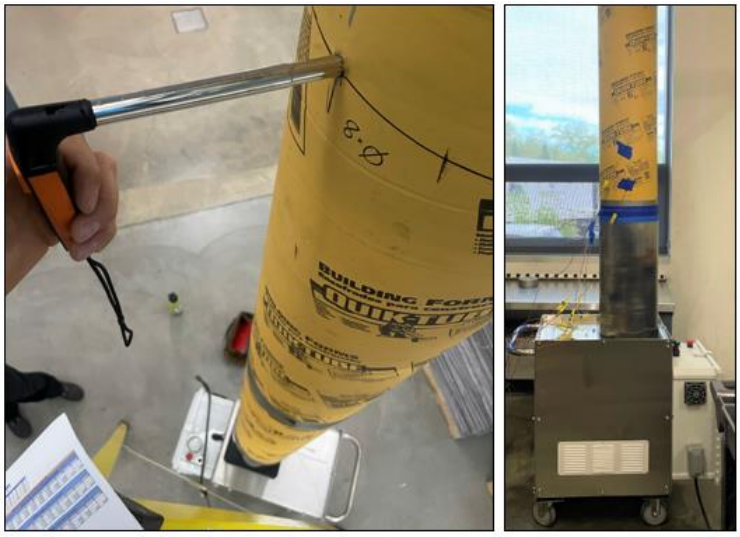

Figure 4.20: Volumetric airflow test setup. The inside diameter of the large yellow tube is equal to the diameter of the VacciRAPTOR's airflow field (inside diameter = 26cm, length = 10x inside diameter, flow measurement location = 8x inside diameter downstream.

Table 4.4: Volumetric flowrate measurement locations per ASHRAE 111-1988 log-linear rule.

Position relative to the inner wall (diameter fraction)								
Position	**1**	**2**	**3**	**4**	**5**	**6**	**7**	**8**
Diameter Fraction	0.021	0.12	0.18	0.35	0.66	0.82	0.88	0.98
Diameter Location (cm)	0.546	3.04	4.78	8.97	17.0	21.2	23.0	25.5

Figure 4.21 illustrates the measured volumetric flow profile in the duct with and without the presence of the top cap. The top cap (grey plastic cap shown in the lower right of ***Figure 4.16 on page 45***) blocks the escape of harmful UV light while permitting air flow for cooling. The "No Top Cap" measurement in ***Figure 4.21*** is a measure of the maximum achievable volumetric flow rate through the illumination chamber with the 275CFM-rated blower. The "With Top Cap" measurement indicates the volumetric flowrate through the VacciRAPTOR when the top cap is present. As per ASHRAE 111-1988, finding the average value of the flow measurements at each of the 8 traverse points determines the average volumetric flow rate. The average value for the No Top Cap measurements is 125CFM and the With Top Cap measurement is 94CFM. As such, it shown that 75% of the maximum achievable volumetric flow rate is permitted with this top cap design.

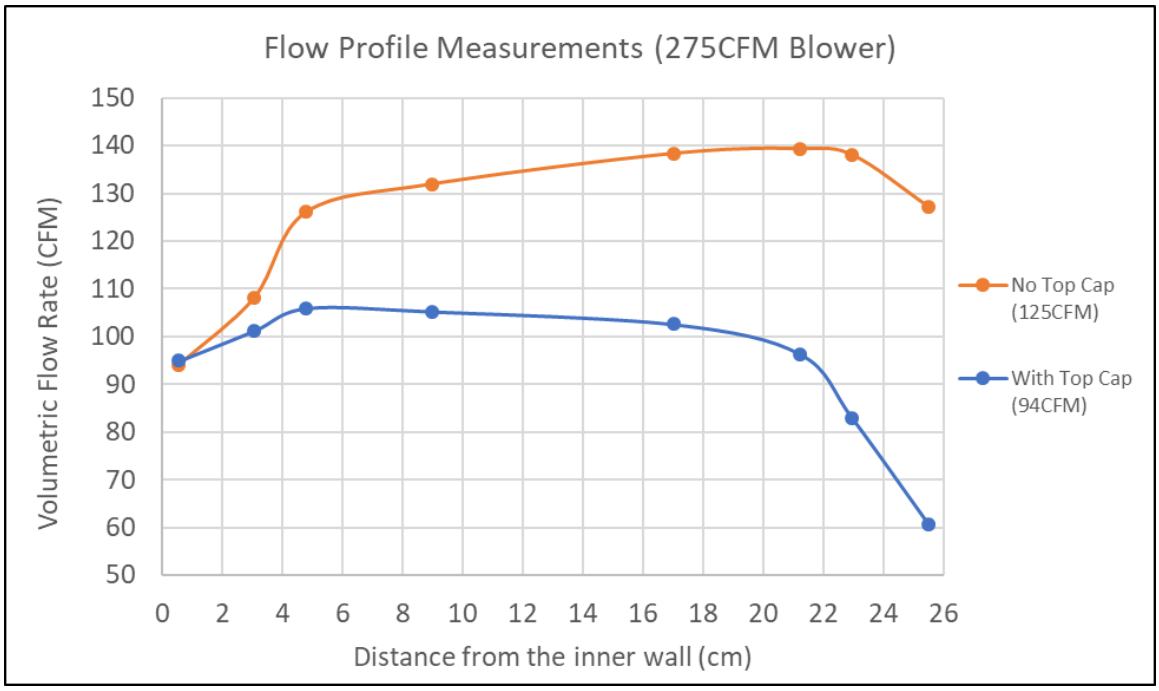

Figure 4.21: As per ASHRAE Standard 111-1988, taking the average value of each measurement at each of the measurement locations (determined by the log-linear rue for traverse points on a circular duct) yields the estimated total volumetric flow rate

within the duct. With the 275CFM blower, air flows at a volumetric flow rate of approximately 125CFM without the presence of the top cap while in the presence of the top cap, a volumetric flow rate of approximately 94CFM is achieved.

The tests determined that under steady operating conditions, air temperature rises from 20°C to 28.4°C from inlet to exit (ΔT = 8.4°C) and the volumetric air flow rate through the chamber is approximately 94CFM (Q = 94CFM). The ambient pressure was recorded at the time of testing to be 85 kPa. Inserting these values into the equation below reveals that the amount of heat that must be rejected to maintain the lamps at an operating temperature within the illumination chamber that is approximately equal to their operating temperature in an open, quiescent room (~63°C) is approximately 377W.

$$Q' = \rho Q C_p \Delta T = 377W$$

where the film temperature (T_{film}) is the median value between the inlet and exit air temperatures and

Q' = heat rejection

ρ = density of air evaluated at T_{film} and ambient pressure (ideal gas law)

Q = volumetric flow rate of air

C_p = specific heat of air at T_{film} (assumed constant over the temperature range) = 1,005 J/kgK

ΔT = difference in temperature between exit and inlet air streams

4.5.4 Ensuring that Liquid Pathogen Solution Temperatures are Sufficiently Low During Inactivation

The whole virion inactivation method employed by the VacciRAPTOR is intended to rely on the photochemistry of riboflavin and UV light. Exposing the whole virion solution to heat can

cause inactivation through a process known as pasteurization. Pasteurization, however, may cause unwanted damage to the virus structure that may decrease its potency as an antigen for the purpose of vaccination. As such, it is important that the flowing solution remain within acceptable temperature bounds to minimize heat-induced viral structure damage. It is essential the viral solution remains below 37-40°C during treatment and preparation. Optimally, the solution should maintain a temperature of approximately 10°C. The following paragraphs describe the methods and results of characterizing the temperature rise of the flowing liquid solution as a function of residence time within the UV illumination chamber. Residence time is defined as the amount of time it takes a unit of liquid solution to traverse the entire length of tubing that is present within the illumination chamber.

Test methods were developed assuming that the riboflavin + whole virion solution has comparable thermodynamic properties to water. In other words, it was assumed that the rate of heat absorption into the liquid is the same for both water and the RB + whole virion solution. The VacciRAPTOR was turned on and allowed to reach steady state operating temperatures. The device requires about 20 minutes to reach steady state operating conditions. A reservoir of water was chilled to and held at a constant 5°C (± 1°C) and flowed through the VacciRAPTOR once it reached steady state operating temperatures. The 5°C water was flowed through a full-size coil at flow rates between 50mL/min and 430mL/min which correspond to residence times between 257 seconds and 30 seconds, respectively. Flow rates greater than 430mL/min were not tested directly because the peristaltic pump being used was unable to deliver flow rates greater than 430mL/min. Residence time was calculated using the following derivation.

Given

$$Residence\ Time = \frac{length\ of\ tubing}{liquid\ mean\ velocity} = \frac{l}{V}$$

and

$$Liquid\ Mean\ Velocity = \frac{volumetric\ flow\ rate}{tube\ cross\ sectional\ area} = \frac{Q}{A}$$

then

$$Residence\ Time = \frac{lA}{Q}$$

where

l = *length of reactor coil tubing*

A = *tube cross-sectional area*

Q = *volumetric flow rate*

Figure 4.22 below shows the measured temperature increase for various residence times along with the logarithmic trendline created from the nine data points. In order to dose a solution with 1.5J/mL of UV radiant energy, the solution must remain within the illumination chamber for approximately 13 seconds. Therefore, the residence time for all coil sizes is 13 seconds. The trendline equation in ***Figure 4.22*** estimates that the liquid solution will increase in temperature by approximately 0.4°C after ~13 seconds of residence time.

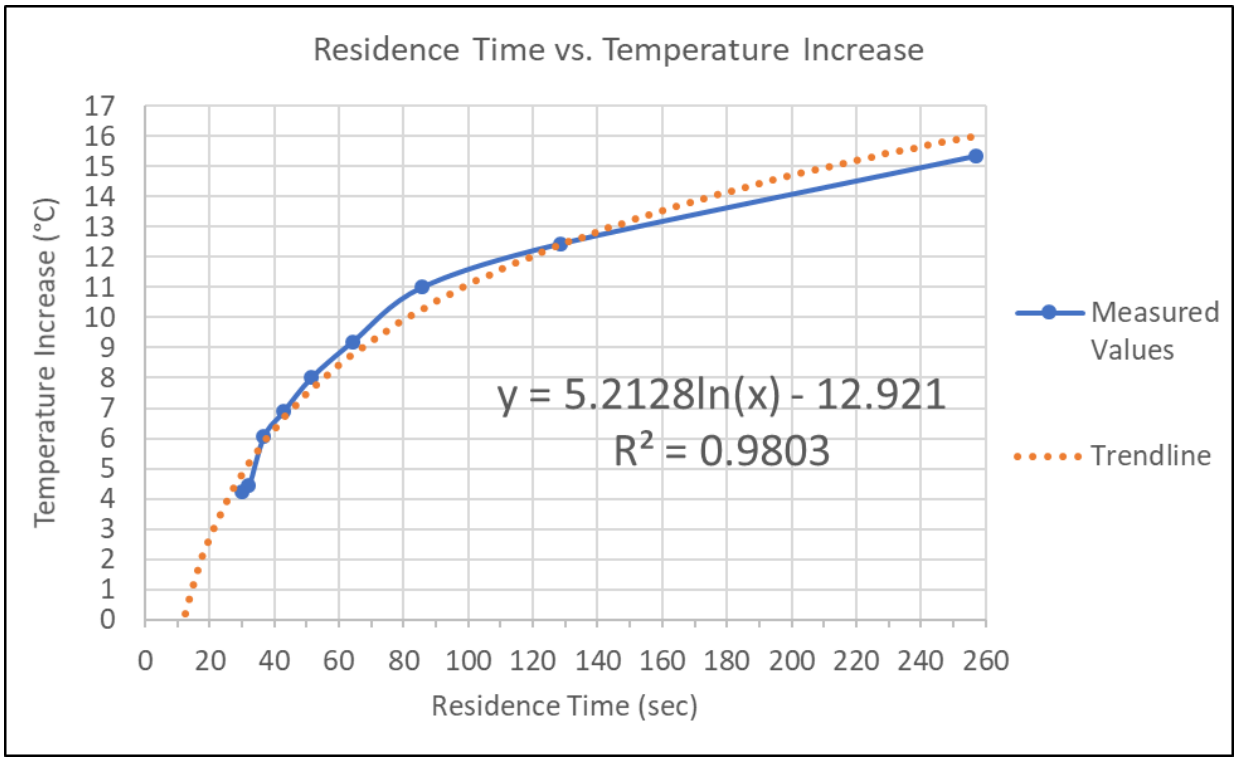

Figure 4.22: The residence time vs. temperature increase curve above indicates that temperature increase in the liquid treatment solution is negligible for all residence times that are representative of a UV radiant energy dosage of 1.5J/mL. This dosage corresponsds to a residence time of ~13 seconds and a temperature increase of ~0.4°C.

This minimal temperature increase is negligible. Even if the dosage of radiant energy were doubled to 3.0J/mL (i.e. if residence time were doubled), the resulting temperature rise would be about 4°C. Since minimal temperature rise was exhibited in the liquid at residence times that are representative of true operating residence times, maintaining the liquid riboflavin + whole virion solution at temperatures near optimal (10°C) and well below the upper limit (37-40°C) is readily achieved by the VacciRAPTOR.

4.6 Control System

The VacciRAPTOR's control system is comprised of a single on/off "emergency-stop" style button and a potentiometer selector knob that selects lamp operation programs as shown in ***Figure 4.23 below***. When the on/off selector is switched to the "on" position, the blower

automatically turns on to ensure that the lamps cannot be turned on without the blower also being turned on. Lamp operation is controlled by Arduino code. The Arduino controller code is available in ***Appendix A***. The lamp operation modes are selected by varying the position of a 10-position potentiometer. In position zero, all lamps are turned off. In positions 1-9, the lamps turn on in consecutive pairs after a five second delay. For example, in position 1 lamps 1-2 turn on. In position 2, lamps 1-4 turn on. In position 3, lamps 1-6 turn on, etc. The lamps are also wired in pairs because the ballasts are designed to operate the lamps in pairs.

Figure 4.23: Emergency stop button (red knob), lamp program selector (black knob), and layout of lamp ballasts and other electronic equipment within the VacciRAPTOR.

Assembled in line with the power cable that provides power to the VacciRAPTOR lamps and blower is a HOBO plug load logger (i.e., power meter). This power meter is used to display the real time power consumption of the device. After a warmup period of approximately 20 minutes, the power consumption of the device levels off at approximately 580W ***Figure 4.24***. If a lamp malfunctions or goes out, the power reading will drop. The power reading is an indication of whether a lamp has gone out within the device. As is shown in ***Figure 4.25 below*** if a lamp

goes out, the steady state power consumption of ~585W will drop by ~60W. Although the lamps used in the device have a rated power consumption of 36W, the power meter shows that each lamp consumes 30W and the entire device consumes ~585W. The power reading will drop by 60W rather than 30W when a lamp goes out or malfunctions because they are wired in pairs.

Figure 4.24: HOBO plug load monitor and logger that displays real time power consumption of the device

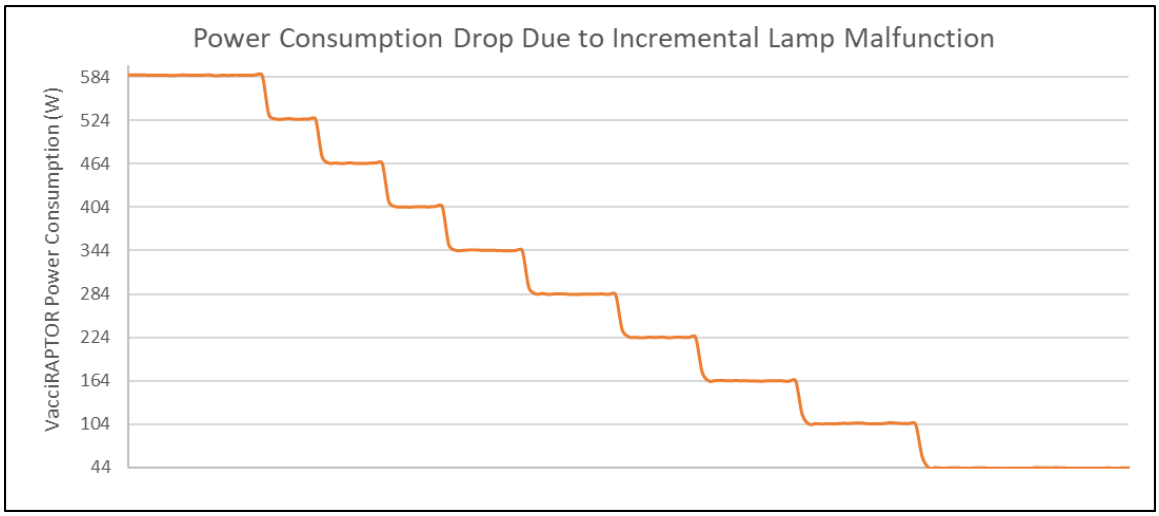

Figure 4.25: This profile shows incremental power consumption drop due to incremental lamp malfunction. If a lamp malfunctions, the power consumtion reading drops by 60W.

CHAPTER 5 SPECTRAL IRRADIANCE AND KILL KINETICS OF NARROWBAND AND BROADBAND UV ILLUMINATION FOR RIBOFLAVIN-UV FACILITATED PATHOGEN REDUCTION

5.1 Spectral Irradiance of Narrowband UV LEDs and the VacciRAPTOR's Broadband UV Lamp Illumination Field

5.1.1 Background

Narrowband UV LEDS are a new technology that have a much narrower emission spectra than broadband UV lamps. A study was performed to compare differences in pathogen kill kinetics both with and without the presence of riboflavin across various narrowband UV LED emission spectra. See ***Chapter 5.2***. In preparation for that study, the spectral irradiance of the narrowband UV LEDs being used needed to be characterized. The American Biomedical Group Incorporated (ABGI) built a device that was intended to irradiate horse blood with UV light to study immune response in horses after a portion of the horse's blood was irradiated with narrowband UV light. This device served as a great platform for performing pathogen kill kinetics. The ABGI device is equipped with 20 UV LEDs. There are five rows of four UV LEDs. Each row of four LEDs outputs narrowband UV radiation at either 265, 275, 285, 310, or 325nm. ***Chapter 5.1*** discusses the methods, results, and conclusions of the spectral irradiance characterization study performed using these five high intensity narrowband UV LED emitters.

5.1.2 Methods

To measure the spectral irradiance of each of the five UV LEDs, a custom-designed cap was attached to the end of a spectrometer to block out extraneous light while fully capturing the emitted beam of UV radiation. The custom cap blocked ambient light and ensured that

measurements were taken at a constant angle and distance from the illumination source. Further, the cap was designed to ensure that, given a 30° light source emission angle, the spacing between the probe tip and the emission source would capture 100% of the light emission directly on the surface of the spectrometer probe tip. ***Figure 5.1 below*** shows the custom blue cap attached to the spectrometer tip and the ABGI blood irradiator device.

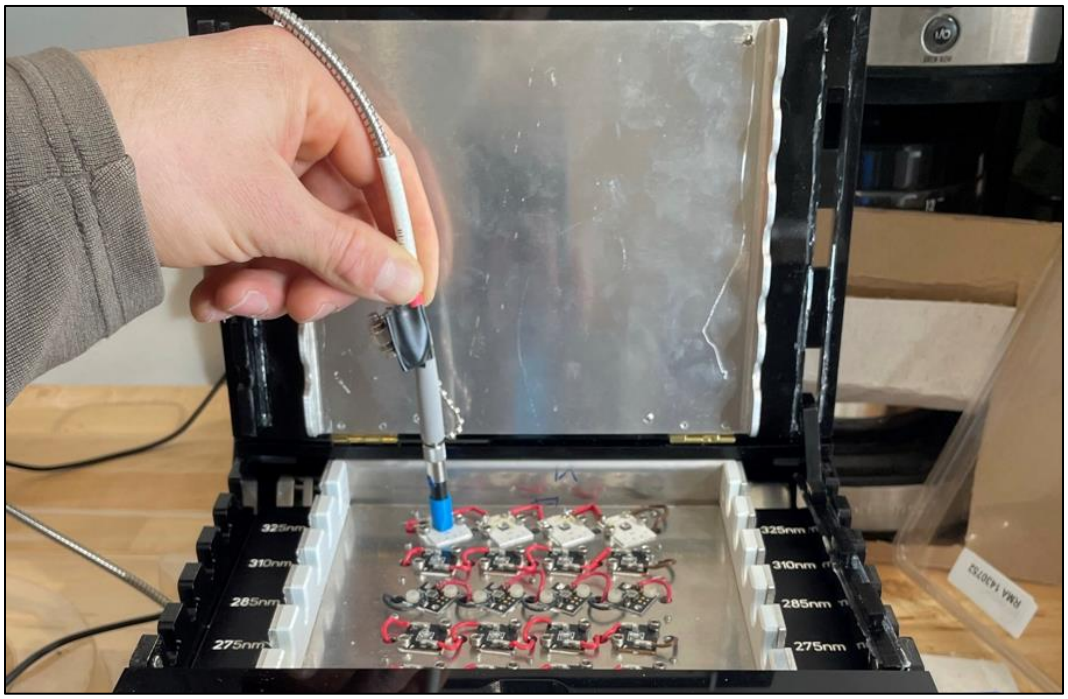

Figure 5.1: The American Biomedical Group Blood Irradiator device was used to compare the influence of narrowband UVB radiant energy at vasrious wavelengths on pathogen kill kinetics. The kill conetics were compared across five nominal UVB wavelengths (265, 275, 285, 310, and 325nm) both with and without the presence of riboflavin.

5.1.3 Results

Figure 5.2 below compares each UV LED's irradiance spectra to the UV lamp irradiance spectra of the VacciRAPTOR's 18-lamp illumination field (Daavlin 36W broadband UV lamp). Note that the primary vertical axis corresponds to the VacciRAPTOR's lamp spectral irradiance, and the secondary vertical axis pertains to the LED spectral irradiance. The UV LEDs exhibit spectral irradiance amplitudes that are approximately 10 to 20 times greater than the 18-lamp

spectral irradiance. The UV LEDs also exhibit irradiance values (area under the curve) that are 1.4 to 7.6 times greater than the VacciRAPTOR's irradiance values. Even though the spectral irradiance (amplitude) and total irradiance (area under the curve) of the UV LEDs are greater than that of the UV lamps, the electromagnetic radiation emitted by the LEDs is delivered to a much smaller surface area. The high intensity irradiance spectra of the LEDs irradiate a surface area that is roughly 14,700 times smaller than the irradiated surface area within the VacciRAPTOR's illumination chamber (0.119 cm^2 compared to 1,756 cm^2). The average radiant power output of the UV LEDs tested here is 12.2mW and the radiant power output of the VacciRAPTOR'S 18-lamp illumination field is 36,200 mW. In other words, the VacciRAPTOR has a radiant power output that is equivalent to that of approximately 3,000 UV LEDs.

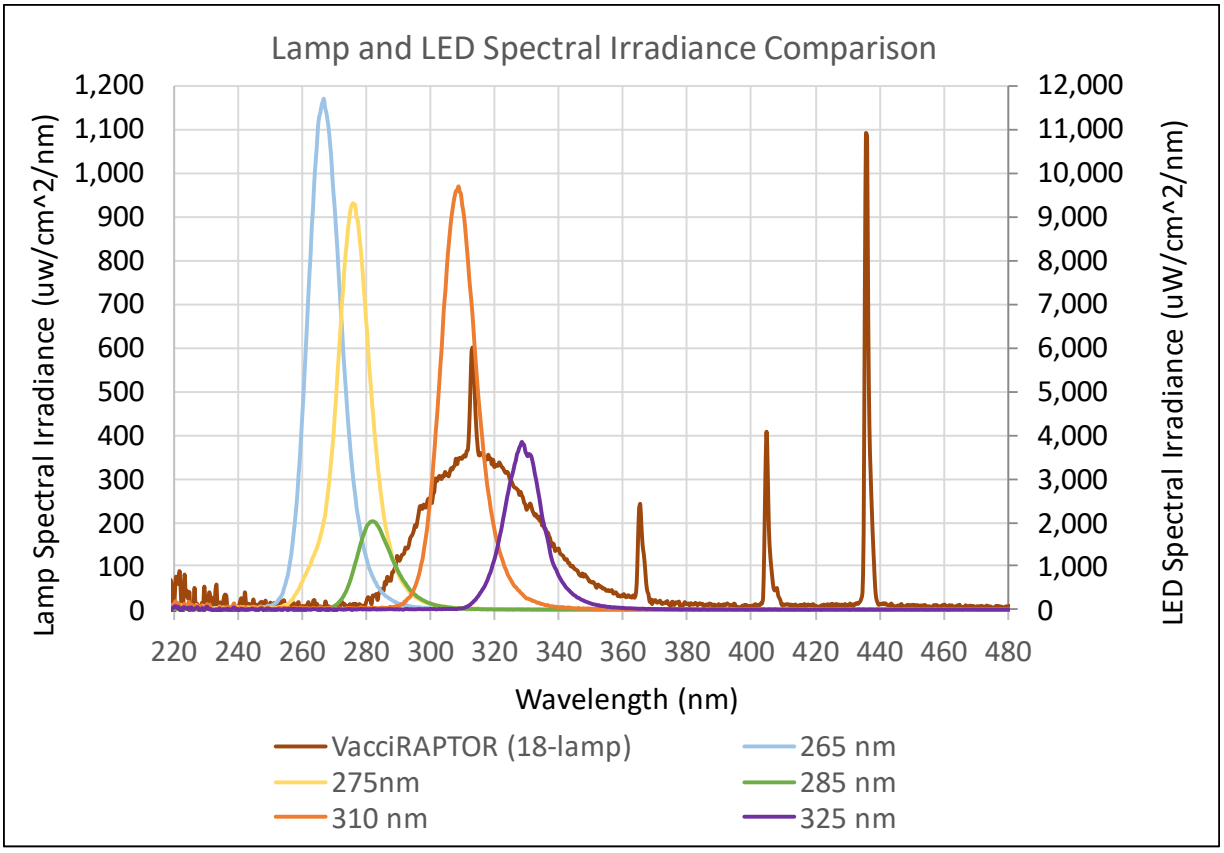

Figure 5.2: UV Lamp and UV LED spectral irradiance comparison. The primary vertical axis pertains to the VacciRAPTOR's UV lamp spectral irradiance while the secondary vertical axis pertains to the UV LED spectral irradiance.

Table 5.1 below shows that 95 to 96% of each LEDs irradiance falls within a narrow 60 to 85nm wide band (Δλ), on average each LED emits 12.2 mW of radiant power per LED, and that per LED, the average treatment capacity is 0.401 mL/min. The key result in this table is the treatment capacity (rightmost column). The treatment capacity results are used in ***Chapter 5.2*** to determine the flowrates needed to deliver a cumulative dose of 1.5J/mL to the viral solution.

The treatment capacity calculated in ***Table 5.1*** is the flowrate required to for a single LED to deliver an energy dosage of 1.5J/mL. The treatment capacity listed for the VacciRAPTOR is the flowrate required for the entire 18-lamp illumination chamber to deliver 1.5J/mL of UV energy. The calculations use the same methods as those outlined in ***Chapter 4.3.4***. The treatment capacity here does not account for UV transmission losses through the tubing.

Table 5.1: Irradiance, incident surface area, radiant power, and treatment capacities for the VacciRAPTOR's 18-lamp illumination field and individual narrowband UV LEDs. The treatment capacity assumes an energy dosage of 1.5J/mL.

Device Name	Wavelength Range (λ) (nm)	Δλ (nm)	% of Total Irradiance in Range (%)	Irradiance (mW/cm^2)	Incident Surface Area (cm^2)	Radiant Power (mW)	Treatment Capacity (mL/min)
VacciRAPTOR (18 lamps)	220 to 480	260	75%	20.6	1,756	36,200	1,450
265 nm LED	240 to 300	60	96%	156	0.119	18.6	0.743
275 nm LED	250 to 310	60	95%	130	0.119	15.5	0.619
285 nm LED	250 to 320	70	95%	29.0	0.119	3.45	0.138
310 nm LED	280 to 350	70	95%	140	0.119	16.7	0.666
325 nm LED	290 to 375	85	95%	58.8	0.119	7.00	0.280
					LED Average	**12.2**	**0.489**

5.1.4 Conclusions

In summary, at least 95% of the narrowband UV irradiance occurs in these narrowband LEDs at a bandwidth of approximately 60 to 85nm while 75% of the irradiance from the

broadband lamps in the VacciRAPTOR occurs over a much larger 260nm bandwidth. Narrowband UV LEDs output irradiance that is 1.4 to nearly 8x greater than that of the VacciRAPTOR's illumination field, but the beam of irradiance is over a much smaller incident surface area. As such, even though irradiance is much higher with these UV LEDs, the radiant power is much lower. The test methods used in ***Chapter 5.2*** utilize the calculated treatment capacity results in ***Table 5.2 below*** to deliver incremental 0.5J/mL doses of UV radiant energy. A sample calculation of provided below the table.

Table 5.2: Comparing irradiance and resulting treatment capacities at energy dosages of 0.5J/mL for select high intensity, narrowband UV LEDs.

Device Name	Wavelength Range (λ) (nm)	Δλ (nm)	% of Total Irradiance in Range (%)	Irradiance (mW/cm^2)	Incident Surface Area (cm^2)	Treatment Capacity @0.5J/mL (mL/min)
265 nm LED	240 to 300	60	96%	156	0.119	2.23
275 nm LED	250 to 310	60	95%	130	0.119	1.86
285 nm LED	250 to 320	70	95%	29.0	0.119	0.41
310 nm LED	280 to 350	70	95%	140	0.119	2.00
325 nm LED	290 to 375	85	95%	58.8	0.119	0.84

$$Treatment\ Capacity$$

$$= Irradiance \times Incident\ Surface\ Area\ \times \frac{1}{Radiant\ Energy\ Dosage}$$

$$= 156\frac{mW}{cm^2} \times 0.119 cm^2 \times \frac{1}{0.5\ {}^{J}/_{mL}} \times \frac{1\,J}{1{,}000 mJ} \times \frac{60 sec}{1 min} = 2.23\frac{mL}{min}$$

5.2 Narrowband UV LED Kill Kinetics of Riboflavin-UV Facilitated Pathogen Inactivation

5.2.1 Background

Presently, the literature on the effects of ultraviolet light spectra and dosages for pathogen inactivation are contradictory [21]. Literature has not come to an agreement on which wavelength or which combinations of wavelengths and dosages of electromagnetic radiation most precisely perform the function of pathogen reduction/inactivation without causing indiscriminate damage. Most riboflavin-UV pathogen inactivation research has been performed from the perspective of limiting blood transfusion-transmitted infections (TTIs) as opposed to the perspective of whole virion inactivation for vaccine production. Whether limiting blood TTIs or producing inactivated virus solutions for vaccine use, the goals are the same: inactivating pathogen without causing indiscriminate damage to the product.

In an attempt to clarify uncertainty around optimal UV spectra for riboflavin-UV facilitated pathogen reduction, a research group from the Clinical Transfusion Research Center (CTRC) in China performed experiments comparing the efficacy of *Escherichia coli* (*E coli*) inactivation using three UV spectra—broadband (275-400nm) and narrowband (centered on 311nm and 365nm)—at various UV light doses [21]. The results from the study showed that of the three spectra compared, the narrowband UV centered on 311nm "optimally reduced the *E coli* titer…[and] had a good inactivation effect on *E coli* and phages, eliminating many viruses, and resulted in acceptable platelet quality after riboflavin-UV treatment…" [21]. This result agrees with the assertion from Goodrich and colleagues who observed that "the wavelength used will depend on the type of pathogen reduction compound selected and the type of blood component being pathogen reduced. For platelets, the light source may provide light of about 270 to about 700nm, and more preferably about 308nm to about 320nm" [22].

5.2.2 Methods

To further clarify uncertainty around optimal UV spectra for riboflavin-UV facilitated pathogen reduction, collaborative study between research groups at Colorado State University's Infectious Disease Research Center (IDRC) and the Energy Institute was performed to compare whole virion kill kinetics at increasing UV light doses across a range of narrowband UV LED illumination sources. This study specifically examined kill kinetics of Zika virus (family Flaviviridae, strain PRVABC59) in aqueous media both with and without the presence of riboflavin after receiving various doses of narrowband UV light. The ABGI blood irradiator device described in ***Chapter 5.1*** was used to irradiate a flowing solution of whole Zika virus in aqueous media at narrowband UV wavelengths centered at 265, 275, 285, 310, and 325nm. Kill kinetics were assessed at each wavelength after light dosages of 0.5J/mL 1.0J/mL and 1.5J/mL.

As shown in ***Figure 5.3 below***, using a peristaltic pump, the first pass of the viral solution was pumped from Bag (1), across a UV irradiation field where the solution was dosed with 0.5J/mL of UV light, and then was pumped into Bag (2). A 35mL sample was removed from Bag (2) after the first pass to assess log kill due to a total UV dosage of 0.5J/mL. In a second pass, the solution was pumped back from Bag (2) into Bag (1) after being dosed with an additional 0.5J/mL of UV light to accumulate a total dosage of 1.0J/mL. After the second pass, a 35mL sample was removed from Bag (1) to assess log kill due to a total UV dosage of 1.0J/mL. In a third pass, the solution was pumped from Bag (1) into Bag (2) after again being dosed with an additional 0.5J/mL of UV light to accumulate a total dosage of 1.5J/mL. A 35mL sample was removed from Bag (2) to assess to assess log kill due to a total UV dosage of 1.5J/mL.

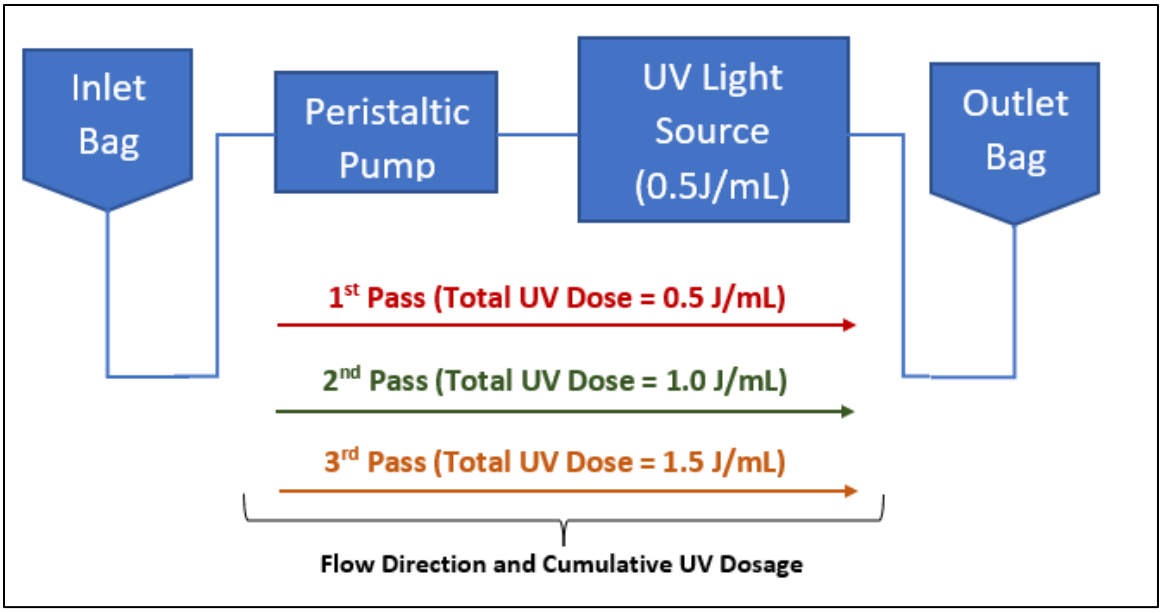

Figure 5.3: Test setup schematic for narrowband UV irradiation of Zika virus in aqueous media with and without riboflavin.

5.2.3 Results

The results from the collaborative study performed by CSU's IDRC and Energy Institute corroborate the conclusions inferred from the action spectra curve that was first introduced in ***Figure 3.3 on page 13***. For reference, this figure is reproduced below and relabeled as ***Figure 5.4***. The action spectra curve (yellow line) in ***Figure 5.4*** shows that at wavelengths below 290nm, RB reduces log virus kill while at wavelengths greater than 290nm, RB improves log virus kill. The same trend is observed in the narrowband UV LED study with Zika virus. ***Figure 5.5 below*** shows that for all wavelengths below 290nm (265, 275, and 285nm), log virus kill decreases in the presence of RB while for wavelengths greater than 290nm (310 and 325nm), log virus kill increases in the presence of RB.

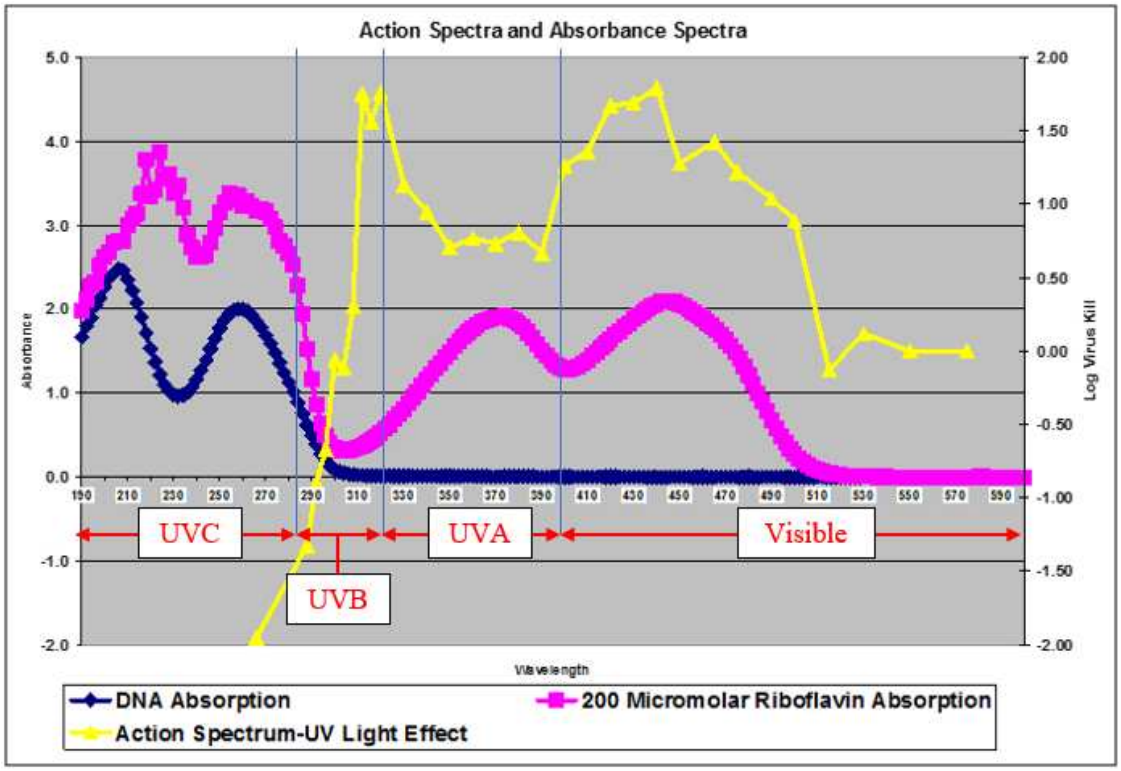

Figure 5.4: The action spectrum (yellow line) indicates the difference in pathogen kill levels with and without RB. The action spectra are positive above 290nm. This indicates that kill levels are greater with RB when exposed to UV light wavelengths greater than 290nm [14].

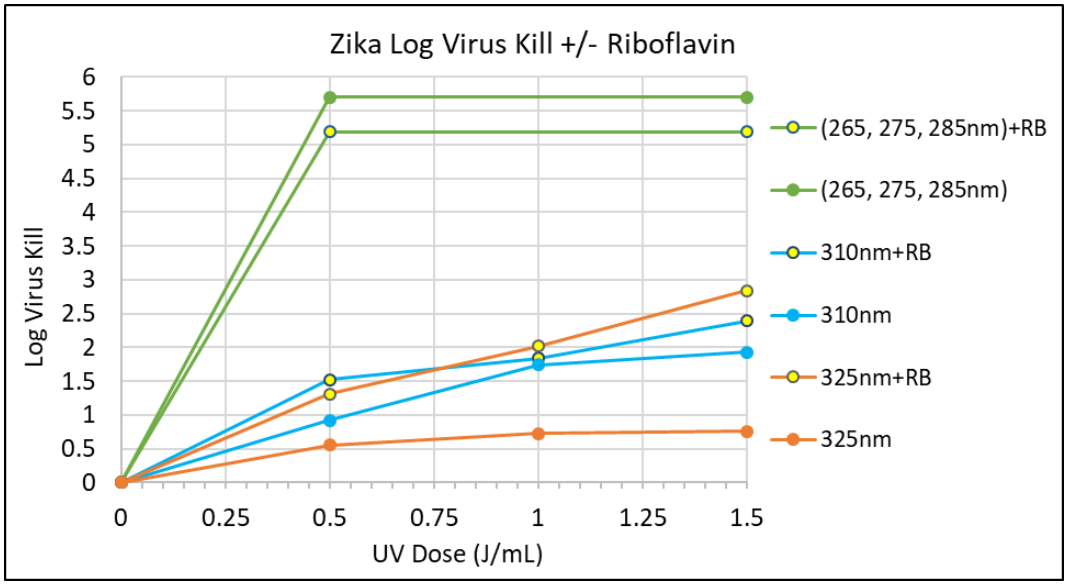

Figure 5.5: Log Zika virus kill with and without riboflavin after receiving narrowband UVB light dosages of 0.5, 1.0, and 1.5J/mL.

When looking at the log virus kill trends for the samples without RB in ***Figure 5.5***, the data trends as expected. Recall that shorter wavelength light is more energetic than longer wavelength light. Log kill is higher when exposed to shorter (i.e. higher energy) wavelengths. Without RB, log kill is the highest with 265, 275, and 285nm wavelengths (5.7 log reduction), lower with 310nm (1.93 log reduction), and lowest with 325nm (0.76 log reduction).

When looking at relative log virus kill levels for samples with RB in ***Figure 5.5 above***, it is seen that low wavelength light (265, 275, 285nm) is the most effective at reducing Zika viral titer, followed by 325nm, then 310nm light. From the curves in ***Figure 5.5***, action spectra of the riboflavin-UV photochemistry can be deduced. The action spectrum in ***Figure 5.4 above*** peaks near the intersection of the UVA and UVB regions at approximately 310 and 325nm and is negative below ~290nm. Thus, it is anticipated that Zika titer reduction due to riboflavin-photochemistry would be optimal near the peak between ~310nm and ~325nm and negative for the 265, 275, and 285nm wavelength LEDs.

Figure 5.6 below compares the RB action spectra at the wavelengths tested and suggests that inactivation is most dependent on riboflavin photochemistry at 325nm. Since 325nm light is less energetic than 310nm light, it is also probable that 325nm light is optimal for riboflavin-UV facilitated pathogen reduction because 325nm light is less likely to cause indiscriminate damage than 310nm light.

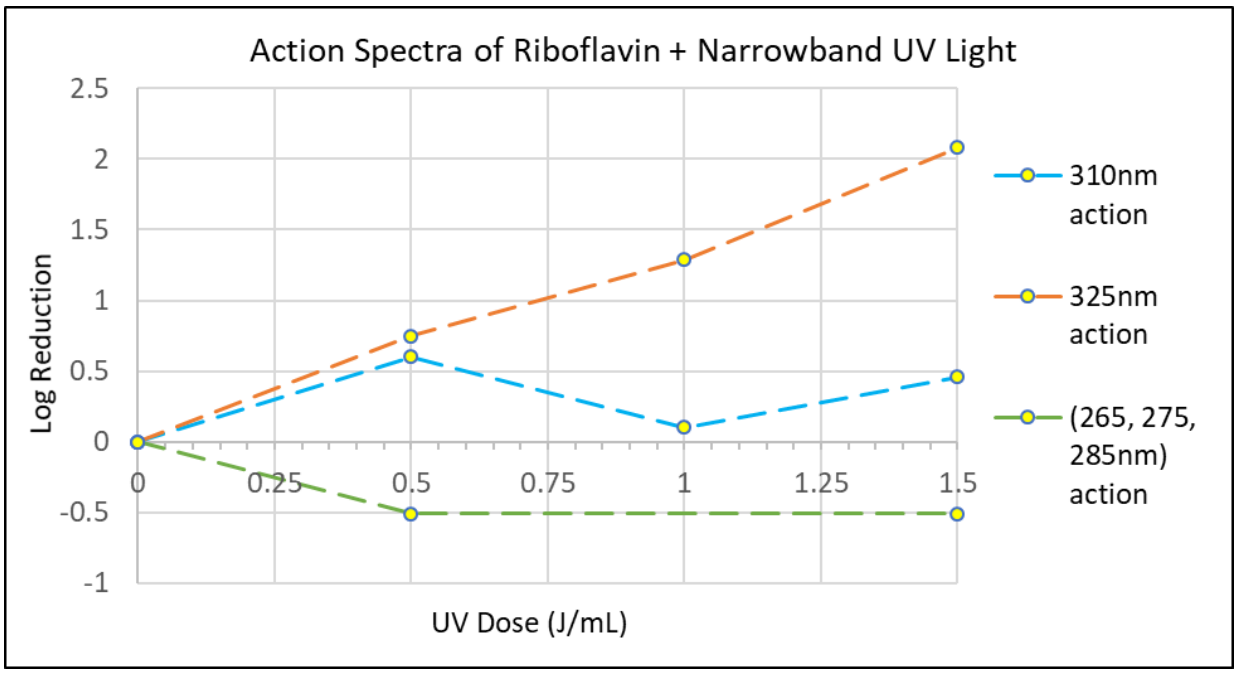

Figure 5.6: Action spectra of riboflavin and UV light on Zika virus in aqueous media at various wavelengths.

5.2.4 Conclusions

Many of the trends observed in this study agree with the literature: higher energy, lower wavelength UV radiation exposures yield greater log virus kill than lower energy, higher wavelength UV radiation; at wavelengths below 290nm, the addition of riboflavin reduces log kill while at wavelengths greater than 290nm, riboflavin enhances log kill via riboflavin photochemistry. Additionally, kill kinetics appear to employ riboflavin photochemistry most heavily at 325nm compared to 265, 275, 285, and 310nm.

Additional narrowband riboflavin-UV testing is necessary to characterize and assess the statistical significance of the differences observed between the action spectra of 310 and 325nm riboflavin-UV facilitated pathogen reduction for Zika virus. Additional testing is also necessary to determine the applicability of these results across various virus types. The CTRC study referenced here suggests that 311nm UV light may be optimal [21] and the CSU IDRC/Energy Institute study suggests that 325nm light may be optimal over 310nm UV light. In order to

narrow in on and draw firm conclusions about the optimal UV spectra for riboflavin-UV facilitated pathogen reduction, additional testing is necessary.

5.3 VacciRAPTOR Kill Kinetics of Riboflavin-UV Facilitated Pathogen Inactivation

5.3.1 Background

Colorado State University's Infectious Disease Research Center (IDRC) and Energy Institute collaborated to perform riboflavin-UV facility pathogen kill kinetic testing using the VacciRAPTOR with Zika virus (family Flaviviridae, strain PRVABC59). Zika virus is classified as a Biosafety Level 2 (BSL2) microbe. The Center for Disease Control defines BSL2 microbes as microbes that pose moderate hazards to laboratorians and the environment. BSL2 microbes are typically indigenous and associated with diseases of varying severity. Zika virus was used for proof-of-concept testing of the VacciRAPTOR prototype. This is the same virus that was used in ***Chapter 5.2*** to study kill kinetics using narrowband UV LEDs.

5.3.2 Methods

To perform the kill kinetic testing with Zika virus, stock Zika virus titers were prepared in a lab at the IDRC. For each test replicate, a 500mL bulk viral solution composed of 415mL of PBS, 35mL of 500μmol/L riboflavin, and 50mL of stock virus grown in media was prepared and mixed into a 1,000mL blood bag. Once the viral solution was mixed, three 3mL "pre-treatment" samples were removed from the bag and saved for plaque assay preparation of the pre-treatment condition.

As is illustrated in ***Figure 5.7 below***, the bulk solution was pumped three consecutive times from one 1,000mL blood bag (Inlet Bag), past the peristaltic pump, into the VacciRAPTOR illumination chamber and coil, and then into a 1,000mL post-treatment bag (Outlet Bag). After each consecutive pass through the device, the bulk solution accumulates an additional 0.5J/mL UV energy dosage and, after each pass, three 3mL samples are removed from the bulk solution and saved for plaque assay preparation. ***Figure 5.8 below*** is a photo taken during testing. The bag being pointed to is the inlet bag and the bag on the left is the outlet or "post-treatment" bag.

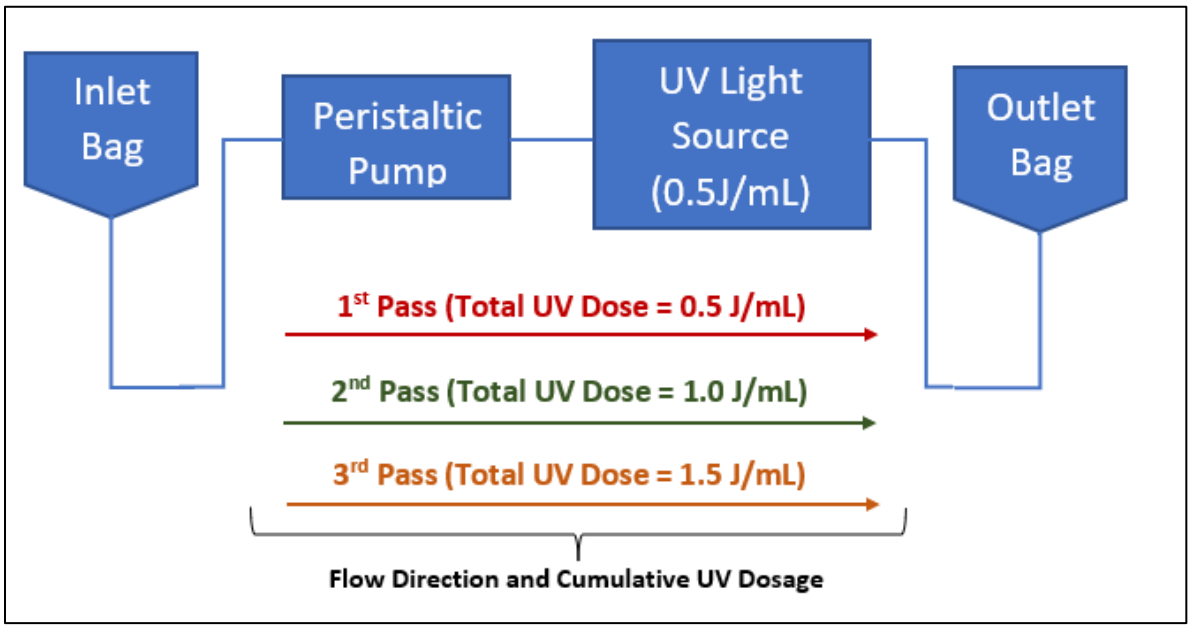

Figure 5.7: Test setup and procedure schematic for VacciRAPTOR kill kinetic testing with Zika virus.

Figure 5.8: Bulk zika virus solution flowing from the inlet bag (see bag being pointed to), through the VacciRAPTOR illumination chamber, and out into to the outlet bag. Credit: John Eisele/Colorado State University Photography

After dosing the bulk solution with three 0.5J/mL dosages of UV energy and removing three 3mL samples after each treatment, each of the four treatment conditions (pre-treatment, 0.5J/mL, 1.0J/mL, and 1.5J/mL) were plaque assayed. Plaque assays were performed to develop kill kinetic curves and understand the proof-of-concept performance of the VacciRAPTOR for riboflavin-UV facilitated Zika inactivation. Detailed sterilization and test procedure instructions are provided in ***Appendix B***.

5.3.3 Results

The inactivation testing results show that VacciRATPOR successfully and repeatably inactivates Zika virus. The VacciRAPTOR inactivates Zika at an average inactivation rate of 4.6 $\log_{10}$PFU/mL per J/mL of UV energy dosage. The inactivation rate is the absolute value of the

slope of kinetic kill curves show in ***Figure 5.9 below***. The legend in ***Figure 5.9*** names the four data sets and the level of detection (LOD). The data set labeled "Z-7.8" indicates a Zika stock viral sample whose starting titer was 7.8 $\log_{10}$PFU/mL. The three data sets labeled with "Z-7.3" indicates a Zika stock viral sample whose starting titer was 7.3 $\log_{10}$PFU/mL. Three test replicates were performed with the Z-7.3 viral stock and are labeled in the figure as "(rep. 1), (rep. 2), and (rep. 3)". ***Table 5.3 below*** provides a table of the data values shown in the preceding figure. Figure 5.10 below shows images of the plaque assays from the Z-7.8 data set.

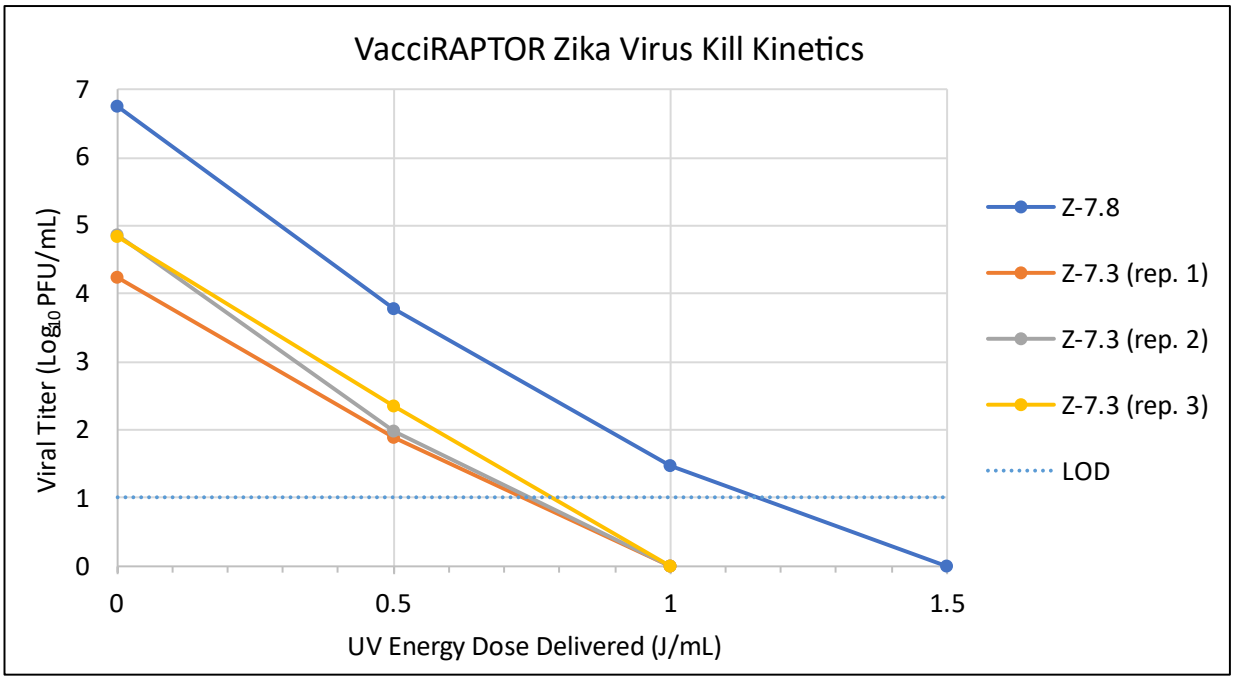

Figure 5.9: VacciRAPTOR Zika virus kill kinetic testing results.

Table 5.3: Results table of Zika virus inactivation testing comparing viral titer values after each cumulative UV energy dose.

Sample	Viral Titer (Log_{10} PFU/mL)			
	Z-7.8	Z-7.3 (rep. 1)	Z-7.3 (rep. 2)	Z-7.3 (rep. 3)
Pre-Tx	6.76	4.23	4.86	4.83
0.5 J/mL	3.78	1.88	1.98	2.34
1.0 J/mL	1.48	<1	<1	<1
1.5 J/mL	<1	<1	<1	<1
Inactivation Rate (Log10PFU/mL per J/mL)	4.5	4.2	4.9	4.8

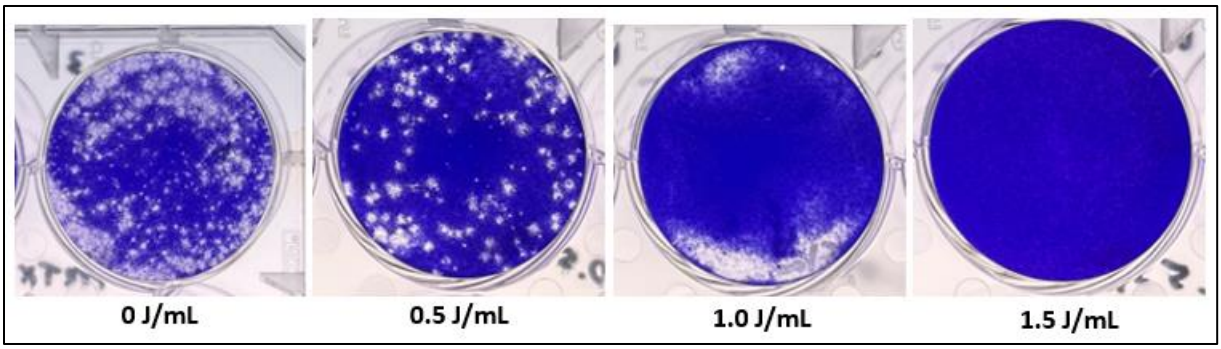

Figure 5.10: Plaque assay images from the Z-7.8 data set exhibit the progressive decrease in viral plaques due to cumulative UV energy dosages. Credit: Alina Vise/Colorado State University

5.3.4 Conclusions

The above results confirm the proof-of-concept of the VacciRAPTOR as a high throughput pathogen inactivation device. Two conclusions can be drawn from the results presented above. To begin with, one can conclude that inactivation energy is proportional to the magnitude of the viral titer. Comparing data set Z-7.8 to Z-7.3 shows that kill kinetics using the SolaVAX method are dependent on magnitude of the "pre-treatment" viral titer. In the pre-treatment condition, the Z-7.8 sample has a viral titer of 6.76 $\log_{10}$PFU/mL while the Z-7.3 pre-treatment data has an average viral titer of 4.64 $\log_{10}$PFU/mL. The higher viral titer required an additional UV energy dosage of about 0.4 to 0.5J/mL to reach the limit of detection.

Additionally, the results suggest that the rate of Zika inactivation using the SolaVAX method in the VacciRAPTOR is about 4.6 $\log_{10}$PFU/mL per J/mL of UV energy dosage. Both viral titers exhibit comparable rates of inactivation (slopes of the curves). Additional testing is required to determine the antigen potency of the inactivated Zika virus. This additional testing will determine how discrete the inactivating damage was to the viral structure. It is predicted that the VacciRAPTOR produces an antigen whose potency is comparable to that of the Mirasol PRT system since both devices employ the SolaVAX process and have nearly equivalent emission spectra. Further, testing is required to determine the robustness of the VacciRAPTOR. It remains unknown whether the VacciRAPTOR will also perform successfully with different viruses of different structure and with other pathogen such as parasites.

CHAPTER 6 DESIGNING FOR EFFICIENCY – A COMBINED LIFE CYCLE ASSESSMENT AND TECHNOECONOMIC ANALYSIS COMPARING NARROWBAND UV LEDS AND BROADBAND UV LAMPS FOR PATHOGEN INACTIVATION

6.1 Background

Presently, the VacciRAPTOR prototype utilizes broadband UV phototherapy tube lamps to deliver UV radiant energy to a live virion solution that flows through the device. It is common industry knowledge that, for visible spectrum illumination purposes, LED light sources are more energy efficient than fluorescent tube lamp light sources (~50 Lumen/Watt for LEDs vs. ~30 Lumen/Watt or less for fluorescent tube lamps) [5].

UV tube lamps are not a novel technology and there is a strong market demand for these types of lamps for use in phototherapy applications. UV LEDs on the other hand, are a newer technology with a relatively low market demand in comparison to UV lamps. As such, UV LED costs remain high in comparison to standard, non-UV LEDs such as those one would find in office lighting, bike lights, and headlamps. For example, medium and high intensity UV LEDs often cost around $30-$35 per unit while high intensity non-UV LEDs can cost as little as $1 or less.

Life cycle assessment (LCA) is the assessment of environmental impacts related to a product, service, or process from raw materials to waste removal [23]. A literature review yielded valuable information regarding the LCA data for LED lamps as they compare to Compact Fluorescent Lamps (CFL). No LCA information was found regarding UV phototherapy lamps. No direct LCA comparison was found for LEDs and fluorescent tube lights. Fluorescent tube lights (FL) are the most comparable lighting type to the UV phototherapy fluorescent lamps used in the present VacciRAPTOR design.

A literature review was performed for related LCA and TEA studies. The United States Department of Energy (DOE) performed an LCA that compares traditional incandescent lamps, CFLs, and LED lamps. This study showed that, on average, the "use" phase of all three types of these lamps accounted for 90% of total life-cycle energy [24]. The remaining 10% of life cycle energy was consumed during manufacturing and transportation [24]. The DOE's study also concluded that the use phase not only dominates energy usage, but it also dominates environmental impacts assessed [24].

Another LCA was performed comparing LED and CFL environmental impacts by a research group in Italy. This study further confirmed that the environmental impact of these two light sources is dominated by the use phase of the technology which contributed 96% to 99% of the total global warming potential in the study's LCA [25]. The literature review suggests that limiting the scope of this study to the use phase only is a reasonable assumption that may capture 90% to 99% of the total lifetime energy consumption and CO2-eq emissions for the UV light sources considered here [24, 25].

It is important to note the literature review showed that all data regarding LCAs of lighting sources focused on lighting in the visible spectrum (i.e., lighting for visible illumination). No information was found that assessed lighting in UV applications. The functional unit for visible spectrum lighting is typically related to visible output per time (e.g., lumen-hours, lux-hours, etc.). The study here assessed lighting based on a UV light application rather than a visible light application. The VacciRAPTOR is designed to deliver 1,500 Joules of UV-spectrum radiant energy to each liter of virion solution flowing at a volumetric flow rate of up to 71.2 Liters/hour. Accordingly, the functional unit of this study is one liter of treated virion

solution. In other words, the study normalizes the energy consumption and resulting CO2-eq emissions on a "per liter of treated virion solution" basis.

Additionally, a brief Techno-Economic Analysis (TEA) follows the LCA in the study. The TEA assumes that all capital expenses are overnight costs of each devices' energy consuming sub-systems (cooling fan, peristaltic pump, and UV light source). Operational costs are limited to the cost of energy consumption for each device over its assumed lifetime of 10 years. The TEA is used to further guide second generation prototyping decisions, namely, to guide whether the second-generation prototype should be designed using UV LEDs or whether it should maintain UV phototherapy lamps to provide the required UV radiant energy dosage.

6.2 Methods and Materials

To assess the potential environmental and economic impacts of utilizing UV LEDs versus UV Lamps in the VacciRAPTOR, a life cycle assessment (LCA) and techno-economic analysis (TEA) were performed. As noted in the following sections, the LCA and TEA performed here have narrow scopes due to the specific goals outlined in the following study details.

6.2.1 Goal of the combined LCA TEA

The intended application of this combined LCA TEA is to compare the use phase of the VacciRAPTOR using UV phototherapy lamps compared to using UV LEDs to deliver UV radiant energy to a flowing liquid of virion solution. There are two primary design constraints that influence the light source requirements. The light sources must be able to:

1. Deliver 1,500 Joules of UVA/UVB radiant energy to each liter of virion solution that flows through the device (i.e., radiant UV energy delivered per volume = 1,500 J/L)

2. Deliver UVA/UVB radiant energy at an intensity (mW/cm^2) that is equivalent to the intensity of the VacciRAPTOR's 18-lamp illumination field. For this study, the illumination sources' emission spectra were compared between 300nm and 340nm rather than 220nm to 480nm. The reasoning for narrowing the emission spectra in this analysis is outlined in ***Chapter 6.2.2.4 Data/Inventory Analysis***.

This study was carried out to guide design decisions for the second prototype of the VacciRAPTOR. The combined LCA TEA was used to compare "use" phase energy consumption and capital costs for designs using either UV phototherapy lamps or UV LEDs. The intended audience is the research team that is involved in the development of the VacciRAPTOR. The results will be used in comparative assertions that are presently intended to be released publicly.

6.2.2 Scope of the combined LCA TEA

The product system studied is a novel technology that is being developed to deliver UV radiant energy to a flowing virion solution to inactivate the virion without causing excess damage to its structure (i.e., causing excess damage that reduces the antigen potency). The device is intended to be a highly scalable, flow-through unit. At this early stage in the device's development, there are two primary concerns that relate to the scope of the LCA TEA:

1. Minimize greenhouse gas (GHG) emissions specifically related to the energy consumption of the device during the use phase
2. Understand the capital costs and energy consumption costs of employing UV phototherapy lamps versus UV LEDs in the design

6.2.2.1 Functional Unit

The functional unit used in the LCA study is Liter of virion solution treated. This functional unit is used because the function of the VacciRAPTOR is to produce a given volume of inactive (treated) virion solution. The functional unit used in the TEA study is device lifetime. The primary interest of the TEA is to comparing lifetime capital and use costs of the device.

6.2.2.2 System Boundary

The system boundary is limited to the "use" phase of the device. There are three energy consuming units on the device: the cooling blower, the UV light source, and the peristaltic pump. ***Figure 6.1 below*** illustrates the LCA fundamental direct inputs (electricity), system boundary, and outputs. ***Figure 6.2 below*** illustrates the TEA system boundary which is limited to the overnight capital costs and electricity use costs for the use phase only.

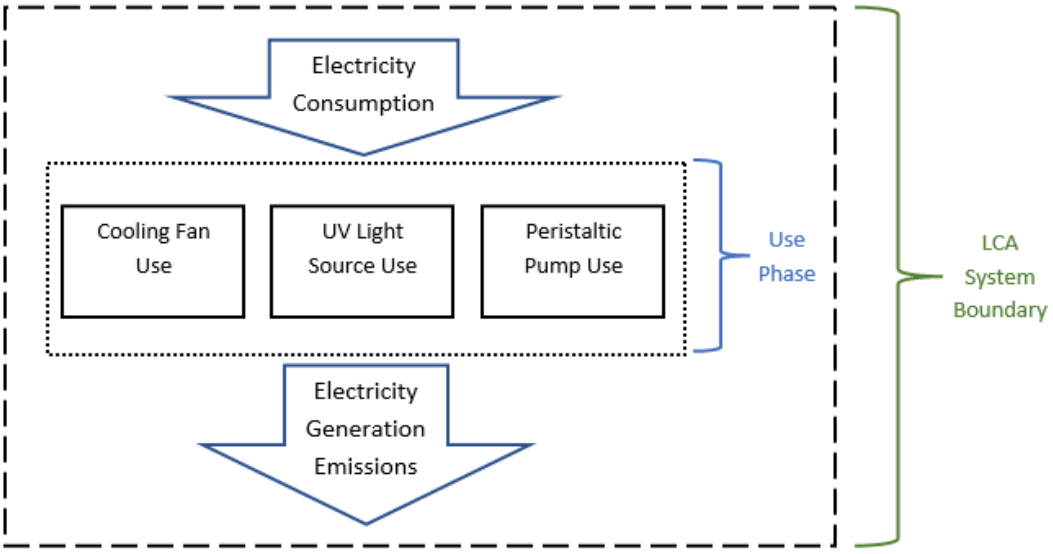

Figure 6.1: The LCA system boundary is limited to the use phase of the device.

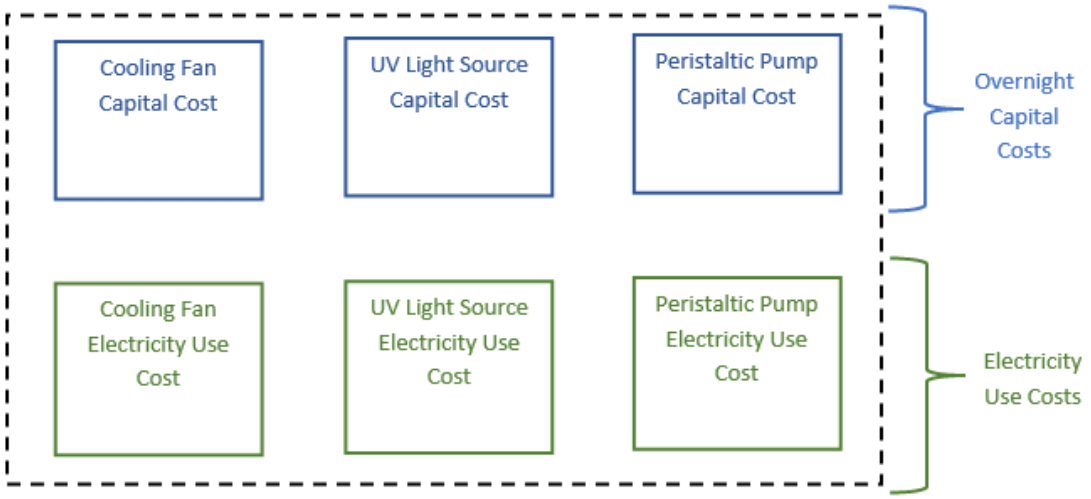

Figure 6.2: The TEA system boundary is limited to overnight capital costs and lifetime electricity use costs.

6.2.2.3 Impact Assessment

In this study, one impact category was selected to describe the energy and environmental performance of the UV lamp versus UV LED device design. This study assesses impact based on global warming potential (GWP) on a per gram of CO2-equivalence (g-CO2-eq). The emissions assessed are indirect emissions associated with the generation of the electricity that is used to power the device. Additional details are outlined in the following section.

6.2.2.4 Data/Inventory Analysis (LCA and TEA data)

VacciRAPTOR UV Radiant Energy Delivery Data Collection

All of the spectral data (irradiance, peak intensity, radiant flux, wavelength, etc.) is primary data that was obtained using a spectrometer. A spectrometer was used to measure the spectral light emission for the VacciRAPTOR and select high-output UV LEDs whose peak intensities are centered at 310nm and 325nm.

It is important to note that in light of a literature review of Martin et al. [14, 15], Goodrich et al. [16], and Yin et al. [21], it is assumed that the majority of the desired inactivation due to UV-riboflavin photochemistry in the UVA/UVB region occurs between approximately

300nm and 340nm with major inactivation peaks centered at 310nm and 325nm. In the 300nm to 340nm region, it is understood that the UV-riboflavin photochemistry specifically targets pathogen nucleic acid at the location that promotes replication. Specifically targeting and damaging this nucleic acid location renders the pathogen inactive by discretely damaging the replication site without causing extraneous damage that reduces the resulting antigen's potency.

At wavelengths less than ~300nm where the UVB region approaches the UVC spectrum, the UV radiation becomes energetic enough to cause non-discriminatory damage to the pathogen. While inactivation occurs readily below 300nm, the excess damage can reduce the resulting antigen potency. At wavelengths greater than ~340nm, the UV-riboflavin photo chemical begins to change regimes where the dominant mechanism for inactivation is due to a reaction that generates reactive oxygen species. These oxygen species cause irreversible nucleic acid damage through various oxidative reactions that cause in activation. Similar to UV radiation dosages at wavelengths below ~300nm, dosages at wavelengths above ~340nm will also cause excess damage to the virus structure that reduce the resulting antigen's potency [14, 15, 16].

To represent the central assertion that the majority of the desired UV-riboflavin inactivation occurs between 300nm and 340nm, ***Figure 3.3 from page 13*** is reproduced below as ***Figure 6.3***. Here, the emission spectra of the VacciRAPTOR's 18-lamp emission spectra (red line) and two high-intensity narrowband UV LEDs centered on 310nm and 325nm (orange and dark purple lines, respectively) are overlayed on the graph. This shows that the spectral irradiance of the VacciRAPTOR's emission spectrum and the 310nm and 325nm narrowband LED spectra fall within the wavelengths of the most prominent portion of the UVA/UVB riboflavin action spectrum (i.e., between approximately 300nm and 340nm).

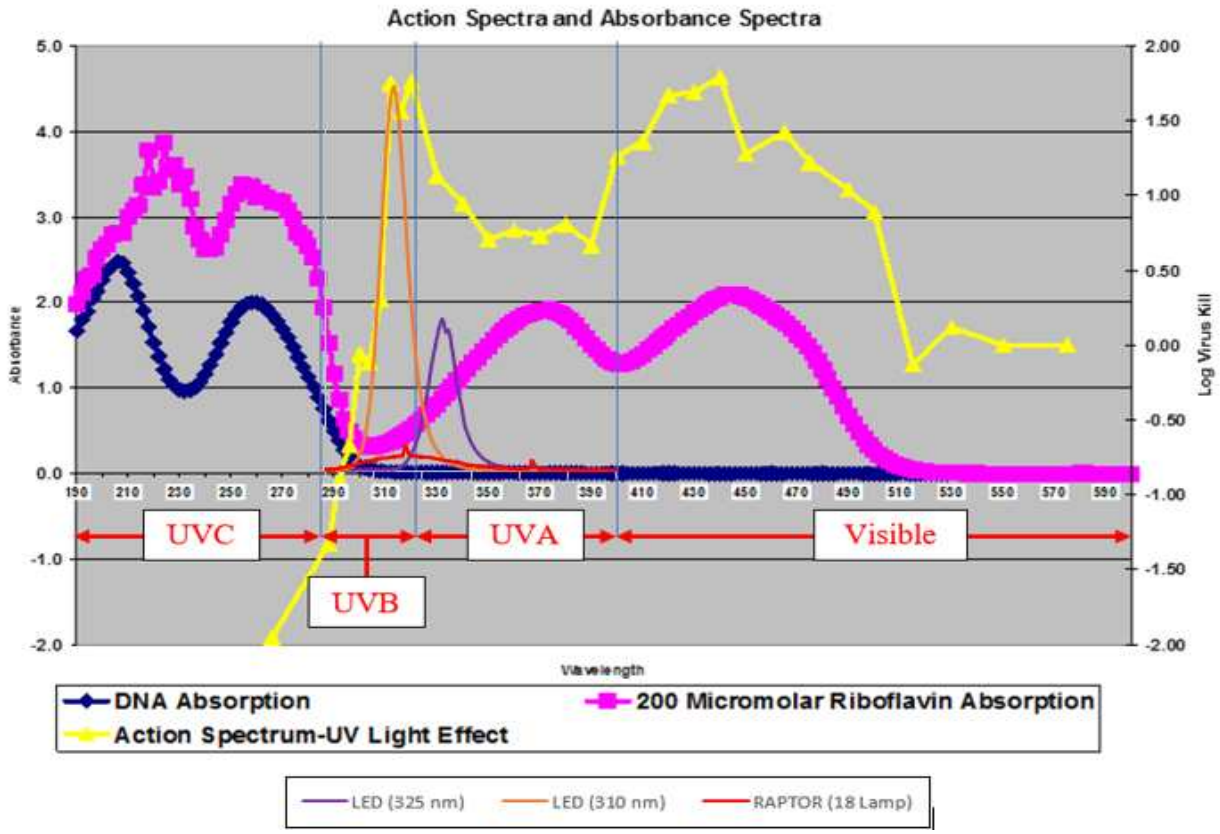

Figure 6.3: Action and absorbance spectra of riboflavin and DNA [14] with an overlay of narrowband UV LED (325nm and 310nm) emission spectra and the VacciRAPTOR's 18-lamp broadband emission spectra.

Given the assertion that the most desirable inactivation results are yielded by an irradiance spectrum between approximately 300nm and 340nm and to appropriately compare the radiant broadband lamps used in the VacciRAPTOR to high-intensity UV LED's, this combined LCA TEA ignores all radiant energy delivery outside of the 300 to 340nm range. Herein, only the irradiance and radiant power values measured within this wavelength (λ) range are considered. As shown in ***Table 6.1 below***, this truncates the VacciRAPTOR's 18-lamp emission energy to 43% of the total emission energy while the 325nm and 310nm LED emission energy are truncated only slightly to 86% and 94% of their total emission energy, respectively. Also note that the analysis assumes that the LED-based illumation field is comprised of (50%) 325nm LEDs and (50%) 310nm LEDs.

Table 6.1: Illumination field performance when assessed between 300nm and 340nm. In this range, the VacciRAPTOR 18-lamp illumination field outputs 21,100mW of radiant power while a single pair of 325nm and 310nm UV LEDs output 22.2mW. Assuming 50% of the LED matrix are 325nm and 50% are 310nm, 1900 total LEDs are required to produce an equivalent maximum treatment capacity to that of the VacciRAPTOR at 51L/hr.

Device Name	Nominal λ (nm)	Range λ (nm)	Energy % in Range (%)	Irradiance (mW/cm^2)	Incident Surface Area (cm^2)	Radiant Power (mW)	Total Power (mW)	LED Equiv. (#)	Max. Treat. Cap. (L/hr)
RAPTOR 18-Lamp	Multi-spectral	300-340	43%	12.0	1,756	21,100	21,100	n/a	51
LED - 325nm	325	300-340	86%	53.9	0.119	6.41	22.2	1,900	51
LED - 310nm	310	300-340	94%	133	0.119	15.8			

In summary, the key result of the primary data analysis is the number of UV LEDs that are required to create a UV LED-based illumination field that demonstrates an equivalent treatment capacity to that of the 18-broadband UV lamp version between 300 and 340nm. The analysis reveals that approximately 1,900 UV LEDs ((950) 325nm LEDs and (950) 310nm LEDs) are needed to provide an equivalent treatment capacity of 51L/hr with a UV energy dosage of 1,500J/L. Note that the treatment capacity of the VacciRAPTOR presented in the ***Table 6.1 above*** is 51L/hr and not 71L/hr as is shown in ***Table 4.3 on page 38***. The treatment capacity in ***Table 6.1*** only accounts for radiant power delivered between 300 and 340nm while the treatment capacity in ***Table 4.3*** accounts for radiant power delivered between 280 and 480nm.

Power Consumption Ratings for the Cooling Fan, UV Light Sources, and Peristaltic Pump

The power consumption rating of the cooling fan (275CFM blower[2]), peristaltic pump[3], the UV Lamps[4], and UV LEDs [5,6] were obtained from the specification sheets for each unit. ***Table 6.2 below*** summarizes the power ratings of each individual system as well as the total power rating for the entire device. Note that power rating for the 1,900 UV LEDs assumes that the device employs a 50/50 mix of 310nm and 325nm LEDs. It was also assumed that the cooling fan operates at the nominal power rating listed on the specification sheet (54 W). Further, it was assumed that the peristaltic pump operates at the maximum power rating provided on the specification sheet (50 W). The peristaltic pump's maximum power rating was assumed to provide a "worst case scenario" for the energy use contribution due to pump operation. It is also anticipated that during operation, the pump will need to operate at 90% to 100% of its maximum power capacity to pump fluid at the required volumetric flow rate.

Table 6.2: Individual system and total device power rating comparison

Subsystem	Individual Unit Power Rating (W)	Quantity	Subsystem Power Rating (W)
Cooling Fan (nom)	54	1	54
Peristaltic Pump (max)	50	1	50
UV Lamp (nom)	36	18	648
UV LED (nom)	9.3	1,900	17,700
Device	**Total Power Rating (W)**		
UV 18 Lamp (nom)	752		
UV 1,900 LED (nom)	17,800		

[2] Source (cooling fan): https://www.grainger.com/product/DAYTON-OEM-Blower-Rectangular-3HMH7
[3] Source (peristaltic pump): https://www.interscience.com/IMG/pdf/interscience_flexipump_ft_en.pdf
[4] Source (Daavlin 36W phototherapy lamp): https://daavlin.com/hcp/products/
[5] Source (325nm UV LED): https://www.violumas.com/wp-content/uploads/2022/02/WS5252C40L3-325-Rev020822.pdf
[6] Source (310nm UV LED): https://www.violumas.com/wp-content/uploads/2021/08/VS7272C48L6-310-Rev080621.pdf

The UV light source power rating for the UV phototherapy lamps is based on the nominal power rating of each UV lamp (36 W/ea.). There are 18 lamps used by the device, so the total power rating of lamp illumination system is 648W (18 lamps * 36W/lamp = 648W). The power rating of the UV LEDs at 310nm and 325nm are 1.9W/each and 16.8W/each, respectively. Since this analysis assumes a 50/50 mix of 310nm and 325nm LEDs, the average LED power consumption is 9.3W/each (1,900 UV LEDs * 9.3 W per LED = 17,700W). Note that the estimated total power rating of the UV 1,900 LED lighting system is over 23x greater than that of the UV 18 lamp system.

Overnight Capital Costing Data

Capital costs for the three energy consuming systems in the VacciRAPTOR were included in the TEA (cooling fan, peristaltic pump, and UV light source). ***Table 6.3 below*** summarizes the overnight capital cost inputs for each energy consuming system. The capital cost of the cooling fan is rounded to the nearest whole dollar from a common supplier at $140[7]. The capital cost of the peristaltic pump was obtained from quote provided by the pump manufacturer and was rounded to the nearest whole dollar at $3,900[8].

Table 6.3: Overnight capital costs for each individual system and the total for each device

System	UV 18 Lamp	UV 1,900 LED
Cooling Fan	$ 140	$ 140
UV Light Source	$ 1,350	$ 62,700
Peristaltic Pump	$ 3,900	$ 3,900
TOTAL	$ 5,390	$ 66,740

[7] Source (cooling fan): https://www.grainger.com/product/DAYTON-OEM-Blower-Rectangular-3HMH7
[8] Source (peristaltic pump): https://www.interscience.com/flexipump-pro-dispensing-pump-71?lang=en

The capital cost of the UV phototherapy lamps is significantly less than the cost of an equivalent UV LED system. The cost of the UV lamps used in the device was obtained from a purchase order receipt from the lamp manufacturer Daavlin[9]. Each lamp costs $75. There are 18 lamps in use on the device so the total capital cost of the lamps on the device is $1,350.

The capital cost of the UV LEDs was obtained from the manufacturer of the specific make and model LEDs that are suitable for the VacciRAPTOR. Each of the LED types for the wavelengths of interest cost approximately the same per unit at an average value rounded to $33 each[10]. This unit price includes volume pricing at 500 units. Therefore, the total capital cost of the 1,900 UV LEDs is estimated to be $62,700 (46x greater than that of the UV LED lamps).

Average Cost of Electricity in the United States

The Energy Information Administration (EIA) reports that as of April 2022, the average cost of electricity in the United States is 11.74 cents/kWh [26]. The TEA model here assumes this average cost of electricity. ***Table 6.4 below*** summarizes the hourly operating costs (electricity consumption only) of each device given a cost of 11.74 cents/kWh.

Table 6.4: Average cost of electricity and resulting hourly operating costs (electricity consumption only)

Metric	Value
Average cost of electricity per kWh	$ 0.1174
Hourly operating costs	
UV 18 Lamp (nom)	$ 0.088
UV 1,900 LED (nom)	$ 2.090

[9] Source (Daavlin 36W UV lamp): https://daavlin.com/hcp/products/
[10] Source (Violumas COB UV LED modules): https://www.violumas.com/uv-leds/cob-modules/

Emissions Data Source (g CO2-eq/kWh of energy generation)

The emissions per energy generation metric used in this report was sourced from the 2020 emissions by geographical regional data reported by the EIA [27]. As illustrated by ***Figure 6.4 below***, there is significant variation in the regional emissions per generation throughout the US. Note that the median value for the NERC regional data is 407 g-CO2-eq/kWh and the US overall average value is 388 g-CO2-eq/kWh. All emissions estimations carried out in this report use the US overall average reported value of 388 g-CO2-eq/kWh of generation. The average, overall value is of interest in this study. The variation by region is provided below for reference only and is outside the scope of this report.

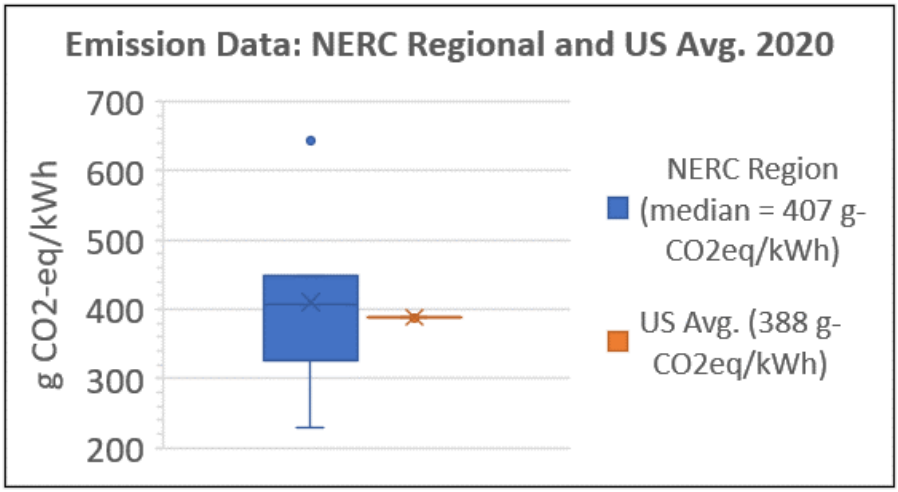

Figure 6.4: NERC regional and US average emissions per kWh of generation [27].

Lighting System Lifetime Data

Lifetime estimates of the lighting systems reviewed in this study were not available directly from the manufacturers. Industry reported average lifetimes for traditional LEDs and traditional compact fluorescent lamps (CFLs) assert that that LEDs have an average lifespan of 50,000 to 100,000 hours and CFLs have an average lifespan of 10,000 hours [28]. In this study, it is assumed that the UV lamps have a lifetime of 10,000 hours and the UV LEDs have a lifetime

of 50,000 hours. 50,000 hours was selected for the UV LEDs to be conservative. The lifetime of the lighting sources a major assumption with large uncertainty that effects the TEA results. LCA results are uninfluenced by this assumption.

6.3 Results and Discussion

6.3.1 Results & Discussion: Life Cycle Assessment (LCA)

The global warming potential (GWP) profile related to the assessed devices is shown in ***Table 6.5 below***. It is overwhelmingly clear in ***Figure 6.5 below*** that the UV 18 Lamp device causes a lower use-phase environmental impact compared to the UV 1,900 LED device per L of treated virion solution. The GWP impact for the UV 18-lamp device is 5.7 g-CO2-eq/L and the impact of the UV 1,900 LED device is nearly 24x greater at 136 g-CO2-eq/L. For the UV 18 Lamp device, 86% of the GWP impact contribution is due to the operation of the UV lamps. For the UV 1,900 LED device, 99% of the GWP impact contribution is due to the operation of the UV LEDs.

Table 6.5: Comparison between the GWP impacts assessed for the use phase of the UV 18 Lamp and UV 1,900 LED devices; total impact and impact of each energy consuming unit (functional unit = 1 L of treated virion solution)

UV 18 Lamp					
Impact Category	**Unit**	**Total**	**Cooling Fan**	**Peristaltic Pump**	**UV Source**
GWP (nom)	g CO2-eq	5.7	0.41	0.38	4.9
UV 1,900 LED					
Impact Category	**Unit**	**Total**	**Cooling Fan**	**Peristaltic Pump**	**UV Source**
GWP (nom)	g CO2-eq	136	0.41	0.38	135

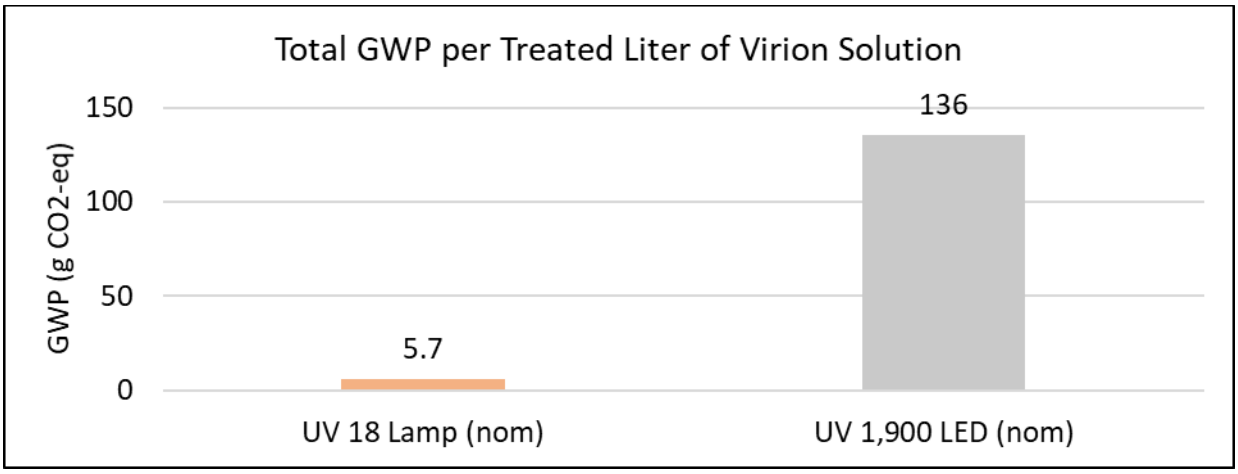

Figure 6.5: Total use phase GWP comparison between the 18-lamp device and the equivalent 1,900 LED device

A sensitivity analysis was performed to determine the sensitivity of a +/-20% change in the size of each electricity consuming system for each of the UV lighting options. As expected, since 86% to 99% of the total system emissions are a result of the lighting power consumption, changing the size of the cooling fan or the peristaltic pump yields a minor change to the total system emissions of the UV 18 Lamp device and yields a negligible change in total system emissions of the UV 1,900 LED device.

When changing the lighting system size by +/-20%, there is an overall change in the total system size by nearly +/- 20% as well. ***Figure 6.6 below*** is a graphical representation of the sensitivity analysis for each device. ***Figure 6.5*** and ***Figure 6.6*** clearly indicate that that the UV 18 Lamp System offers a much lower GWP system for the use phase of the device.

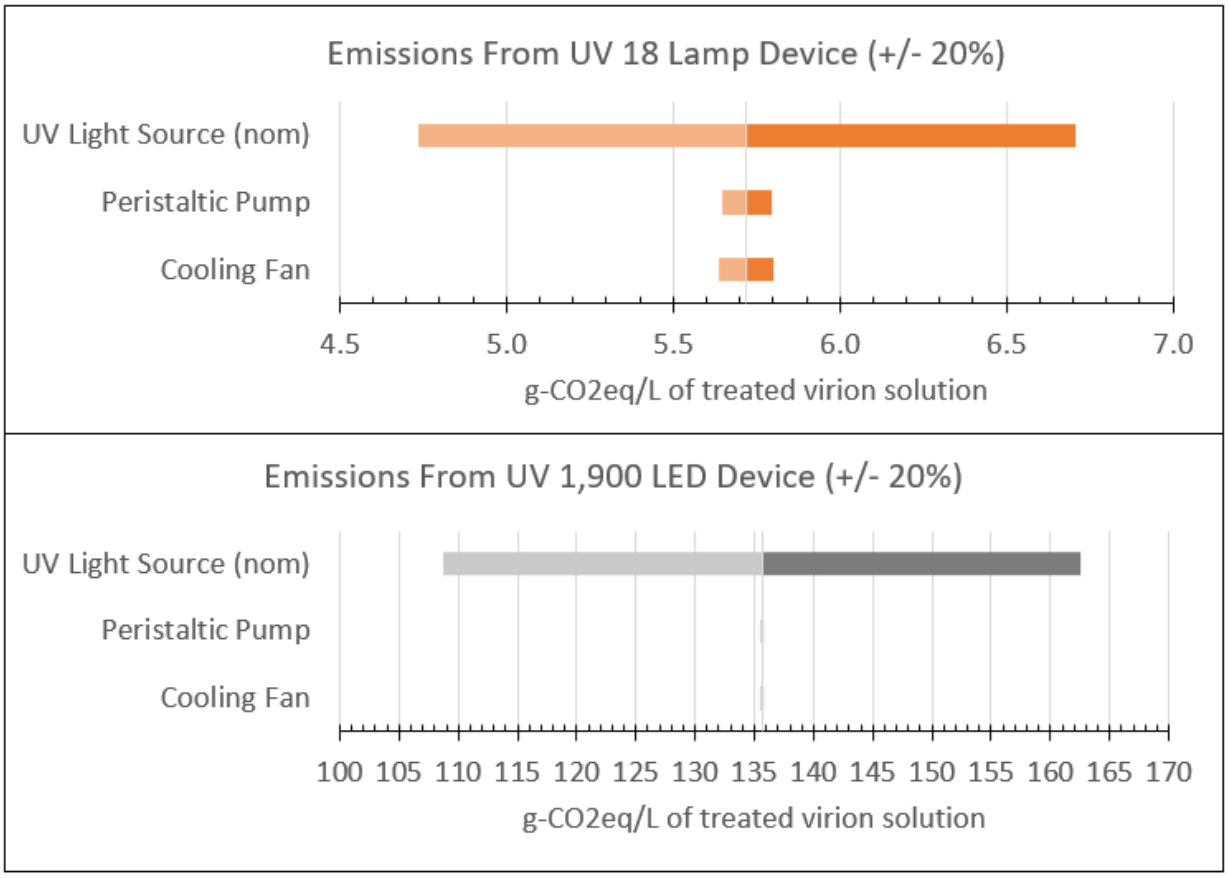

Figure 6.6: Sensitivity analysis for the UV 18 lamp device and the UV 1,900 LED Device (functional unit = 1 L of treated virion solution)

6.3.2 Results & Discussion: Techno-Economic Analysis (TEA)

Table 6.6 below summarizes the individual sub-system items and total device overnight capital costs for the UV 18 Lamp and UV 1,900 LED devices. The TEA assumes that all capital costs are incurred overnight, and all items are procured without loans. ***Table 6.7 below*** summarizes the lifetime electricity consumption costs for each device. As noted in the table title, the analysis asserts three primary assumptions for the reported lifetime electricity consumption costs:

- The cost of electricity 11.74 cents/kWh and remains constant over the lifespan of the device [26].

- The service life of the device is 10 years.
- The device operates 1,000 hours per year.

Table 6.6: Overnight capital costing for each device sub-system and total device cost

System	UV 18 Lamp	UV 1,900 LED
Cooling Fan	$ 140	$ 140
UV Light Source	$ 1,350	$ 62,700
Peristaltic Pump	$ 3,900	$ 3,900
TOTAL	$ 5,390	$ 66,740

Table 6.7: Total costing given overnight capital costs and lifetime energy consumption costs (assumes 11.74 cents/kWh, 10-year device lifespan, and 1,000 hours of operation per year)

UV 18 Lamp		
TEA Impact Category		**Value**
Overnight Capital	$	5,390
Lifetime Energy Consumption	$	883
TOTAL	$	6,273
UV 1,900 LED		
TEA Impact Category		**Value**
Overnight Capital	$	66,740
Lifetime Energy Consumption	$	20,897
TOTAL	$	87,637

The overnight capital cost of the UV 1,900 LED device is approximately 12x greater than the UV 18 Lamp device, and the lifetime electricity consumption costs are approximately 24x greater than the UV 18 Lamp device. It is clearly illustrated by ***Figure 6.7 below*** that the UV 18 Lamp device offers a far more attractive economic solution when considering the type of UV radiant energy delivery system.

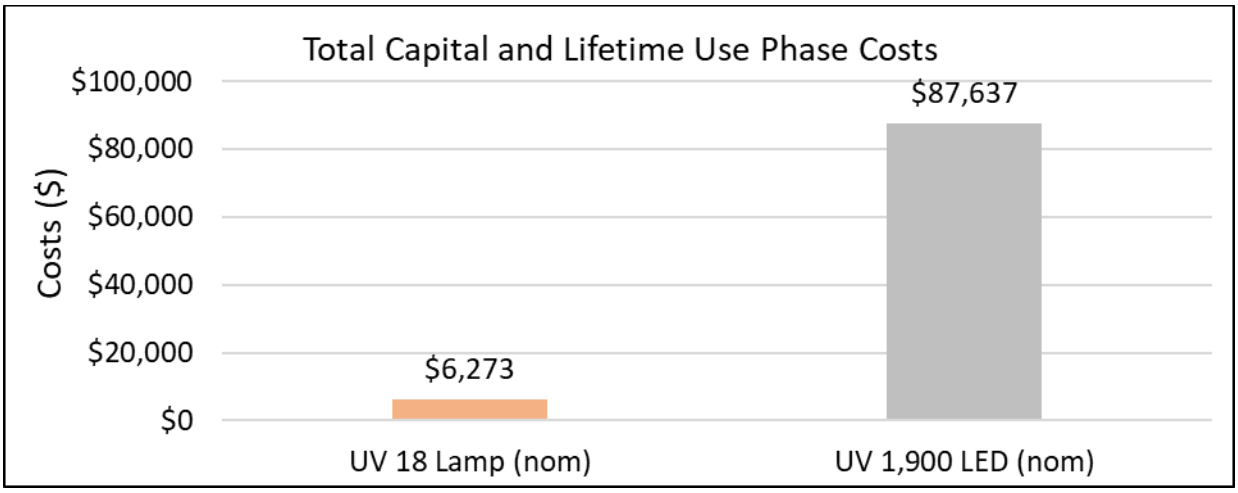

Figure 6.7: Total lifetime costs (overnight capital and lifetime energy consumption)

6.4 Conclusions and Implications

This study presents the evaluation and comparison of two types of UV radiant energy sources for use in the VacciRAPTOR rapid vaccine prototype that is being developed in collaboration between Colorado State University's Energy Institute and Infectious Disease Research Center. The assessment considers the use phase of the life cycle of the device prototype in its current UV 18 Lamp configuration and compares it to an equivalent device design (UV 1,900 LED) that utilizes UV LEDs to deliver UV radiant energy.

6.4.1 Conclusion: Life Cycle Assessment (LCA)

Using UV lamps to deliver the desired UV radiant energy to the flowing liquid virion solution has proven to be better solution for minimizing GWP environmental impacts. Given a GWP of 5.7 g-CO2-eq per Liter of treated virion solution for the UV 18 Lamp device compared to 136 g-CO2-eq for the UV 1,900 LED device, the UV Lamp solution is approximately 24x less environmentally impactful than the UV LED solution.

6.4.2 Conclusion: Techno-Economic Analysis (TEA)

Using UV lamps to deliver the desired UV radiant energy to the flowing liquid virion solution has proven to be a better economic solution for minimizing the overall cost of the device. Given total overnight capital and lifetime energy consumption costs of $6,300 for the UV 18 Lamp device compared to over $88,000 for the UV 1,900 LED device, the UV Lamp solution is approximately 14x less expensive than the UV LED solution.

6.4.3 Implications of the Combined LCA TEA and Potential Advancements in the Science of UV-Riboflavin Pathogen Inactivation

Although the results of the study clearly show that the UV Lamp device is preferred from the standpoint of minimizing GWP and economic impact by an order of magnitude, this does not necessarily mean that the UV LED solution is not valuable or should not be explored. To date, the science of UV-riboflavin photochemistry for use in whole virion vaccine production is in its infancy. Efficacy using broadband UV lamps has been proven in an animal challenge model for the SARS CoV-2 virus by Ragan et al. [5], but investigations comparing antigen potency via narrowband inactivation compared to broadband inactivation have not been performed.

There is immense scientific value in prototyping a UV LED device so that antigen potency via broadband UV exposure can be directly compared to antigen potency via narrowband UV exposure. If results show that the potency of antigen produced via narrowband UV inactivation is an order of an order of magnitude higher than the potency of antigen produced via broadband UV inactivation, a UV LED device may ultimately produce a higher quality product and have an environmental and economic impact that is comparable to that of the UV 18 lamp device.

In light of the combined LCA TEA results, it is suggested that two actions be taken. Given the significantly lower environmental and economic impacts of the UV 18 lamp device, the 18 lamp device should continue to be developed towards commercial readiness. Additinolly, it is suggested that a narrowband UV LED device be developed. In the early stages of developing a narrowband UV LED device, it is suggested that the device be use fewer than 1,900 UV LEDs in order to reduce power consumption and cost during initial development. Once inactivation tests have been performed with both devices, the antigen potency should be directly compared. If antigen potency via narrowband UV LED inactivation is significantly higher than antigen potency via broadband UV lamp inactivation, it may be valuable to pursue a commercially viable UV LED inactivation device.

CHAPTER 7 CONCLUSIONS

7.1 Summary of Findings

The process of developing a high-throughput rapid vaccine production device provided many insights into the processes of UV and riboflavin-UV facilitated pathogen inactivation. CSU produced a high throughput device that successfully and repeatably inactivates Zika virus. The devices scales to treat anywhere from 9 to over 70L/hr of virion solution. This equates to a human SARS-CoV-2 vaccine production rate of approximately 13,000 to over 100,000 vaccine doses per hour.

When testing the performance of high-intensity UV LEDs it was concluded that riboflavin-UV photochemistry is most strongly employed by narrowband UV LEDs whose nominal wavelengths are centered at 310nm and 325nm. If one were to design a device that utilizes a 50/50 mix of 310nm and 325nm LEDs whose radiant power per pair of LEDs is ~22mW, the device would require ~1,900 LEDs to yield the same treatment capacity as the VacciRAPTOR's 18 broadband UV lamp configuration.

A combined life cycle assessment (LCA) and technoeconomic analysis (TEA) indicate that, given the 18-lamp configuration compared to the 1,900 LED configuration, the 18-lamp configuration is 24x less impactful from a carbon footprint perspective and 12x less impactful from an economic perspective. Further study is necessary to understand the implications environmental impacts associated with lamp versus LED disposal as well as lamp versus LED lifetime. Even though the UV LED configuration may consume 24x more energy and cost 12x more than the 18-lamp device, there is immense scientific value in designing the LED prototype and comparing the potency of antigen produced by both the UV lamp device and a UV LED device. Narrowband UV LEDs with 310nm and 325nm nominal emission spectra may yield an

antigen whose potency is much greater than the potency of antigen produced by the current broadband UV lamp configuration due to the differing mechanisms of riboflavin-UV induced inactivation.

7.2 Suggestions for Future Work

In the continued development of a high-throughput rapid vaccine production device, an alternative pursuit to the broadband UV lamp illumination field is a narrowband UV LED illumination field. Exploring whole virion riboflavin-UV inactivation with narrowband UV LEDs may provide insight into maximizing the potency of antigen produced via the SolaVAX method and the VacciRAPTOR technology.

Several avenues exist for improving the safety of the current device. Three primary improvements are suggested. The device is currently configured with an emergency stop button that kills power to the lamps and the fan. Integrated into this circuit, power to the peristaltic pump should also be killed by the emergency stop button. Another suggestion for safety improvement is to integrate HEPA filtration at the outlet of the top cap to filter air that exits the device. The third primary safety improvement suggestion is to pull air through the illumination chamber rather than to push air through it. The "pulling" configuration would produce a vacuum in the illumination chamber rather than pressurizing the illumination chamber as occurs in the "pushing" configuration. In the event of a rupture in the tubing within the illumination chamber, all three of these measures would greatly improve the safety of the device.

Testing procedures can be improved by reconfiguring the tubing assembly methods. Integrating a y-connector with an inlet selector knob onto the inlet side of the tubing and immediately downstream from the inlet bag would produce two primary benefits. During the

sterilization process, one could select for NaOH or ethanol to flow though the tubing assembly and flip the selector at the y-connector to then pull PBS through another line to chase the NaOH out of the tubing. During the testing process, when the bulk viral solution inlet bag empties, one could select another inlet path that pulls HEPA filtered air through the coil so that filtered air could chase behind the solution and assist in fully evacuating the solution from the tubing and tubing coil.

Further, programming logic into the device's operation to not only display real time power consumption to but also alert the user and stop the pump if power consumption drops sufficiently low to indicate that lamp failure may have occurred. These measures are essential for quality and safety control going forward.

REFERENCES

[1] J. Louten, "Chapter 8 - Vaccines, Antivirals, and the Beneficial Uses of Viruses," in *Essential Human Virology*, Academic Press, 2016, pp. 133-154.

[2] "The History of Vaccines," The college of Physicians of Philadelphia, 17 January 2018. [Online]. Available: https://www.historyofvaccines.org/content/articles/different-types-vaccines. [Accessed 3 February 2022].

[3] E. Soler and L. M. Houdebine, "Preparation of recombinant vaccines. Biotechnology Annual Review,," *Elsevier,* vol. 13, no. https://doi.org/10.1016/S1387-2656(07)13004-0, pp. 65-94, 2007.

[4] World Health Organization, "WHO Coronavirus (COVID-19) Dashboard," World Health Organization, 05 August 2022. [Online]. Available: https://covid19.who.int/. [Accessed 05 August 2022].

[5] I. K. Ragan, L. M. Hartson, T. S. Dutt, A. Obregon-Henao, R. M. Maison, P. Gordy, A. Fox, B. R. Karger, S. T. Cross, M. L. Kapuscinski, S. K. Cooper, B. K. Podell, M. D. Stenglein, R. A. Bowen, M. Henao-Tamayo and R. P. Goodrich, "A Whole Virion Vaccine for COVID-19 Produced via a Novel Inactivation Method and Preliminary Demonstration of Efficacy in an Animal Challenge Model," *Vaccines,* vol. 9, no. 340, 2021.

[6] S. Marschner and R. P. Goodrich, "Pathogen Reduction Technology Treatment of Platelets, Plasma and Whole Blood Using Riboflavin and UV Light," *Transfusion Medicine and Hemotherapy,* no. 38, pp. 8-18, 2011.

[7] S. D. Keil, N. Hovenga, D. Gilmour, S. Marshner and R. Goodrich, "Treatment of Platelet Products with Riboflavin and UV Light: Effectiveness Against High Titer Bacterial Contamination," *Journal of Visualized Experiments,* no. 102, 2015.

[8] R. Percuoco, "Chapter 1 - Introduction to Imaging," in *Clinical Imaging (Third Edition)*, St. Louis, Mosby, 2014, pp. 1-4.

[9] "How Does Ultraviolet Light Disinfect?," We UV Care, 2022. [Online]. Available: https://www.weuvcare.com/how-does-ultraviolet-light-disinfection/. [Accessed 2 March 2022].

[10] "Spectrometry and Spectroscopy: What's the Difference," ATA Scientific, 17 January 2020. [Online]. Available: https://www.atascientific.com.au/spectrometry/. [Accessed 2 March 2022].

[11] "Riboflavin," National Institutes of Health Office of Dietary Supplements, 22 March 2021. [Online]. Available: https://ods.od.nih.gov/factsheets/Riboflavin-Consumer/. [Accessed 2 March 2022].

[12] V. Kumar, O. Lockerbie, S. Keil, P. Ruane, M. Platz, C. Martin, J.-L. Ravanat, J. Cadet and R. Goodrich, "Riboflavin and UV-Light Based Pathogen Reduction: Extent and Consequence of DNA Damage at the Molecular Level," *Photochemistry and Photobiology,* no. 80, pp. 15-21, 2004.

[13] M. Orlowska, T. Koutchma, M. Grapperhaus, J. Gallagher, R. Schaefer and C. Defelice, "Continuous and Pulsed Ultraviolet Light for Nonthermal Treatment of Liquid Foods. Part 1: Effects on Quality of Fructose Solution, Apple Juice, and Milk," *Food Bioprocess Technol,* June 2012.

[14] C. B. Martin, E. Wilfong, P. Ruane, R. Goodrich and M. Platz, "An Action Spectrum of the Riboflavin-photosenzitized Inactivation of Lambda Phage," *Photochemistry and Photobiology,* no. 81, pp. 474-480, 2005.

[15] C. B. Martin, X. S. Shi, M.-L. Tsao, D. Karweik, J. Brooke, C. M. Hadad and M. S. Platz, "The Photochemistry of Riboflavin Tetraacetate and Nucleosides. A Study Using Density Functional Theory, Laser Flash Photolysis, Fluorescence, UV-Vis, and Time Resolved Infrared Spectroscopy," *Journal of Physical Chemistry B,* no. 106, pp. 10263-10271, 2002.

[16] R. P. Goodrich, M. Cardoso and S. Marschner, "Vitamin B2 and Innovations in Improving Blood Safety," in *B Group Vitamins - Current Uses and Perspectives*, London, IntechOpen, 2018, pp. 127-140.

[17] Philips, "UVB Narrowband Lamps - Phototherapy lamp range brochure," October 2014. [Online]. Available: https://www.lighting.philips.com/main/products/special-lighting/various-uvb-applications/uvb-narrowband. [Accessed 28 February 2022].

[18] R. Grundmann, "Friction Diagram of the Helically Coiled Tube," *Chemical Engineering and Processing: Process Intensification,* vol. 19, no. 2, pp. 113-115, 1984.

[19] E. F. Schmidt, " Wfirmeiibergang und Druckverlust in Rohrschlangen," *G'zemieJng.Tech.,* vol. 39, pp. 781-789, 1967.

[20] V. Gnielinski, "Zur Berechnung des Druckverlustes in Rohrwendelin," *VT Verfahrenstechnik,* no. 17, pp. 683-690, 1983.

[21] Y. Yin, L. Li, L. Gong, H. Xu and Z. Liu, "Effects of riboflavin and ultraviolet light treatment on pathogen reduction and platelets," *Transfusion,* vol. https://doi.org/10.1111/trf.16053, no. 60, pp. 2647-2654, 2020.

[22] L. Goodrich, R. P. Goodrich, D. Gampp and R. Lockerbie, "Solution contianing platelet activation inhibitors for pathogen reducing and storing blood platelets". United State of America Patent WO 03/090794 A1, 26 April 2002.

[23] W. Clopffer, "Life Cycle Assessment: From Beginning to the Current State," *Environmental Science & Pollution Res.,* vol. IV, no. 4, pp. 223-228, 1997.

[24] Building Technologies Office US Department of Energy, "Life Cycle Assessment of Energy and Environmental Impacts of LED Lighting Products," April 2013.

[25] P. Principi and R. Fioretti, "A comparative life cycle assessment of luminaires for general lighting for the office e compact fluorescent (CFL) vs Light Emitting Diode (LED) a case study," *Journal of Cleaner Production,* no. 83, pp. 97-107, 2014.

[26] Energy Information Administration (EIA), "Electric Power Monthly Table 5.6.A. Average Price of Electricity to Ultimate Customers by End-Use Sector," April 2022. [Online]. Available:

https://www.eia.gov/electricity/monthly/epm_table_grapher.php?t=epmt_5_6_a. [Accessed 22 July 2022].

[27] Energy Information Administration, "Electricity - Emissions by geographical region for CO2, SO2, and NOx," 2020. [Online]. Available: https://www.eia.gov/electricity/data/emissions/. [Accessed 16 July 2022].

[28] StouchLighting, "Lighting Comparison: LED vs Fluorescent and CFL," 13 January 2016. [Online]. Available: https://www.stouchlighting.com/blog/fluorescent-vs-led-vs-cfl#:~:text=New%20LEDs%20can%20last%2050%2C000,other%20commercially%20available%20lighting%20technology.. [Accessed 16 November 2021].

[29] Philips Lighting, "Phototherapy Lamp Range Brochure," October 2014. [Online]. Available: https://www.lighting.philips.com/main/products/special-lighting/various-uvb-applications/uvb-narrowband. [Accessed 23 February 2022].

APPENDIX A – ARDUINO CONTROLLER CODE

```
int analogPin = A1;
int pot = 0.0;
int val = 0;
int lights[10] = {13,3,4,5,6,7,8,9,10,11};
void setup() {
  // put your setup code here, to run once:
pinMode(3,OUTPUT);
pinMode(4,OUTPUT);
pinMode(5,OUTPUT);
pinMode(6,OUTPUT);
pinMode(7,OUTPUT);
pinMode(8,OUTPUT);
pinMode(9,OUTPUT);
pinMode(10,OUTPUT);
pinMode(11,OUTPUT);
pinMode(12,OUTPUT);
pinMode(13,OUTPUT);
Serial.begin(9600);
for(int i = 0;i<10;i++){
      digitalWrite(lights[i],HIGH);
    }
}
```

```
void loop() {
  // put your main code here, to run repeatedly:
  pot = analogRead(A1);
    if(pot<=5){
      val = 0;
      digitalWrite(12,HIGH);
      digitalWrite(3,HIGH);
      digitalWrite(4,HIGH);
      digitalWrite(5,HIGH);
      digitalWrite(6,HIGH);
      digitalWrite(7,HIGH);
      digitalWrite(8,HIGH);
      digitalWrite(9,HIGH);
      digitalWrite(10,HIGH);
      digitalWrite(11,HIGH);
      delay(1000);
   }
//  else if(pot<=57.5){
//    val = 1;
//    digitalWrite(12,LOW);
//      digitalWrite(3,LOW);
//      digitalWrite(4,HIGH);
//      digitalWrite(5,HIGH);
```

```
//      digitalWrite(6,HIGH);
//      digitalWrite(7,HIGH);
//      digitalWrite(8,HIGH);
//      digitalWrite(9,HIGH);
//      digitalWrite(10,HIGH);
//      digitalWrite(11,HIGH);
//      delay(1000);
//  }
//  else if(pot<=165){
//      val = 2;
//      digitalWrite(12,LOW);
//      digitalWrite(3,LOW);
//      digitalWrite(4,LOW);
//      digitalWrite(5,HIGH);
//      digitalWrite(6,HIGH);
//      digitalWrite(7,HIGH);
//      digitalWrite(8,HIGH);
//      digitalWrite(9,HIGH);
//      digitalWrite(10,HIGH);
//      digitalWrite(11,HIGH);
//      delay(1000);
//  }
//  else if(pot<=289){
```

```
//      val = 3;
//      digitalWrite(12,LOW);
//      digitalWrite(3,LOW);
//      digitalWrite(4,LOW);
//      digitalWrite(5,LOW);
//      digitalWrite(6,HIGH);
//      digitalWrite(7,HIGH);
//      digitalWrite(8,HIGH);
//      digitalWrite(9,HIGH);
//      digitalWrite(10,HIGH);
//      digitalWrite(11,HIGH);
//      delay(1000);
//  }
//  else if(pot<=429){
//      val = 4;
//      digitalWrite(12,LOW);
//      digitalWrite(3,LOW);
//      digitalWrite(4,LOW);
//      digitalWrite(5,LOW);
//      digitalWrite(6,LOW);
//
//      digitalWrite(7,HIGH);
//      digitalWrite(8,HIGH);
```

```
//     digitalWrite(9,HIGH);
//     digitalWrite(10,HIGH);
//     digitalWrite(11,HIGH);
//     delay(1000);
//
//  }
//  else if(pot<=578){
//     val = 5;
//     digitalWrite(12,LOW);
//     digitalWrite(3,LOW);
//     digitalWrite(4,LOW);
//     digitalWrite(5,LOW);
//     digitalWrite(6,LOW);
//     digitalWrite(7,LOW);
//     digitalWrite(8,HIGH);
//     digitalWrite(9,HIGH);
//     digitalWrite(10,HIGH);
//     digitalWrite(11,HIGH);
//     delay(1000);
//  }
//  else if(pot<=720){
//     val = 6;
//     digitalWrite(12,LOW);
```

```
//      digitalWrite(3,LOW);
//      digitalWrite(4,LOW);
//      digitalWrite(5,LOW);
//      digitalWrite(6,LOW);
//      digitalWrite(7,LOW);
//      digitalWrite(8,LOW);
//      digitalWrite(9,HIGH);
//      digitalWrite(10,HIGH);
//      digitalWrite(11,HIGH);
//      delay(1000);
//  }
//  else if(pot<=852){
//      val = 7;
//      digitalWrite(12,LOW);
//      digitalWrite(3,LOW);
//      digitalWrite(4,LOW);
//      digitalWrite(5,LOW);
//      digitalWrite(6,LOW);
//      digitalWrite(7,LOW);
//      digitalWrite(8,LOW);
//      digitalWrite(9,LOW);
//      digitalWrite(10,HIGH);
//      digitalWrite(11,HIGH);
```

```
//      delay(1000);
//  }
//  else if(pot<=963){
//     val = 8;
//    digitalWrite(12,LOW);
//      digitalWrite(3,LOW);
//      digitalWrite(4,LOW);
//      digitalWrite(5,LOW);
//      digitalWrite(6,LOW);
//      digitalWrite(7,LOW);
//      digitalWrite(8,LOW);
//      digitalWrite(9,LOW);
//      digitalWrite(10,LOW);
//      digitalWrite(11,HIGH);
//      delay(1000);
//
//  }
  else if(pot<=1017){
    val = 9;
    digitalWrite(12,LOW);
      digitalWrite(3,LOW);
      digitalWrite(4,LOW);
      digitalWrite(5,LOW);
```

```
      digitalWrite(6,LOW);
      digitalWrite(7,LOW);
      digitalWrite(8,LOW);
      digitalWrite(9,LOW);
      digitalWrite(10,LOW);
      digitalWrite(11,LOW);
      delay(1000);
  }
  else if(pot<=1028){
//    val = 10;
//    digitalWrite(12,LOW);
//     digitalWrite(3,LOW);
//     digitalWrite(4,LOW);
//     digitalWrite(5,HIGH);
//     digitalWrite(6,LOW);
//     digitalWrite(7,LOW);
//     digitalWrite(8,LOW);
//     digitalWrite(9,LOW);
//     digitalWrite(10,LOW);
//     digitalWrite(11,LOW);
//     delay(1000);
    digitalWrite(12,LOW);
      digitalWrite(3,HIGH);
```

```
    digitalWrite(4,HIGH);
    digitalWrite(5,HIGH);
    digitalWrite(6,HIGH);
    digitalWrite(7,HIGH);
    digitalWrite(8,HIGH);
    digitalWrite(9,HIGH);
    digitalWrite(10,HIGH);
    digitalWrite(11,HIGH);
    delay(1000);
  for(int i = 1;i<10;i++){
    digitalWrite(lights[i],LOW);
    delay (10000);
    digitalWrite(lights[i],HIGH);
    delay (4000);
}
}
 Serial.print(pot);
 Serial.print(", ");
 Serial.println(val);
```

APPENDIX B – ZIKA INACTIVATION TEST PROCEDURE

The instructions below are intended to provide the backbone of the testing instructions. Certain details such as safety and hazardous waste containment are beyond the scope of these instructions. These instructions are general guidelines that indicate key variables in the process such as liquid volumes, general sterilization procedures, and general operating procedures.

1. Calibrate the peristaltic pump using the 1/8th size calibration coil and calibration water bags
    a. See peristaltic pump user manual for calibration procedures
    b. Calibrate the pump by flowing approximately 500mL of water a flow rate of 544 mL/min
2. Turn on the VacciRAPTOR fan and lamps allow the device to warm up
    a. Monitor the power meter to ensure that the power meter reaches steady state readings of approximately ~585W (+/- 10W) after about 20 minutes of warmup time.
    b. While the lamps are warming up, perform the following coil sterilization steps.
3. Coil sterilization
    a. Prepare 1.0M NaOH for sterilization of the coil
    b. Run 200mL of 1M NaOH through the coil at 544ml/min
    c. Flush residual NaOH from the with 200mL of PBS
    d. Flush and collect an additional 100mL of PBS through the coil and ensure the PBS has a PH of 7.0. This ensures that all residual NaOH has been removed from the tubing.
4. Bulk virus solution preparation for a total prepared volume of 500mL

a. In a 1L blood bag, combine 50mL of stock Zika virus, 35 mL of riboflavin, and 415 mL of PBS (50 + 35 + 415 = 500mL mixture)

5. Connect 1L sterile blood bags to the sterilized coil
    a. Connect prepared bulk virus solution to the inlet side of the tubing coil
    b. Connect an empty bag to the outlet side of the tubing coil
6. Turn off the VacciRAPTOR lamps (do not turn off the fan)
    a. Insert the coil into the illumination chamber
    b. Secure the tubing clamp
    c. Secure the top cap
    d. Turn the lamps back on and ensure that steady state power consumption is achieved again at ~585W (+/- 10W). It should only take a few minutes for this to occur since the lamps were only turned off briefly and are still warm.
7. Insert the inlet tubing coil into the peristaltic pump and set pump to 544 ml/min. Do not turn on the pump yet.
    a. Ensure pumping will occur in the correct direction
    b. Undo all clamps on the tubing so that liquid will flow
    c. Turn on the pump and monitor treatment progress to ensure flow continues until the bag is empty.
    d. When the bag is empty, turn off the pump and clamp the tubes near the base of the inlet and exit bags.
    e. Turn off the lamps.
    f. Remove the tubing assembly from the pump and the illumination field.
8. Remove three 3mL samples from the outlet bag.

9. Sterilize the tubing coil before the second bulk solution treatment
    a. Flow 200mL of 70% ethanol through the coil.
    b. Flush the coil with 200mL of PBS
10. Attach a new, sterile bag to the outlet side of the tubing assembly and connect the treated bag to the inlet side of the tubing assembly.